UNIVERSIDADE FEDERAL DE UBERLÂNDIA
FACULDADE DE ENGENHARIA QUÍMICA
PROGRAMA DE PÓS-GRADUAÇÃO EM ENGENHARIA QUÍMICA

FINE AND ULTRAFINE APATITE FLOTATION DERIVED FROM TAILINGS

FLOTAÇÃO DE FINOS E ULTRAFINOS DE APATITA PROVENIENTE DE REJEITOS

Thessa Fuzaro Mendes

Uberlândia
2025

UNIVERSIDADE FEDERAL DE UBERLÂNDIA
FACULDADE DE ENGENHARIA QUÍMICA
PROGRAMA DE PÓS-GRADUAÇÃO EM ENGENHARIA QUÍMICA

FINE AND ULTRAFINE APATITE FLOTATION DERIVED FROM TAILINGS

FLOTAÇÃO DE FINOS E ULTRAFINOS DE APATITA PROVENIENTES DE REJEITOS

Thessa Fuzaro Mendes

PhD Thesis submitted to the Graduate Program in Chemical Engineering at the Federal University of Uberlândia as a partial requirement for obtaining the title of PhD in Chemical Engineering, with a concentration area in Research and Development of Chemical Processes.

Advisor: Prof. PhD. Marcos Antonio de Souza Barrozo

Prof. PhD. Elenice Maria Schons Silva

Uberlândia

2025

Ficha Catalográfica Online do Sistema de Bibliotecas da UFU
com dados informados pelo(a) próprio(a) autor(a).

M538 Mendes, Thessa Fuzaro, 1989-
2025 Flotação de finos e ultrafinos de apatita proveniente de rejeitos [recurso eletrônico] / Thessa Fuzaro Mendes. - 2025.

Orientador: Marcos Antonio de Souza Barrozo.
Coorientadora: Elenice Maria Schons Silva.
Tese (Doutorado) - Universidade Federal de Uberlândia, Pós-graduação em Engenharia Química.
Modo de acesso: Internet.
DOI http://doi.org/10.14393/ufu.te.2025.412
Inclui bibliografia.
Inclui ilustrações.

1. Engenharia química. I. Barrozo, Marcos Antonio de Souza, 1961-, (Orient.). II. Silva, Elenice Maria Schons,1980-, (Coorient.). III. Universidade Federal de Uberlândia. Pós-graduação em Engenharia Química. IV. Título.

CDU: 66.0

Bibliotecários responsáveis pela estrutura de acordo com o AACR2:
Gizele Cristine Nunes do Couto - CRB6/2091
Nelson Marcos Ferreira - CRB6/3074

Bloco de Assinatura 124681 - Sequencial 2 Selecionar para Assinatura

UNIVERSIDADE FEDERAL DE UBERLÂNDIA
Coordenação do Programa de Pós-Graduação em Engenharia Química
Av. João Naves de Ávila, 2121, Bloco 1K, Sala 206 - Bairro Santa Mônica, Uberlândia-MG, CEP 38400-902
Telefone: (34)3239-4249 - www.ppgeq.feq.ufu.br - secppgeq@feq.ufu.br

ATA DE DEFESA - PÓS-GRADUAÇÃO

Programa de Pós-graduação em:	Engenharia Química				
Defesa de:	Tese de Doutorado, 8/2025, PPGEQ				
Data:	21 de julho de 2025	Hora de início:	14:00	Hora de encerramento:	17:00
Matrícula da Discente:	12113EQU010				
Nome da Discente:	Thessa Fuzaro Mendes				
Título do Trabalho:	Flotation of fine and ultrafine apatite tailings				
Área de concentração:	Desenvolvimento de Processos Químicos				
Linha de pesquisa:	Processos de Separação				
Projeto de Pesquisa de vinculação:	Flotação da apatita em coluna				
ODS-ONU:	ODS 12 – Consumo e Produção Responsáveis				

Reuniu-se por meio de webconferência, a Banca Examinadora, designada pelo Colegiado do Programa de Pós-graduação em Engenharia Química, assim composta: Professores Doutores: João Inácio Soletti - CETEC/UFAL, Maria do Carmo Ferreira - DEQ/UFSCar, Michelly dos Santos Oliveira - CEFET-MG/ *Campus* Araxá, Ricardo Corrêa de Santana - PPGEA/UFU, Elenice Maria Schons Silva - FENG/UFCAT, coorientadora, e Marcos Antonio de Souza Barrozo - PPGEQ/UFU, orientador da candidata.

Iniciando os trabalhos o presidente da mesa, Prof. Dr. Marcos Antonio de Souza Barrozo, apresentou a Comissão Examinadora e a candidata, agradeceu a presença do público e concedeu à discente a palavra para a exposição do seu trabalho. A duração da apresentação da discente e o tempo de arguição e resposta foram conforme as normas do Programa.

A seguir, o presidente concedeu a palavra, pela ordem sucessivamente aos examinadores, que passaram a arguir a candidata. Ultimada a arguição, que se desenvolveu dentro dos termos regimentais, a Banca, em sessão secreta, atribuiu o resultado final considerando a candidata:

Aprovada

Esta defesa faz parte dos requisitos necessários à obtenção do título de Doutor.

O competente diploma será expedido após cumprimento dos demais requisitos, conforme as normas do Programa, a legislação pertinente e a regulamentação interna da UFU.

Nada mais havendo a tratar foram encerrados os trabalhos. Foi lavrada a presente ata que após lida e achada conforme foi assinada pela Banca Examinadora.

Documento assinado eletronicamente por **Marcos Antonio de Souza Barrozo**, **Professor(a) do Magistério Superior**, em 22/07/2025, às 11:25, conforme horário oficial de Brasília, com fundamento no art. 6º, § 1º, do Decreto nº 8.539, de 8 de outubro de 2015.

Documento assinado eletronicamente por **Ricardo Correa de Santana**, **Professor(a) do Magistério Superior**, em 22/07/2025, às 11:31, conforme horário oficial de Brasília, com fundamento no art. 6º, § 1º, do Decreto nº 8.539, de 8 de outubro de 2015.

Documento assinado eletronicamente por **Elenice Maria Schons Silva**, **Usuário Externo**, em 22/07/2025, às 15:35, conforme horário oficial de Brasília, com fundamento no art. 6º, § 1º, do Decreto nº 8.539, de 8 de outubro de 2015.

Documento assinado eletronicamente por **MARIA DO CARMO FERREIRA**, **Usuário Externo**, em 22/07/2025, às 15:35, conforme horário oficial de Brasília, com fundamento no art. 6º, § 1º, do Decreto nº 8.539, de 8 de outubro de 2015.

Documento assinado eletronicamente por **Michelly dos Santos Oliveira**, **Usuário Externo**, em 22/07/2025, às 15:42, conforme horário oficial de Brasília, com fundamento no art. 6º, § 1º, do Decreto nº 8.539, de 8 de outubro de 2015.

Documento assinado eletronicamente por **João Inácio soletti**, **Usuário Externo**, em 23/07/2025, às 09:42, conforme horário oficial de Brasília, com fundamento no art. 6º, § 1º, do Decreto nº 8.539, de 8 de outubro de 2015.

A autenticidade deste documento pode ser conferida no site https://www.sei.ufu.br/sei/controlador_externo.php?acao=documento_conferir&id_orgao_acesso_externo=0, informando o código verificador **6529226** e o código CRC **86A77C1E**.

"Porque eu sei os planos que tenho para vocês', declara o Senhor, 'planos de prosperá-los e não de causar-lhes dano, planos de dar-lhes esperança e um futuro." (Jr 29:11)

AGRADECIMENTOS

A jornada do doutorado foi intensa, desafiadora e transformadora. Chegar até aqui não foi um caminho solitário, e por isso sou profundamente grata a todas as pessoas que, direta ou indiretamente, fizeram parte dessa conquista.

Agradeço, primeiramente e acima de tudo, a Deus, por me sustentar em todos os momentos, capacitar-me para realizar este trabalho e iluminar meu caminho.

Ao meu marido, pelo apoio inabalável e pela colaboração essencial para que eu pudesse me dedicar ao doutorado. Sem sua compreensão e parceria, essa jornada teria sido ainda mais árdua.

Ao meu filho Levi, que sempre me perguntava se eu já tinha terminado o doutorado e que, mesmo sem saber, foi a maior fonte de força para eu continuar. Seu nascimento no início desta jornada trouxe desafios imensos, mas também uma motivação indescritível para seguir em frente.

À minha mãe e irmã que sempre oraram por mim, mesmo sem compreender totalmente os motivos que me levaram a escolher esse caminho. O amor e a fé de vocês foram uma base firme em minha vida.

À minha amiga Angélica, que foi muito mais do que uma amiga – foi uma verdadeira mentora. Seu apoio, sua orientação e sua presença tornaram essa trajetória mais leve e significativa.

Aos meus orientadores, Professores Doutores Marcos Barrozo e Elenice Schon pela confiança, apoio incondicional e incentivo constante à pesquisa. Sua orientação foi essencial para que este trabalho se concretizasse. Um agradecimento especial ao professor Marquinhos, que não permitiu que eu desistisse. Foi uma honra tê-lo ao meu lado, sempre me incentivando nessa jornada.

Aos meus alunos de iniciação científica, Enrico, Mikael, Julia, Ana Elisa, Filipe e Leandro que contribuíram imensamente para esta pesquisa e me ensinaram tanto ao longo do caminho. Foi uma honra compartilhar conhecimento com vocês. Muito obrigada Julia e Ana Elisa por terem sido meu apoio quando eu mais precisei.

Aos meus amigos do PEQ, Aliny, Denis, Thales, Vanessa, Cliff, Camila, Luiza e Felipe que estiveram ao meu lado desde o mestrado e sempre me apoiaram. Vocês moram no meu coração e fazem parte desta conquista.

A todas as pessoas que, de alguma forma, colaboraram para que eu pudesse concluir esta etapa – desde aqueles que cuidaram do Levi para que eu pudesse estar no laboratório até

os que estiveram do meu lado durante as análises e experimentos. Cada gesto de apoio foi fundamental.

Meus sinceros agradecimentos aos técnicos, Rafael, Ulisses e Cristiane, e colegas do Laboratório de Sistemas Particulados da FEQUI-UFU, que forma imprescindíveis e tiveram um papel essencial nesse processo.

O doutorado foi mais do que um aprendizado acadêmico – foi um processo de crescimento pessoal e emocional. Aprendi que o conhecimento é desafiador, mas também libertador. Espero poder contribuir para a formação de futuros pesquisadores e que, de alguma forma, eu tenha inspirado aqueles ao meu redor a não desistirem dos seus sonhos, mesmo quando tudo parece apontar o contrário.

A todos vocês, o meu mais sincero e profundo agradecimento.

TABLE OF CONTENTS:

LIST OF FIGURES:

LIST OF TABLES:

LIST OF SYMBOLS

d_{50}	Diameter of 50% of the particle distribution size
d	Particle diameter
d_b	Bubble diameter
Ec	Collision efficiency
M_c	Mass of the concentrate
M_F	Mass of the feed
p	Parameter p of sigmoide model
P_a	Attachment probability
P_c	Collision probability
P_{Coll}	Collection probability
P_d	Detachment probability
R	Recovery of apatite
R^2	Model parameter
Re	Reynolds number
RI	Response index
SR_{Fe2O3}	Selectivity ratio of Fe_2O_3
SR_{SiO2}	Selectivity ratio of SiO_2
$x_{ap,c}$	Calcium oxide grade in the concentrate
$x_{ap,F}$	Calcium oxide grade in the feed
x_1	Collector dosage
x_2	Depressant dosage
x_3	Type of collector
x_4	pH
x_5	Solid concentration during conditioning
x_6	Dispersant dosage
y_g	P_2O_5 grade in concentrate of empirical equation
y_r	Apatite recovery in concentrate of empirical equation

ABSTRACT

Phosphorus, primarily sourced from phosphate ore deposits, is vital for industry and agriculture. The depletion of high-grade ores has necessitated the processing of lower-grade deposits, leading to the production of fine (10-50 μm) and ultrafine (<10 μm) particles, which pose significant beneficiation challenges. In Brazil, phosphate reserves are predominantly of igneous origin, with apatite as the principal phosphate mineral. Moreover, the froth flotation remains the most effective technique for apatite concentration; however, its efficiency declines for fine and ultrafine particles due to poor particle-bubble interactions, a persistent challenge in tailings processing. This study investigates the selective flotation of apatite from tailings generated during phosphate ore processing, focusing on optimizing flotation conditions to improve recovery and grade. Batch flotation tests in laboratory cells and column flotation were conducted to evaluate six key flotation variables: collector type and dosage, depressant dosage, pH, solid concentration during conditioning, and dispersant dosage. The results revealed that rice oil soap was a more effective collector than Agem A3 (vegetable fatty acid mixture) for both fine and ultrafine tailings flotation. For fine ore (d_{32}= 17.98 μm) flotation, a combination of high-intensity conditioning (HIC) and column flotation, under optimized conditions of 51.78% conditioning solid concentration, 474.13 ppm collector dosage, 346.63 ppm depressant, pH 10.18, and no dispersant, achieved a P_2O_5 grade of 34.82% and 92.16% apatite recovery. For ultrafine apatite (d_{32}=2.43 μm) flotation, cell flotation tests revealed limitations, as none of the tested conditions simultaneously met the required P_2O_5 grade and minimum apatite recovery. However, optimization via HIC followed by column flotation, with 40% solid concentration during conditioning, 52.83 ppm collector, 711.31 ppm depressant, pH 12, and 250 ppm sodium silicate dispersant, achieved a P_2O_5 grade of 26.10% and 43.94% recovery, demonstrating that even ultrafine particles can be successfully processed without desliming. These findings highlight the importance of precise reagent dosage, control of solid concentration during conditioning, pH regulation and the effectiveness of HIC in enhancing particle-bubble interactions, thereby enabling improved apatite recovery from challenging fine and ultrafine tailings. This study contributes to more sustainable and efficient phosphate beneficiation practices.

Key words: Froth flotation, Fine particles, Ultrafine particles, Tailings

RESUMO

O fósforo, proveniente principalmente de minério fosfático, é vital para indústria e agricultura. O esgotamento de minérios de alto teor exigiu o processamento de depósitos de menor teor, levando à produção de partículas finas (10-50 μm) e ultrafinas (<10 μm), que representam desafios significativos de beneficiamento. No Brasil, as reservas de fosfato são predominantemente de origem ígnea, sendo a apatita o principal mineral de fosfato. E a flotação por espuma continua sendo a técnica mais eficaz para a concentração de apatita; no entanto, sua eficiência diminui para partículas finas e ultrafinas devido às interações ruins entre bolhas e partículas, um desafio persistente no processamento de rejeitos. Este estudo investiga a flotação seletiva de apatita de rejeitos gerados durante o processamento de minério de fosfato, com foco na otimização das condições de flotação para melhorar a recuperação e o teor. Foram realizados testes de flotação em batelada utilizando células e colunas de flotação para avaliar seis variáveis principais de flotação: tipo de coletor, dosagem de coletor, dosagem de depressor, pH, concentração de sólidos durante o condicionamento e dosagem do dispersante. Os resultados revelaram que o óleo de arroz saponificado foi um coletor mais eficaz do que o Agem A3 (mistura de ácidos graxos vegetais) para a flotação de rejeitos finos e ultrafinos. Para a flotação de minério fino (d_{32}= 17,98 μm), condições otimizadas envolvendo a combinação do condicionamento de alta intensidade (CAI) e a flotação em coluna, sob condições de 51,78% de concentração de sólidos durante o condicionamento, 474,13 ppm de dosagem de coletor, 356,63 ppm de depressor, pH 10,18 e nenhum dispersante, atingiu um teor de P_2O_5 de 34,82% e 92,16% de recuperação de apatita. Para a flotação do minério fino (d_{32}=2,43 μm), os testes de flotação em célula revelaram limitações, pois nenhuma das condições testadas atendeu simultaneamente ao teor de P_2O_5 exigido e à recuperação mínima de apatita. No entanto, o emprego de CAI seguido de flotação em coluna, com as condições otimizadas de 40% de concentração de sólidos durante o condicionamento, 52,83 ppm de coletor, 711,31 ppm de depressor, pH 12 e 250 ppm de dispersante de silicato de sódio, alcançou um teor de P_2O_5 de 26,10% e 43,94% de recuperação. Esses resultados destacam a importância da dosagem precisa de reagentes, do controle da concentração de sólidos durante o condicionamento, da regulação do pH e da eficácia do CAI no aprimoramento das interações bolha-partícula, possibilitando, assim, uma melhor recuperação de apatita a partir de rejeitos finos e ultrafinos desafiadores. Este estudo contribui para práticas de beneficiamento de fosfato mais sustentáveis e eficientes.

Palavras-chave: Flotação em espuma, Partículas finas, Partículas ultrafinas, Rejeito

1. INTRODUCTION

Phosphorus (P) is a vital element derived from phosphate ore reservoirs, playing a critical role in agriculture, industry, and various technological applications. Phosphate ores are primarily sourced from two geological formations: sedimentary and igneous deposits. In Brazil, most phosphate ore deposits are of igneous origin, with apatite being the predominant phosphate mineral. The quality of these deposits is commonly expressed in terms of phosphorus pentoxide (P_2O_5) grade, which indicates the concentration of phosphorus available for apatite beneficiation and subsequent use (SANTANA *et al.*, 2011; VALDERRAMA *et al*., 2024).

With the increasing global demand for phosphorus and the depletion of high-grade ore deposits, the need to process low-grade ores has become more pressing. These ores often require more complex concentration techniques to achieve viable recovery rates. As a result, significant research has focused on developing efficient beneficiation methods for low-grade phosphate ores and their tailings, particularly for fine (10-50 μm) and ultrafine (<10 μm) particles. The generation of mineral fines arises from multiple sources, with a substantial portion produced during grinding to achieve adequate particle liberation. In other cases, extremely fine grinding is necessary due to declining ore grades and the increasing complexity of ore bodies (RUBIO *et al*., 2007).

Froth flotation is the most widely employed method for concentrating apatite and plays a fundamental role in phosphate beneficiation. This process operates in three phases: solid, liquid, and gas, where the target mineral, suspended in water, undergoes selective surface modification through chemical reagents (ALSAFASFEH; ALAGHA, 2017). Apatite, like most minerals, is naturally hydrophilic, meaning it has an affinity for water and does not spontaneously attach to air bubbles. To enable flotation, collectors are introduced to adsorb onto the apatite surface, altering its wettability and inducing hydrophobicity, which makes particle-bubble attachment possible. Simultaneously, depressants are added to maintain the hydrophilicity of gangue minerals, preventing their flotation. When air is dispersed into the system, hydrophobic apatite particles adhere to air bubbles, forming stable aggregates that rise to the surface and accumulate as froth, which is then collected as the concentrate. Meanwhile, hydrophilic gangue particles remain in the aqueous phase and are removed as tailings. The efficiency of this process depends on optimizing the balance between hydrophobicity induction and gangue suppression to maximize apatite recovery while minimizing impurities (BULATOVIC, 2007; KUPKA; RUDOLPH, 2018).

Despite its effectiveness, flotation performance declines significantly when applied to fine and ultrafine particles due to challenges in particle-bubble interactions. The recovery of these particles is hindered by their inherent physical properties, such as low mass, limited momentum, and high interfacial free energy. These characteristics reduce the probability of particle-bubble collision and attachment, promote the formation of overly stable froths, and result in slow flotation kinetics. Additionally, conventional flotation machines generate coarse bubbles that are less effective at capturing fine particles, further limiting recovery. Consequently, a significant portion of fine minerals is often discarded as slimes prior to flotation due to the absence of efficient recovery methods (CAPPONI *et al.*, 2023).

The efficiency and selectivity of the flotation process are strongly influenced by particle-bubble interactions, which involve hydrodynamic and kinetic phenomena. These interactions occur in three stages: collision, adhesion, and the formation of particle-bubble aggregate, with adhesion being the most critical for successful separation (CHENG *et al.,* 2017). Optimizing flotation conditions, such as reagent dosage, bubble size, and hydrodynamic conditions, is fundamental to improving recovery rates (REIS, 2019). Additionally, phosphate tailings generated from beneficiation plants represent a valuable secondary resource. Through appropriate flotation techniques, these tailings can be reprocessed to recover residual apatite, producing concentrates suitable for fertilizer production. Enhancing resource utilization while minimizing environmental impact contributes to a more sustainable and efficient phosphate processing industry (ALSAFASFEH *et al.*, 2022).

A common strategy for recovering fine and ultrafine phosphate from slimes involves removing ultrafine particles from the flotation feed to minimize their negative impact on performance. This is typically achieved through desliming, which enhances phosphate recovery and prevents slime coating, a phenomenon that interferes with flotation (MATIOLO *et al.*, 2019). Froth flotation, the primary method for phosphate recovery, exploits differences in the physicochemical properties of apatite and gangue minerals. In general, apatite is recovered via direct flotation using fatty acid collectors, while starches act as depressants to selectively separate it from the ore (SEVEROV; FILIPPOVA; FILIPPOV, 2022).

To enhance the flotation of fine and ultrafine particles, recent research has explored advanced techniques and novel reagents. Capponi *et al.* (2023) demonstrated that micro- and nanobubbles in column flotation improve recovery by promoting bubble attachment and separation efficiency. Zhao and Zhang (2024) investigated hydrophobic agglomeration, showing that oleic acid significantly increased apatite particle size and slurry viscosity, enhancing flotation performance. Zhang *et al.* (2024) found that interfacial nanobubbles (INBs)

on hydrophobic surfaces improve particle-bubble interactions, leading to better flotation recovery and selectivity for microfine particles. Alsafasfeh and Alagha (2017) explored upgrading P_2O_5 content in tailings from a phosphorus production plant using direct froth flotation. By optimizing pulp density, pH, and flotation time, they increased the P_2O_5 grade from 21.57% to 28.4%, achieving a recovery rate above 73%. The study also highlighted the crucial role of sodium silicate as a dispersant in flotation performance.

Despite advanced flotation techniques, recovering fine and ultrafine particles remains a significant challenge, especially in processes that do not include desliming. Understanding the behavior of ultrafine apatite particles is crucial, as their recovery is still not well understood, and existing techniques often fail to meet industrial standards. Optimizing flotation conditions is essential, as fine particles must reach a P_2O_5 grade of at least 30% with over 60% apatite recovery, while ultrafine particles require a minimum P_2O_5 grade of 24% and at least 40% recovery (ALSAFASFEH; ALAGHA, 2017; OLIVEIRA *et al.*, 2011; REIS *et al.*, 2023; VALDERRAMA *et al.*, 2024).

To contextualize the evolution of research on the flotation of fine and ultrafine apatite particles, Figure 1 presents a timeline outlining the principal advances from 2003 to 2021 by the Particulate Systems Laboratory (PSL) at the Federal University of Uberlândia (UFU). This chronology illustrates the increasing academic interest in refining operational parameters, developing innovative reagents, and understanding the physicochemical mechanisms governing the selective recovery of these particles under various flotation configurations. It is important to note, however, that none of these investigations specifically focused on the recovery of fine and ultrafine apatite particles originating from tailings.

Figure 1.1 - Timeline of the principlam advances in apatite flotation from 2003 to 2021 by PSL at UFU.

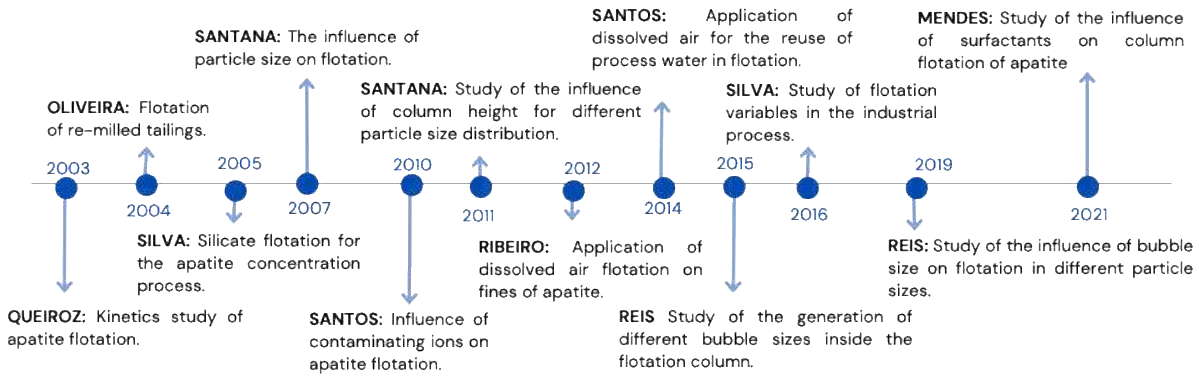

Source: Author (2025).

The aim of this study was to achieve selective flotation of apatite from fine and ultrafine tailings generated during phosphate ore processing. To this end, batch flotation tests in a laboratory cell and column flotation were conducted to systematically investigate and optimize the froth flotation process for the selective recovery of apatite. The study focuses on six key flotation variables: collector type and dosage, depressant dosage, pH, solid concentration during conditioning, and dispersant dosage. This study is driven by the imperative to recover valuable minerals from these tailings, which have already undergone initial extraction and comminution, and explores their potential as a significant secondary resource. By minimizing tailings accumulation, reducing environmental impacts, and maximizing resource utilization, this research aims to promote sustainable practices within the phosphate sector. Furthermore, integrating mineral recovery with environmental stewardship can reduce operational costs compared to primary ore processing, enhancing the economic viability of beneficiation. The findings of this study are expected to enhance the understanding of fine and ultrafine phosphate recovery processes, contributing to more sustainable and economically viable exploitation of phosphate resources.

2. LITERATURE REVIEW

2.1. Phosphate ore

Phosphorus is an indispensable and non-renewable element that plays a critical role in sustaining plant and animal life. It is a primary component in the production of fertilizers, which are essential for global agricultural productivity (OLIVEIRA *et al*., 2011). Phosphorus actively participates in key biological processes, including photosynthesis, energy transfer for sugar metabolism, cell division, and nutrient transportation (LAPIDO-LOUREIRO; MELAMED, 2006). As a result, agriculture is the primary driver of phosphorus demand, with global consumption increasing significantly over the decades. For instance, Figures 2.1 and 2.2 illustrate, global consumption of P_2O_5 reached 44106 kt in 2022, while Brazil consumption reached 5809 kt in the same year (IFA, 2019). This trend underscores the importance of ensuring a sustainable supply of phosphate resources to meet the escalating demand.

Figure 2.1 - Consumption of P_2O_5 in the world along the years

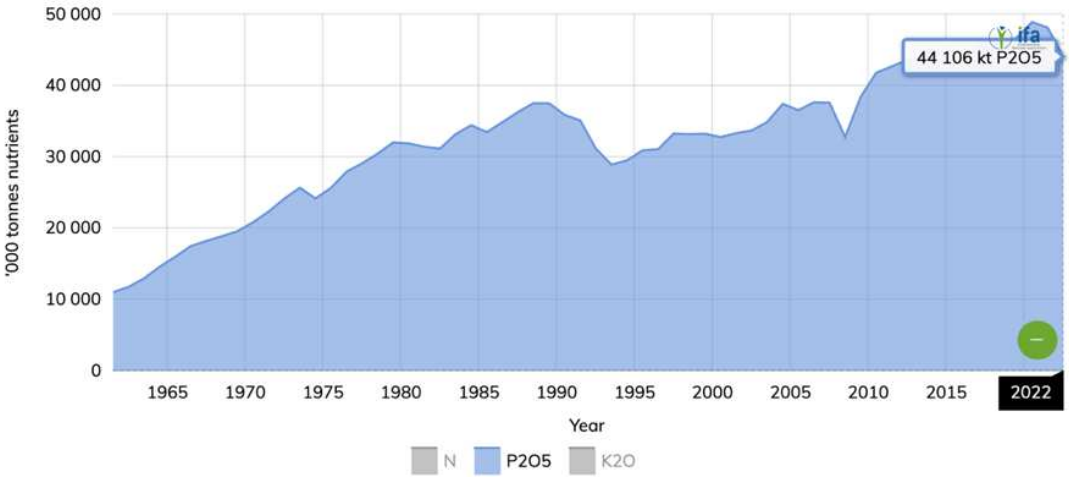

Source: IFA (2019).

Phosphate deposits are classified into five main categories: marine sedimentary, igneous, metamorphic, weathering sedimentary, and biogenic. In Brazil, phosphate ores are predominantly extracted from igneous deposits. However, many of these deposits are low-grade, necessitating beneficiation processes to render them economically viable. The development of advanced technologies for the efficient extraction and processing of phosphate ores is, therefore, crucial to maximize resource utilization and ensure long-term availability (DERHY *et al*., 2020).

Figure 2.2 - Consumption of P_2O_5 in Brazil along the years

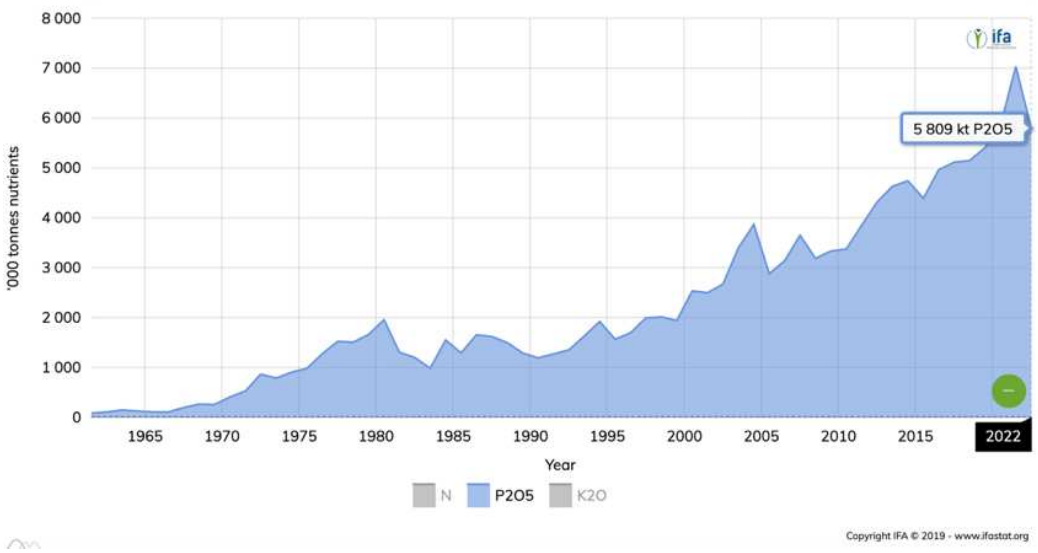

Source: IFA (2019).

Brazil has made substantial investments in the exploration and development of phosphate ores to reduce its dependence on imported fertilizers and address the increasing demand for phosphate-based agricultural inputs. Despite these initiatives, the country has not yet attained self-sufficiency in phosphate production, remaining reliant on external sources to meet its agricultural needs (BENÍCIO, 2022). This fact shows the critical importance of advancing research and innovation to optimize the utilization of Brazil's phosphate reserves. Given the challenges associated with low-grade ores and the need for sustainable practices, the focus on improving flotation techniques for fine and ultrafine apatite particles from tailings becomes increasingly relevant.

2.2. Apatite

Apatite is a group of phosphate minerals widely distributed in the Earth's crust and serves as the primary source of phosphorus for fertilizer production. Despite its abundance, apatite often occurs in low-grade ores or as fine and ultrafine particles, which pose significant challenges for processing due to their complex mineralogy and small particle size (DONG *et al.,* 2021). The mineralogical composition of apatite deposits varies considerably depending on their geological origin. In magmatic or igneous deposits, fluorapatite and hydroxyapatite are predominant, while chloroapatite is less common. In contrast, sedimentary deposits are typically characterized by the presence of carbonate-fluorapatite (francolite) and carbonapatite

(CHULA, 2004). In Brazil, apatite deposits are primarily of igneous origin, with compositions often consisting of a mixture of hydroxyapatite and fluorapatite, accompanied by significant amounts of carbonate-fluorapatite and carbonateapatite (RAMOS, 2018).

The general chemical formula of apatite is $M_{10}(XO_4)_6Z_2$, where M represents alkaline cations (e.g., Ca, Pb, Sr, Na, Mg, Mn, or rare earth elements), X represents trivalent anions (e.g., P, As, V, S, C, or Si), and Z represents monovalent anions (e.g., F, Cl, OH, or Br) (OLIVEIRA, 2007). This structural flexibility allows for extensive ion substitution, leading to a diverse range of apatite types, such as fluorapatite, chloroapatite, and hydroxyapatite, which are distinguished by their dominant anions (F^-, Cl^-, or OH^-, respectively). Additionally, cations such as calcium (Ca^{2+}), manganese (Mn^{2+}), sodium (Na^+), and strontium (Sr^{2+}), as well as anions such as phosphate (PO_4^{3-}), sulfate (SO_4^{2-}), and carbonate (CO_3^{2-}), can be substituted within the crystal lattice. These substitutions are influenced by the mineral's formation environment and the need for charge compensation, resulting in variations in physical and chemical properties (LIU; ZHANG; LI, 2019; SANTANA *et al*., 2011).

The mineralogical complexity of Brazilian apatite deposits necessitates extensive beneficiation to reduce the presence of gangue minerals, such as carbonates and silicates, and to produce high-quality phosphate concentrates suitable for industrial applications (AVELAR, 2018). The low phosphorus content (typically 5-15% P_2O_5) and high carbonate content in these ores further complicate processing, requiring advanced technologies to achieve market-grade specifications (SILVA *et al.,* 2017). Efficient beneficiation methods, particularly for fine and ultrafine particles, are essential to improve recovery rates and concentrate quality, thereby enhancing the economic viability of these resources (LIU; ZHANG; LI, 2019).

Apatite is characterized by its hexagonal crystal system, imperfect cleavage, Mohs hardness of 5, and density ranging from 3.1 to 3.2 g/cm³. It exhibits a vitreous to sub resinous luster and can appear in various colors, including blue, green, brown, violet, or colorless (MARTINS, 2009; RAMOS, 2018). The term "apatite" originates from the Greek word meaning "to deceive" reflecting its historical misidentification with minerals such as tourmaline or beryl (GOUVEIA, 2008). Apatite can form through primary or secondary processes. Primary apatites, associated with high-temperature igneous environments, include fluorapatite, hydroxyapatite, and chloroapatite. Secondary apatites, formed through physicochemical alterations, are typically found in sedimentary deposits and include carbonate-fluorapatite and carbonatohidroxiapatite (RAMOS, 2018).

The surface properties of apatite can vary significantly due to the diverse geological conditions under which it forms. This variability, coupled with the presence of contaminants,

poses a major challenge for the phosphate industry, which must meet stringent market specifications (e.g., 30% apatite content for fines and 24% apatite content for ultrafines and slimes) after beneficiation (ALSAFASFEH; ALAGHA, 2017; LIU; ZHANG; LI, 2019; SANTANA *et al*., 2011). Consequently, ongoing research and innovation in concentration methods are critical to improving the efficiency and sustainability of phosphate ore processing.

2.3. Concentration of apatite

Phosphate ores are rarely found in a state suitable for direct industrial use, necessitating beneficiation for effective utilization. This process involves a series of unit operations aimed at separating valuable phosphate minerals from gangue. The selection of an appropriate separation technique is influenced by particle size and specific physicochemical properties, as heterogeneous solid mixtures demand advanced methods based on factors such as density, magnetism, particle shape, surface charge, radioactivity, or surface chemistry (LEJA, 1982; LIU *et al.,* 2020; PERES; ARAUJO, 2013).

Apatite concentration may present significant challenges due to its complex mineralogy, particularly when derived from igneous sources, where the inherently fine and ultrafine particle size distribution further complicates the beneficiation process. Apatite deposits are often associated with gangue minerals, such as carbonates and silicates, which further complicate the separation process. Effective beneficiation necessitates both the physical liberation of apatite and the manipulation of surface properties to achieve selective separation. In phosphate rock processing, the ore is first subjected to comminution through crushing, followed by size classification via screening. Further milling is employed to reduce particle size, ensuring effective liberation of apatite from gangue minerals. Once physical liberation is achieved, wet magnetic separation is utilized to remove magnetite, thereby improving the purity of the feed (SANTANA, 2011; SILVA, 2016).

Following magnetic separation, desliming is performed to remove fine and ultrafine particles, generally smaller than 37 μm to 10 μm, respectively, depending on the specific process (MATIOLO *et al*., 2017). This step is critical for optimizing flotation efficiency, as ultrafine particles can reduce selectivity and elevate reagent consumption, and elevate pulp viscosity due to slime coatings, which may also over-stabilize the froth (AHMED, 2007; FARROKHPAY; FILLIPOV; FORNASIERO, 2020). By removing slimes from the flotation feed, the process enhances reagent selectivity and mitigates froth stability issues, leading to improved overall flotation performance (MATIOLO *et al.,* 2017).

After desliming, the larger particles are directed to flotation, while the resulting slimes are commonly deposited in tailings ponds. These slimes represent a significant waste of potential resources, as they contain appreciable amounts of recoverable apatite - a non-renewable mineral resource - highlighting an important opportunity for their beneficial reuse. This practice, however, leads to significant environmental repercussions, as the accumulation of vast amounts of mining waste within dams situated close to mining operations poses risks to neighboring communities. This issue is further exacerbated by increasing raw material consumption and the limited availability of effective solutions for managing mining waste (DABBEBI; PERUMAL; MOUKANNAA, 2023).

To achieve selective separation during flotation, the slurry undergoes conditioning, where reagents are added to alter the surface properties of minerals, enhancing selectivity. Froth flotation, a versatile and selective method, is the most widely used technique for concentrating apatite, particularly fine particles (LIU; ZHANG; LI, 2019; SANTANA *et al*., 2011). In Brazilian phosphate processing facilities, a two-stage flotation process is commonly used after desliming, first floating barite and then apatite (MATIOLO *et al.,* 2017).

In general, the recovery of fine and ultrafine phosphate ore involves desliming using hydro-cyclones to remove particles smaller than 10 μm, followed by flotation. Matiolo *et al.* (2019) investigated the effectiveness of various flotation circuits and column sizes for enhancing phosphate recovery from slimes. In their study, samples were deslimed, yielding an underflow with a d_{50} of 18 μm and a P_2O_5 grade of 16% for both samples, which were then subjected to conditioning and flotation. The optimal results achieved were 54% recovery and a P_2O_5 grade of 35%.

An alternative strategy is flotation without prior desliming, utilizing Jameson Cell or column flotation. Teague and Lollback (2012) demonstrated that this approach enables the beneficiation of ultrafine phosphate particles from Paradise South and Dtree ore smaller than 20 μm, conditioning at 35% solid concentration achieving 32% of P_2O_5 grade and recovery rates of up to 80% using Jameson Cells. This method effectively concentrates phosphate from the feed without the need for desliming, providing a viable solution for ultrafine particle recovery.

The primary objective of phosphate rock beneficiation is to produce a final concentrate with a P_2O_5 content exceeding 30% and apatite recovery of up to 60% for fine particles. For ultrafine particles, the target is a P_2O_5 grade of at least 24% with apatite recovery of up to 40%. Achieving these targets is challenging due to the complex mineralogy of these particle sizes of

apatite deposits, requiring precise control of each beneficiation stage (ALSAFASFEH; ALAGHA, 2017; OLIVEIRA *et al.*, 2011; VALDERRAMA *et al.,* 2024).

2.4. Principles of flotation

Froth flotation, developed over a century ago, remains one of the most effective separation techniques based on differences in mineral surface properties. It is particularly significant in mineral processing, as it enables the recovery of valuable minerals from low-grade ores, establishing itself as a fundamental beneficiation method (HADLER; AKTAS; CILLIERS*,* 2005; TAO, 2005). As a widely applied concentration and purification technique, froth flotation operates within a solid-liquid-gas triphasic system, where interfacial properties govern the separation process. The effectiveness of this method relies on a complex interplay of chemical, physicochemical, and physical phenomena occurring within the liberated system (BULATOVIC, 2007).

During comminution, the initial stage in mineral processing, the rupture of both structural and chemical bonds leads to the creation of high-energy, polar surfaces. Conversely, weaker bonds, such as Van der Waals forces, when disrupted, result in low-energy, non-polar surfaces. Minerals naturally exhibit either hydrophilic (water-attracting, polar) or hydrophobic (water-repelling, non-polar) behavior due to their intrinsic electrical properties. This hydrophobicity, quantified by wettability, dictates the stability of interfaces within the solid-liquid and liquid-gas phases. Hydrophilic particles try to minimize their free energy by forming stable interfacial interactions with water molecules, whereas hydrophobic particles possessing lower free energy, may form stable interactions that preferentially associate with air (SILVA, 2016; VERAS, 2010).

In the direct flotation process, selectivity arises from variations in mineral hydrophobicity, either inherent or induced by chemical reagents. Most minerals are naturally hydrophilic; however, during conditioning, specific reagents can modify their surface properties, hindering the collector adsorption on gangue mineral while rendering valuable minerals hydrophobic to facilitate their attachment to air bubbles (BULATOVIC, 2007; KUPKA; RUDOLPH, 2017). This process occurs in a continuously agitated tank, where depressant suppress gangue particles by hindering the collector adsorption, while collectors render target minerals hydrophobic, promoting the formation of stable particle-bubble aggregates (REIS, 2019).

In addition to modifying surface properties, interactions between phases in the pulp and the adsorption of reagents significantly impact critical phenomena such as hydration, dissociation, and adsorption at various system interfaces. Collectors, for instance, serve a dual function: they modify the hydrophobicity of mineral surfaces to facilitate particle-bubble attachment and, in certain cases, act as frothers when selectively adsorbed at the gas-liquid interface, thereby affecting flotation efficiency. Among these processes, reagent adhesion onto particles surface is the most critical, as it directly determines the success of particle-bubble attachment and, consequently, the overall effectiveness of the separation process (CHAVES; LEAL FILHO; BRAGA, 2010).

Adsorption can occur at gas-solid and liquid-solid interfaces and is classified as either physical or chemical, depending on the nature of the adsorbent-adsorbate interactions. Physical adsorption is governed by van der Waals forces, leads to multilayer structures and contributes to phenomena such as mineral surface oxidation. In contrast, chemical adsorption is responsible for induced hydrophobization, altering mineral wettability. This process involves strong interaction, such as ionic bonds, polar covalent bonds, and hydrogen bonds, typically forming monolayers (SANTANA, 2011).

Furthermore, adsorption can be categorized as specific or nonspecific. Nonspecific adsorption is characterized by purely electrostatic interactions between the adsorbate and adsorbent, making it a rapid and reversible process that does not alter the mineral's original surface charge. In contrast, specific adsorption is predominantly governed by mechanisms independent of electrostatic attraction, such as covalent bonding, van der Waals interactions, or hydrogen bonding. This process is typically slow and irreversible, and adsorbed ions can increase, decrease, neutralize, or reverse the electrical charge of the mineral surface (CARVALHO, 2003). Understanding these adsorption mechanisms is crucial for adjust reagent selection and conditioning strategies in ultrafine apatite flotation.

Flotation is inherently complex, as it involves three interacting phases: solid (ore particles), liquid (aqueous solution), and gas (air bubbles). Its complexity arises from the integration of multiple physicochemical phenomena and subprocesses, some of which are not yet fully understood. Among these, the particle-bubble interactions are fundamental, as it dictates the selective separation of hydrophobic particles from hydrophilic ones. Only hydrophobic particles can attach to air bubbles and be carried to the surface by the rising bubbles. This attachment results from a dynamic interplay of physicochemical and hydrodynamic factors within a system composed of solid particles, air bubbles, and an aqueous solution containing chemical reagents (BRABCOVÁ *et al.,* 2014; NGUYEN; EVANS, 2004).

The interaction between particles and bubbles is the most critical factor in the flotation process. Therefore, understanding the underlying subprocesses is essential to achieve optimal recovery of the target mineral. The primary subprocesses include (SANTOS, 2010):

- True flotation, characterized by the selective collision and attachment of particles to air bubbles;
- Hydrodynamic entrainment, where particles are carried into the froth zone by upward flow of water;
- Physical entrapment, in which particles become mechanically trapped within particle-bubble aggregates.

The adhesion of mineral particles to air bubbles is the primary mechanism driving particle recovery in flotation, as it enables the majority of valuable minerals to be collected in the concentrate (NGUYEN; EVANS, 2004). While true flotation, a chemically selective process based on surface properties, is the dominant mechanism for separating valuable minerals from gangue, the overall separation efficiency is also influenced by entrainment and entrapment. Unlike true flotation, these non-selective mechanisms can lead to the recovery of both gangue and valuable minerals. Hydrodynamic entrainment, mechanical entrapment, and slime coating (where ultrafine slimes adhere to particle surfaces) are key factors that can affect concentrate quality and process performance. In industrial practice, entrainment is a common subprocess, often necessitating multiple flotation stages, known as circuits, to achieve an economically acceptable concentrate quality (SANTOS, 2010). Figure 2.3 illustrates the mechanisms involved in particle recovery.

Figure 2.3 - Recovery mechanisms

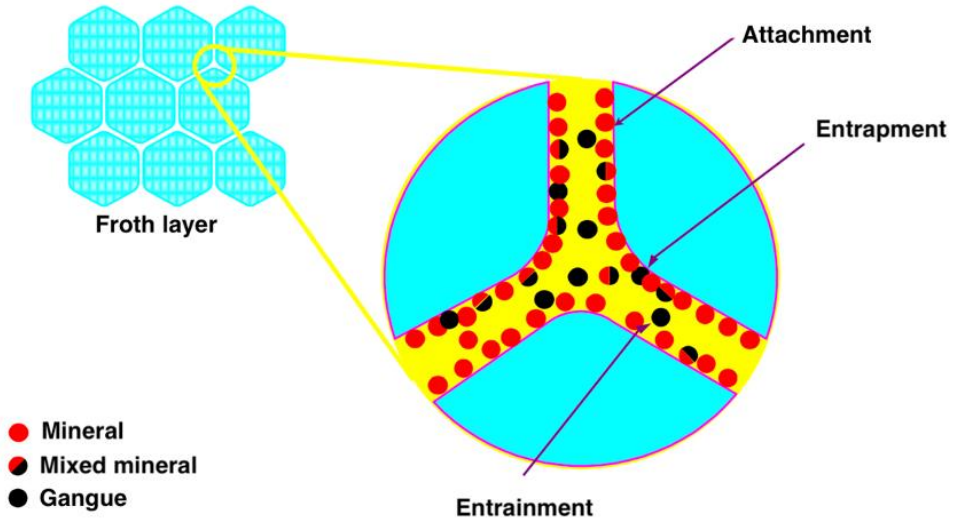

Source: Capponi (2009) apud Santos (2010).

Particle-bubble interaction is a fundamental mechanism governing the selectivity and efficiency of froth flotation (CHENG *et al.,* 2017). The selectivity of the flotation process can be quantified by the particle-bubble collection probability (P_{coll}), which is determined by three subprocess: collision (P_c), attachment (P_a) and detachment (P_d). These subprocesses are mathematically represented by Equation 1 (COLLINS; JAMESON, 1976; WANG; LIU, 2021).

$$P_{coll} = P_{c.}P_{a.}(1 - P_d) \quad (1)$$

It is well-stablished that particles of different sizes exhibit different flotation behavior (SANTANA *et al.,* 2012). Collision occurs when a particle approaches a bubble due to liquid flow and relative motion between them. When the particle and the bubble are sufficiently close, physicochemical interactions begin. Since collision is a nonselective process, it is influenced by physical factors such as particle and bubble size, particle and liquid density, viscosity, and hydrodynamic conditions, including shear force, gravitational force, inertia, momentum, diffusion, Brownian motion, turbulence and others (REIS, 2019). The probability collision efficiency is quantified according to Yoon-Luttrell model which is affected specially by bubble and particle size as described in Equation 2 (JIANG *et al.,* 2025).

$$Ec = \left(\frac{\mathrm{d}}{d_b}\right)^2 \left(\frac{3}{2} + \frac{4Re^{0.72}}{15}\right) \quad (2)$$

In this equation, the collision efficiency (Ec) depends on the particle diameter (d), bubble diameter (d_b), Reynolds number (Re) of the bubble. Collision efficiency decreases with decreasing particle size and increasing bubble size (JIANG *et al.,* 2025). Figure 2.4 illustrates the trajectories of particles near an ascending bubble, which vary depending on their size and density relative to the surrounding liquid. Particles with a density close to that of the liquid typically follow two main trajectories: they either adhere to the flow lines around the bubble (Trajectory 1) or collide through interception. In contrast, colloidal particles may deviate from these trajectories due to Brownian motion (Trajectory 2). When inertial forces dominate, particles slightly deviate from the flow lines (Trajectory 3). Intermediate and coarse particles, particularly those with higher density, possess sufficient inertia to penetrate the flow lines and collide directly with the bubble surface, a process known as inertial collision (Trajectory 4). Additionally, the critical flow line describes a scenario where a particle, propelled by its momentum, only grazes the bubble's surface without making contact (Trajectory 5). Therefore,

particles located within the critical radius (Rc) are expected to collide with the bubble (CAPPONI, 2005).

The critical flow line (limit trajectory) is the path along which a particle moves while merely grazing the bubble's surface without making actual contact. It is assumed that all particles positioned within this critical radius will collide with the bubble's surface. Consequently, the probability of collision is determined by the relative momentum between particles and bubbles, which is governed by factors such as shear force, gravitational force, inertia, and momentum (for coarse and intermediate-sized particles) or diffusion and Brownian motion (for fine and ultrafine particles) (CAPPONI, 2005).

Figure 2.4 - Collision and attachment of a particle whithin the critical radius (Rc) and particles trajectory varying size and density, (1) non-inertia, (2) Brownian, (3) weak inertia, (4) strong inertia, (5) flux line

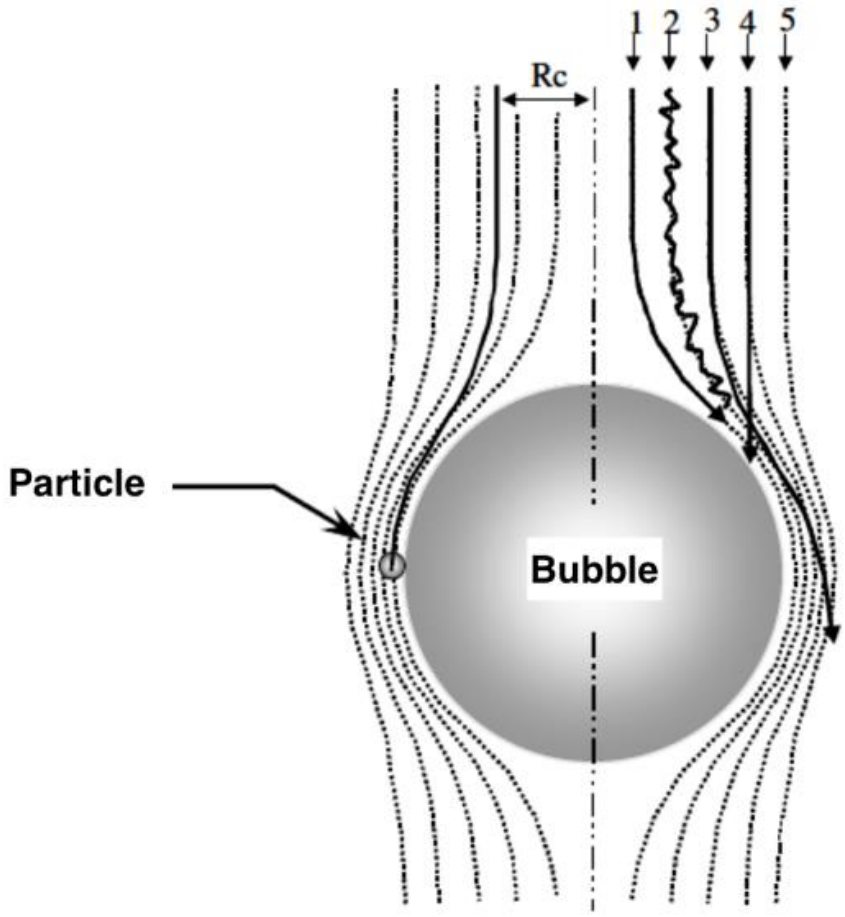

Source: Capponi (2005).

After colliding with the bubble, the particle may slide along its surface through a liquid film, which may result in attachment. However, not all collisions result in attachment. For fine

and ultrafine particles, this process is strongly influenced by the surface properties of the mineral and the adsorption of collectors on their surfaces. Since most minerals are inherently hydrophilic, only those that have been rendered hydrophobic can attach to air bubbles and float. Unlike larger particles, the attachment of fine and ultrafine particles is less affected by hydrodynamic forces and is predominantly governed by surfaces forces (CHENG *et al.,* 2017; MONTE; PERES, 2010; SANTANA, 2011).

The attachment process occurs in three stages: first, the thinning of the intervening water film between a bubble and a particle; second, the rupture of this film and the specific formation of solid-liquid-gas phase contact; and finally, the stabilization of the wetting perimeter as it expands and relaxes from a critical radius, leading to the establishment of the three-phase contact line (NGUYEN; EVANS, 2004).

Attachment in flotation typically occurs when the induction time is shorter than the contact time. The induction time is the time required for a particle and bubble to rupture the thin liquid film separating them, while the contact time between a bubble and a particle comprises two components: the impact time and the sliding time. For fine, ultrafine or low-density particles, however, the impact time is considerably reduced due to the absence of rebound, making the sliding time the dominant factor in the overall contact time. Two critical factors that influence induction time and, by extension, the frequency of attachment are particle size and surface hydrophobicity. Research has shown that induction time decreases with smaller particle sizes and higher contact angles (DAI; FORNASIERO; RALSTON*,* 1999; HEWITT; FORNASIERO; RALSTON*,* 1995).

Attachment probability increases significantly with particle size below 20 μm, which is attributed to the extended sliding time of fine particles around the bubble surface (DOBBY; FINCH, 1987). As a result, fine particles tend to exhibit higher attachment efficiencies compared to coarse particles, even when their induction times are longer. Despite high adhesion potential, the system's low collision probability fundamentally limits selectivity in fine particle flotation, creating a persistent challenge that demands novel approaches for enhanced separation efficiency (WANG; LIU, 2021).

One approach to enhance flotation efficiency is to increase the stirring speed during condition stage, which can improve the attachment probability of particles to bubbles. This is due to the higher probability of collisions for strongly hydrophobic particles under increased agitation (ZHENG *et al.,* 2024). Furthermore, studies by Dai, Fornasiero, Ralston (1999) have demonstrated that smaller bubbles exhibit a greater attachment probability compared to larger bubbles. This is attributed to their faster drainage rates and shorter induction times. As bubbles

ascend from the pulp to the froth phase, the stability of the particle-bubble aggregate depends on whether the attachment forces exceed the combined detachment forces. If this condition is met, the aggregate remains stable and is successfully collected. The probability of detachment, however, is influenced by several factors, including particle inertia, gravity, hydrodynamic drag force, viscous force, hydrostatic pressure, bubble oscillation, centrifugal force resulting from aggregate rotation, and shear flow (SHERMAN, 2018). Additionally, hydrophobic coverage and particle size emerge as equally critical factors, as they fundamentally govern the stability of particle-bubble attachment - where greater hydrophobic coverage enhances adhesion strength, while particle size dictates both collision efficiency and resistance to disruptive forces (ZHANG *et al.,* 2024).

In this context, detachment within the froth phase occurs when previously collected particles are replaced by more hydrophobic ones or when less hydrophobic particles are washed away. Furthermore, mineralized bubbles are prone to coalescence, resulting in a reduced specific surface area, which contributes to aggregate detachment. Consequently, particles that were previously attached to the bubble surface either return to the pulp zone or remain in the froth, where they are subjected to hydrodynamic entrainment (DEMUNER, 2019; WANG *et al*., 2016). Detachment probability decreases with particle size reduction, which can be negligible for fine and ultrafine particles, as a result the collection probability (P_{coll}) equation becomes dependent only on the probability of collision (P_c), attachment (P_a) (Equation 3) (WANG; LIU, 2021).

$$P_{coll} = P_{c.}P_a \tag{3}$$

Fine and ultrafine particles exhibit a reduced induction time, which facilitates their attachment to air bubbles. After attachment, the stability of the particle-bubble aggregates reaches nearly maximum efficiency, making these aggregates highly resistant to separation. Therefore, the primary limitation in flotation efficiency of fine and ultrafine particles is their low collision probability (CHENG *et al.,* 2017; WANG; LIU, 2021). Figure 2.5 illustrates a schematic mechanism of collision, attachment, and particle-bubble aggregate formation. In this process, the hydrophobic particles in the pulp are introduced into the flotation equipment in the presence of air bubble (a). As the particles and bubbles come into close proximity, they may collide (b). Following this, the particles slide along the bubble surface and attach to it, forming a specific contact angle (c). This attachment favors the formation of particle-bubble aggregates (d), which then rise to the froth phase and are collected as concentrate (TESTA, 2008).

Figure 2.5 - Flotation subprocesses

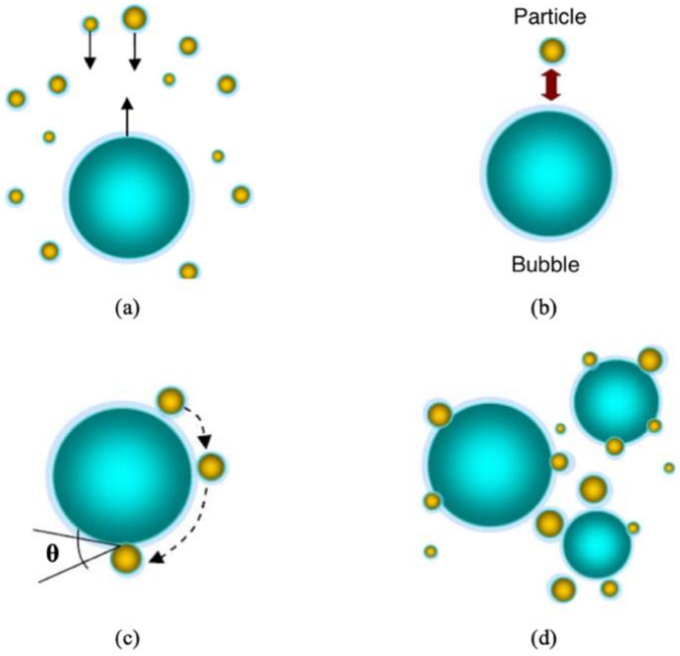

Source: Testa (2008).

2.5. Reagents of flotation

The effectiveness of the froth flotation process relies on modifying the surface properties of minerals, which is achieved using specific reagents such as collectors, depressants, and modifiers (BULATOVIC, 2007). In this context, the selection of reagents is considered crucial, as it can significantly induce the hydrophobicity of the target mineral while maintain the inherent hydrophilicity nature of gangue minerals, ensuring they remain in the pulp phase during flotation. This improvement in selectivity leads to a more efficient separation process (ZHANG *et al.,* 2020). However, the flotation process is often complicated by the similarities in surface properties among minerals (LAFHAJ; FILIPPOV; FILIPPOVA, 2017).

Given its importance, the selection of flotation reagents is fundamental to achieving the desired flotation performance of apatite, ensuring it meets industrial requirements (SIS; CHANDER, 2003). The inherent complexity of mineralogical variability necessitates a thorough understanding of reagent adsorption and its influence on mineral surfaces to optimize flotation performance and meet industrial standards (GUO; LI, 2010; LAFHAJ; FILIPPOV; FILIPPOVA, 2017). Flotation reagents are therefore classified according to their functions, including collectors, depressants, and modifiers.

2.5.1. Collector

Collectors are a diverse group of organic compounds that selectively adsorb onto mineral surfaces, altering their surface properties to induce and enhance hydrophobicity, which is crucial for effective flotation. In apatite flotation, collectors are added during the conditioning stage to induce and increase the hydrophobicity of apatite particles. This enhanced hydrophobicity enables apatite particles to attach to air bubbles during flotation, promoting selective separation. This process is driven by the alignment of collector molecules at the solid-liquid interface, where their non-polar segments extend into the liquid phase while their polar segments bond to the mineral surface (CHAVES; LEAL FILHO; BRAGA, 2010).

Collectors increase the contact angle between the mineral surface and air bubbles, thereby enhancing flotation efficiency by ensuring hydrophobic particles adhere to air bubbles (CHAVES; LEAL FILHO; BRAGA, 2010; SANTANA, 2011). They are generally classified by the charge of their polar groups into categories: anionic collectors, which usually contain sulfhydryl or hydroxyl functional groups, and cationic collectors, commonly derived from amines (SILVA *et al.,* 2017).

Anionic collectors, particularly those sourced from vegetable oils like corn, soybean, and rice bran, are commonly used in low-grade phosphate ore flotation. Due to their chemical properties, they can also function as frothers, and their ionized species may lead to the formation of excessively stable froths (GUIMARÃES; ARAUJO; PERES, 2005). In Brazil, vegetable fatty acid is commonly used. However, these collectors often adsorb either by interaction with calcium sites on the apatite surface, forming calcium carboxylate, or by precipitation near the surface in alkaline pH, which compromises flotation selectivity and efficiency (CAO *et al.,* 2015; CARNEIRO *et al.,* 2023; CARVALHO *et al.,* 2020; RUAN *et al.,* 2019). To overcome this challenge, alternative collectors have been developed, including Flotigam from Clariant® and Agem A3, a vegetable oil-based anionic collector developed by RJMG® Óleo Química. The selection of an appropriate collector type and dosage is crucial for achieving selectivity and recovery in phosphate flotation.

2.5.2. Modifiers

Modifiers are extensively employed in flotation systems to improve the selectivity of mineral separation. These reagents, which include depressants, dispersants, and pH regulators, serve distinct functions that collectively improve flotation performance.

Depressants are introduced during the conditioning stage of phosphate flotation to modify the surface properties of gangue minerals. By maintaining their hydrophilicity, depressants prevent collector adsorption onto gangue minerals, thereby enhance flotation performance (CARNEIRO *et al.,* 2019). Depressants are broadly classified into organic and inorganic compounds. Organic depressants, such as starch, dextrin, and tannin, are widely used due to their effectiveness, while inorganic depressants include sodium silicate, sodium sulfide, potassium dichromate, and sodium cyanide (CHAVES; LEAL FILHO; BRAGA, 2010; NUNES, 2015). In Brazil, gelatinized corn starch is the most commonly used depressant in apatite flotation, selectively adsorbing onto gangue minerals such as carbonates and iron-bearing minerals (PAVLOVIĆ; BRANDÃO, 2003). However, when combined with ionic collectors, starch can induce voluminous froth formation, which may impact froth stability and flotation efficiency (GUIMARÃES; ARAUJO; PERES, 2005; PAVLOVIĆ; BRANDÃO, 2003). Laskowski *et al*. (2007) investigated the adsorption mechanism of polysaccharides, including starch, and observed that adsorption per unit surface area is particle size-dependent and generally stronger on basic metal oxides/hydroxides compared to acidic ones. Furthermore, modified starch might also function as a dispersant by stabilizing mineral particles both electrostatically and sterically.

Dispersants play a critical role in fine and ultrafine particles flotation systems by counteracting particles aggregation. By increasing opposing electrostatic repulsion, dispersants prevent agglomeration, therefore facilitating more elective reagent coating and enhancing flotation performance (MOLIFIE *et al.,* 2023). Sodium silicate is particularly effective as a dispersant, and depending on the pH, can also act as a depressant for silicate gangue minerals (ALSAFASFEH; ALAGHA, 2017; SILVA *et al.,* 2012). Its depressant effectiveness depends on its silicate modulus and decreases at pH levels above 10 (QI; KLAUBER; WARREN, 1993). Beyond preventing agglomeration, sodium silicate reduces pulp viscosity, improves particle-bubble contact, enhances froth drainage, and modifies the zeta potential of minerals, thus preventing electrostatic attraction between gangue and valuable minerals. It can also interact with other flotation reagents, influencing their effectiveness based on flotation conditions and increases particle-bubble collision probability (FARROKHPAY; FILLIPOV; FORNASIERO, 2020; SAJJAD; OTSUKI, 2022).

Regarding pH regulators, they change the concentration of H^+ and OH^- ions in the pulp, altering the surface charge of minerals and enhancing the selectivity of reagent interactions. This change improves collector adherence to target mineral while enhancing depressant action on gangue minerals, thus optimizing selectivity (AARAB *et al*., 2021; BULATOVIC, 2007).

Additionally, pH influences the zeta potential of minerals, the dissociation of collectors and depressants, and the adsorption of ions onto mineral surfaces, which is crucial for pulp stability (DERHY *et al.,* 2020). In apatite flotation, sodium hydroxide is commonly used to maintain an alkaline environment favorable for the process (NUNES, 2015). However, high pH levels can affect froth stability by altering ionic strength and particle-bubble interactions, potentially increasing gangue mineral entrainment and compromising flotation efficiency (ALEKSANDROVA; ELBENDARI, 2021; FARROKHPAY; FILLIPOV; FORNASIERO*,* 2020).

2.6. Flotation machines

The selection of appropriate flotation equipment is critical for achieving optimal performance, alongside considerations of ore properties and reagent characteristics. This choice directly influences key factors such as selectivity, and recovery rates. The primary goal of flotation equipment is to efficiently separate ore into concentrate and tailings, which requires effective interaction between minerals, the liquid phase, reagents, and air. A fundamental function of flotation machines is to disperse air into the pulp, facilitating particle-bubble interactions. The efficiency of flotation equipment is evaluated based on product quality, recovery rates, energy and reagent consumption, and operational and maintenance costs (RUBIO, 2013).

Mechanical cells and flotation columns are the most widely used types of flotation equipment. Mechanical cells generally consist of rectangular tanks with a central impeller that agitates the slurry, maintaining particle suspension and generating air bubbles to enhance particle-bubble contact. These cells operate continuously, with slurry fed on one side and discharged on the opposite side. They are characterized by a turbulent hydrodynamic regime, high flotation kinetics, and a high gas-liquid ratio. However, their complex maintenance requirements and larger horizontal footprint present operational challenges. Although more alternatives have been developed, mechanical cells remain prevalent in the industry due to their reliability and established use (SANTOS, 2010; SILVA, 2016).

In contrast, flotation columns were developed to address the limitations of mechanical cells and offer superior efficiency. They feature a slender vertical design and operate under low-turbulence hydrodynamic conditions, which promote the generation of finer air bubbles. A key advantage of flotation columns is the inclusion of a wash water system, which enhances selectivity by reducing hydrophilic minerals entrainment. These characteristics enable flotation

columns to achieve higher recovery rates and better concentrate quality, particularly for fine and ultrafine particles. Their successful implementation in industrial applications has been widely documented, underscoring their effectiveness in modern mineral processing (PENNA *et al.,* 2003; REIS *et al.,* 2019).

2.6.1. Mechanical cell flotation

Mechanical flotation cells are the most commonly used equipment in mineral processing, with ongoing technological advancements focused on improving air dispersion, reducing reagent consumption, enhancing fine particle recovery, and minimizing installation costs. Figure 2.6 illustrates the schematic diagram of the mechanism of bubble formation in a mechanical flotation cell (WANG; LIU, 2021). These cells typically feature rectangular tanks designed to receive slurry on one side and discharge it on the opposite side. The froth phase rises and overflows into collection launders along the flotation bank, while the depressed material flows through successive cells before final discharge. This setup creates two countercurrent flows: the downward movement of depressed material from the feed to the discharge point and the upward movement of froth, which carries hydrophobic particles to the concentrate (CHAVES; LEAL FILHO; BRAGA, 2010; GUIMARAES, 1995).

Figure 2.6 - Schematic diagrams of the mechanism of bubble formation in a mechanical flotation cell

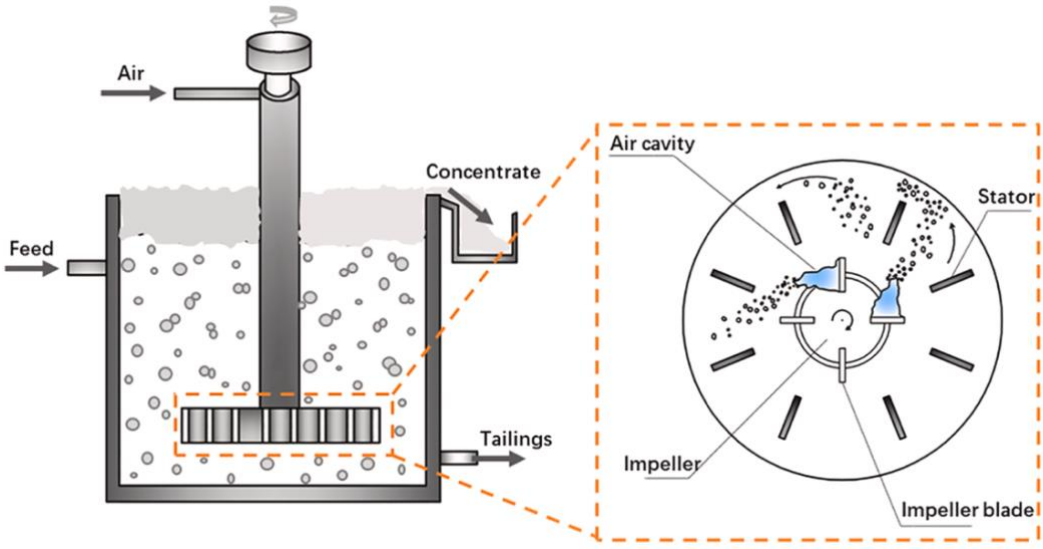

Source: Wang and Liu (2021)

The central component of a mechanical flotation cell is the flotation mechanism, which includes a rotor-stator system located at the bottom of the tank. The rotor, connected to an

external drive via a vertical shaft, rotates within a cylindrical draft tube. Its primary role is to maintain slurry suspension and generate sufficient turbulence to promote effective particle-bubble interactions. The rotor's rotation creates a low-pressure zone, which, in many designs, draws air from the atmosphere. In other configurations, compressed air is introduced to achieve better control over air dispersion. The stator, surrounding the rotor, plays a critical role in breaking the incoming air stream into fine bubbles, typically around 1 mm in diameter. This bubble fragmentation is essential for efficient flotation, as smaller bubbles increase the likelihood of particle-bubble attachment (CHAVES; LEAL FILHO; BRAGA, 2010; CHAVES; RODRIGUES, 2013).

Beyond maintaining suspension and generating bubbles, the rotor must also provide the energy required to transport the depressed material. This necessitates proper rotor positioning within the cell, optimal rotation speed, and an appropriate rotor diameter. Variations in cell design and rotor-stator geometries significantly influence hydrodynamic conditions and, consequently, flotation performance. The choice of flotation mechanism depends on factors such as the ore's mineralogical characteristics, operational requirements, and the need for efficient recovery of fine and ultrafine particles (CHAVES; LEAL FILHO; BRAGA, 2010; CHAVES; RODRIGUES, 2013).

2.6.2. Column flotation

Flotation columns exhibit distinct characteristics compared to mechanical flotation cells, including their unique geometry, low-turbulence hydrodynamic conditions, and the ability to generate smaller-diameter bubbles. Additionally, flotation columns are equipped with wash water systems, which enhance concentrate grade by reducing entrainment of fine and ultrafine particles. These features collectively contribute to their superior recovery rates, particularly in the processing of fine and ultrafine particles, such as apatite. This makes flotation columns a promising alternative for optimizing the recovery of challenging particle size fractions (TAKATA; VALLE, 2013).

As illustrated in Figure 2.7, the scheme of a column flotation which is divided into two zones: the collection zone and cleaning zone. The pulp is typically fed at a position equivalent to two-thirds of the column height, flowing downward (JENA *et al.,* 2008). The collection zone facilitates counter-current contact between particles from the feed and ascending air bubbles generated by the sparger at the base of the column. The hydrophobic particles when collide with the bubbles may form particle-bubble aggregates, which are transported to the cleaning zone

that contains a froth layer, while hydrophilic particles do not attach on the air bubble surface, staying into the pulp phase in the collecting zone and are removed from the column trough the lower section, constituting the non-floated fraction (tailings) (AQUINO; OLIVEIRA; FERNANDES, 2010).

Figure 2.7 - Column flotation scheme

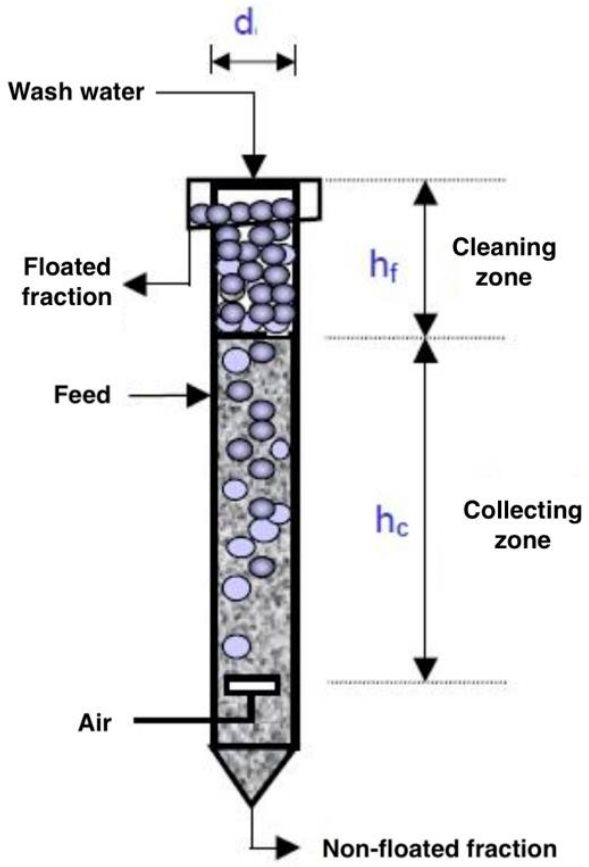

Source: Aquino; Oliveira; Fernandes (2010).

The particle-bubble aggregates rise to the cleaning zone, where wash water is sprayed onto the froth layer at the top of the flotation column. This wash water serves to remove hydrophilic particles entrained by the upward flow of mineralized bubbles and to stabilize the froth layer. The aggregates are then collected at the top of the column as the floated fraction, which is primarily composed of hydrophobic particles. The extended residence time of the bubbles, which are generated at the bottom of the column and rise through its entire height before being collected at the top, combined with the action of wash water, contributes to a higher-grade concentrate (CHAVES; RODRIGUES, 2013; REIS, 2019).

The performance of column flotation is influenced by a wide range of variables, particularly the intrinsic characteristics of the ore, such as particle size distribution,

hydrophobicity, and degree of liberation. Additionally, the type and dosage of reagents, ore conditioning conditions, and operational parameters of the column play significant roles. Key operational variables in the column flotation process include air flow rate, air holdup, wash water flow rate, bias, froth layer height, residence time and bubble size (SANTANA, 2011).

The air flow rate is a critical parameter in column flotation, significantly influencing process efficiency and mineral recovery. Each mineral has an optimal air flow rate range, determined by factors such as mass recovery of the floated fraction, ore particle size distribution, and bubble size. This parameter is closely linked to superficial gas velocity, gas holdup, and bubble diameter. Within the column's stability limits, increasing the air flow rate generally enhances recovery by increasing the number and surface area of bubbles, improving particle-bubble attachment. However, excessively high air flow rates can lead to turbulence or excessive froth formation in the recovery zone, negatively impacting selectivity and recovery efficiency. The superficial gas velocity, defined as the ratio of air flow rate to the column's cross-sectional area, is a key performance indicator, typically maintained between 1 and 3 cm/s under standard operating conditions to ensure optimal particle-bubble interaction and system stability (AQUINO; OLIVEIRA; FERNANDES, 2010).

Gas holdup is defined as the volumetric fraction of gas at a specific point in a column, representing the volume occupied by the gas phase relative to the total volume. It is a dimensionless quantity, typically expressed as a percentage. This parameter depends on several factors, including the air flow rate, bubble size, pulp density, solid loading on the bubbles, and the downward velocity of the pulp (MATIOLO, 2008; TAKATA; VALLE, 2013).

In column flotation, wash water serves three fundamental functions. Firstly, it removes entrained gangue particles from the rising stream, creating a downward water flow known as bias. Secondly, it enhances the stability and height of the froth layer, thereby improving separation efficiency. Lastly, it reduces bubble coalescence by promoting the formation of a densely packed bubble bed, which is crucial for maintaining efficient particle-bubble interactions (AQUINO; OLIVEIRA; FERNANDES, 2010).

The bias represents the residual fraction of wash water that flows through the column and is primarily responsible for the cleaning action within the froth. By convention, the bias is considered positive when this residual flow moves downward, indicating that the wash water flow rate is sufficient to replace the feed water in the floated fraction and to displace a portion of fresh water toward the column's base. The most accurate value of bias can be calculated as the difference between the wash water flow rate and the water flow rate in the tailings (AQUINO; OLIVEIRA; FERNANDES, 2010).

The height of the froth layer strongly influences the selectivity of the flotation process. When using deeper froth layers, if a particle-bubble aggregate breaks or hydrophobic particles detach, these particles can still be recovered, as they must traverse the entire froth zone before being rejected. Its structure can be divided into three distinct regions: (1) the expanded bubble zone, positioned just above the pulp-froth interface, where bubble collisions create shock waves and promote coalescence; (2) the packed bubble zone, which extends from the upper boundary of the first region to the wash water injection point, characterized by moderate coalescence and predominantly spherical bubbles; and (3) the conventional drainage froth, located above the wash water injection point, where bubbles adopt a hexagonal shape and contain minimal liquid (SANTOS, 2005).

Residence time is a critical factor influencing both the grade and recovery of the floated material, with a more pronounced effect on recovery. Variations in residence time can typically be achieved by adjusting the feed solid concentration and flow rate, wash water flow rate, air holdup, and the height of the collection zone in the column. The collection zone must have sufficient height to allow ascending air bubbles to capture hydrophobic particles during their sedimentation. The residence time of particles in both the froth layer and the collection zone is strongly influenced by the air and pulp flow rates, respectively (AQUINO; OLIVEIRA; FERNANDES, 2010). At shorter residence times, the grade of the floated fraction tends to be higher, while recovery is lower, as mineral particles have insufficient time to complete the flotation process. Conversely, at longer residence times, the grade of the floated fraction decreases due to increased entrainment (SANTANA, 2011).

The bubble size distribution (BSD) is one of the most influential variables in the fluid dynamics of gas-liquid systems, as it directly affects the interfacial area available for particle-bubble attachment, which in turn impacts the flotation rate constant. In a flotation column, the interfacial area depends on factors such as bubble size, gas holdup, superficial gas velocity, gas distributor design, phase properties, and column geometry, with gas holdup and bubble size further influenced by the physicochemical properties of the process and the aeration system employed. Bubble size can be controlled by adjusting operational conditions of the aeration system and through the addition of surfactants, as the average bubble size and its distribution are critical in flotation due to their effects on collection efficiency and particle transport. While the use of small bubbles with high surface area enhances the kinetics of particle collection and transport per unit volume of air, excessively small bubbles may exhibit low rise velocities, potentially fall below the downward velocity of the pulp and leading to the loss of collected hydrophobic particles to the non-floated material stream (REIS, 2019; SANTANA, 2011).

2.7. Fine and ultrafine particles

Particle size is a critical factor influencing flotation performance. The classification of particle size varies depending on the author and the mineral under study (ANSARI, 1997; FARROKHPAY; FILLIPOV; FORNASIERO, 2020; MATIOLO *et al.,* 2019; PEASE, 2006; RUBIO, 2007, TRAHAR, 1981, WANG; LIU, 2021). In this work, fine particles are defined as those with diameters between 10 and 50 μm, while ultrafine particles are characterized by diameters smaller than 10 μm (BORROW *et al.,* 2018; PASCOE; DOHERTY, 1997). These size ranges are particularly challenging to treat or recover due to their physical and hydrodynamic properties.

The progressive decline in ore grades has led the mining industry to produce increasingly finer particles to achieve mineral liberation. However, finer particle sizes exacerbate flotation challenges, as these particles are often difficult to process efficiently using conventional methods. Fine and ultrafine particles exhibit properties that hinder their collision and attachment mechanisms with air bubbles, reducing recovery rates (RUBIO *et al.,* 2003). Moreover, these particles (mainly ultrafine) are often removed during conventional recovery processes and retained in tailings ponds as slimes, leading to economic losses and environmental concerns (ANSARI, 1997; FARROKHPAY; FILLIPOV; FORNASIERO, 2020). As a result, there is an urgent need for advanced flotation technologies capable of efficiently processing low-grade ores containing fine and ultrafine particles in an economically viable manner. Addressing these challenges is critical not only for improving recovery rates but also for mitigating the environmental impact of slimes, which are often discarded as waste and contribute to environmental degradation (ANSARI, 1997; FARROKHPAY; FILLIPOV; FORNASIERO, 2020).

Flotation recovery is generally satisfactory for particles within the size range of 10 to 100 μm, though the optimal range depends on the mineral being processed (TRAHAR; WARREN 1976). Figure 2.8 illustrates the conventional relationship between recovery and particle size, which typically follows a parabolic trend (PEASE *et al.*, 2006). Intermediate-sized particles achieve the highest recoveries, while both coarse and fine particles exhibit lower recovery rates. Trahar (1981) noted that particles smaller than 5 μm cannot achieve the same recovery as intermediate-sized particles under any conditions.

Figure 2.8 - Conventional view - "fines do not float"

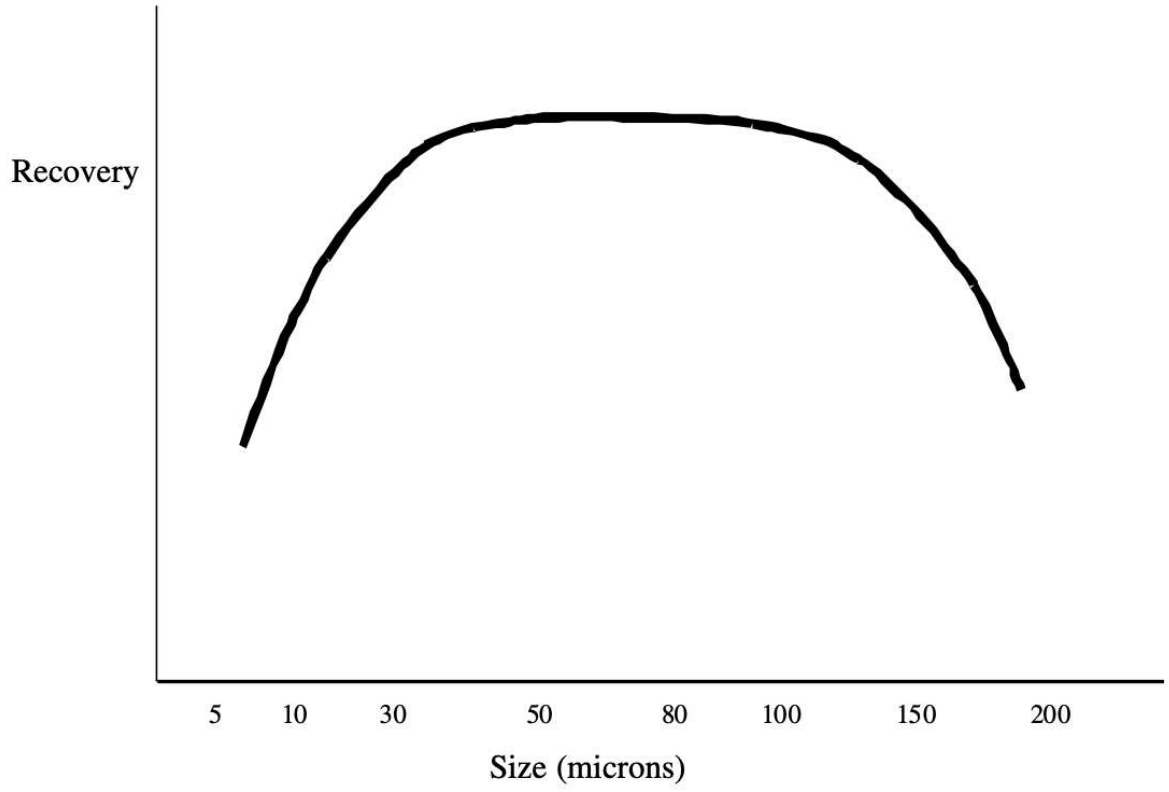

Source: Pease *et al*. (2006).

The inefficient recovery of fine and ultrafine particles alongside coarser particles is well-established. Trahar (1981) demonstrated that treating particles by size fraction, rather than collectively, improves flotation efficiency for each particle size. Pease *et al*. (2006) further showed that a narrow particle size distribution can enhance flotation performance for fine and ultrafine particles, as flotation residence time varies significantly with particle size. Additionally, particles size affects the physicochemical phenomena governing flotation process (SANTANA, 2011).

The behavior of fine and ultrafine particles in flotation has been extensively studied (PEASE *et al.,* 2006; REIS, 2019; RUBIO, 2003; SANTANA, 2011; TEAGUE; LOLLBACK, 2012; TRAHAR; WARREN 1976). Pease *et al.* (2006) observed that fine and ultrafine particles can achieve satisfactory flotation recoveries; however, their behavior differs significantly from that of other particle size fractions. These differences become more pronounced as particle size decreases and are primarily attributed to the following factors:

- High surface area per unit mass, leading to increased reagent consumption;

- Less momentum, causing particles to follow water streams more easily. This reduces their energy for bubble attachment and increases their tendency for entrainment;
- Slower flotation rates, necessitating froth washing to counteract the increased entrainment;
- Increased susceptibility to slime coating, because of their high surface area makes these particles more reactive, while their low momentum reduces the probability of surface deposits being abraded by other particles;
- More sensitivity to water chemistry and ions species in solution;
- High surface area-to-volume ratio, which can result in tenacious froths, making thickening and leading to more difficult filtering process;
- Slower flotation kinetics, fine and ultrafine particles can float with large bubbles but decreasing bubbles size improves flotation rate.

Fine and ultrafine particles can be carried into the froth layer through entrainment or entrapment, where water trapped in air bubbles transports them. If these particles are gangue minerals, they reduce the concentrate grade. In the absence of coarse particles, fine and ultrafine particles recovery primarily depend on true flotation (selective process) and hydraulic entrainment (non-selective) (GEORGE; NGUYEN; JAMESON, 2004).

Decreasing particles size reduces the amount of collector required for adsorption on valuable particles, as fine particles need a lower degree of hydrophobicity to be captured by true flotation, as illustrated in Figure 2.9. Their high surface area enhances reagent adsorption capacity and consumes more available collector in the pulp, favoring true flotation. However, this also means there is no excess collector to adsorb at the gas-liquid interface and act as a frother (TRAHAR, 1981). Additionally, fine particles exhibit distinct surface properties and electrochemical behavior compared to coarser fractions. Their high surface energy increases non-selective reagent adsorption, promoting gangue flotation. Consequently, high recoveries of fine particles are often accompanied by a decline in concentration grade (TRAHAR, 1981).

Froth stability is strongly influenced by fine and ultrafine particles, particularly in terms of dynamic froth stability, which refers to the equilibrium height of the froth within an aerated slurry. Research indicate that fine particles tend to increase froth height and stability (Wang and Liu, 2021; Santana, 2011). However, excessive fine particles can create overly stable, viscous froths that hinder gangue drainage, leading to higher water recovery and increased entrainment of unwanted particles in the concentrate (FARROKHPAY; FILLIPOV; FORNASIERO, 2020).

Figure 2.9 - Qualitative representation of suggested form of the influence of particle size on the relationship between floatability and hydrophobicity

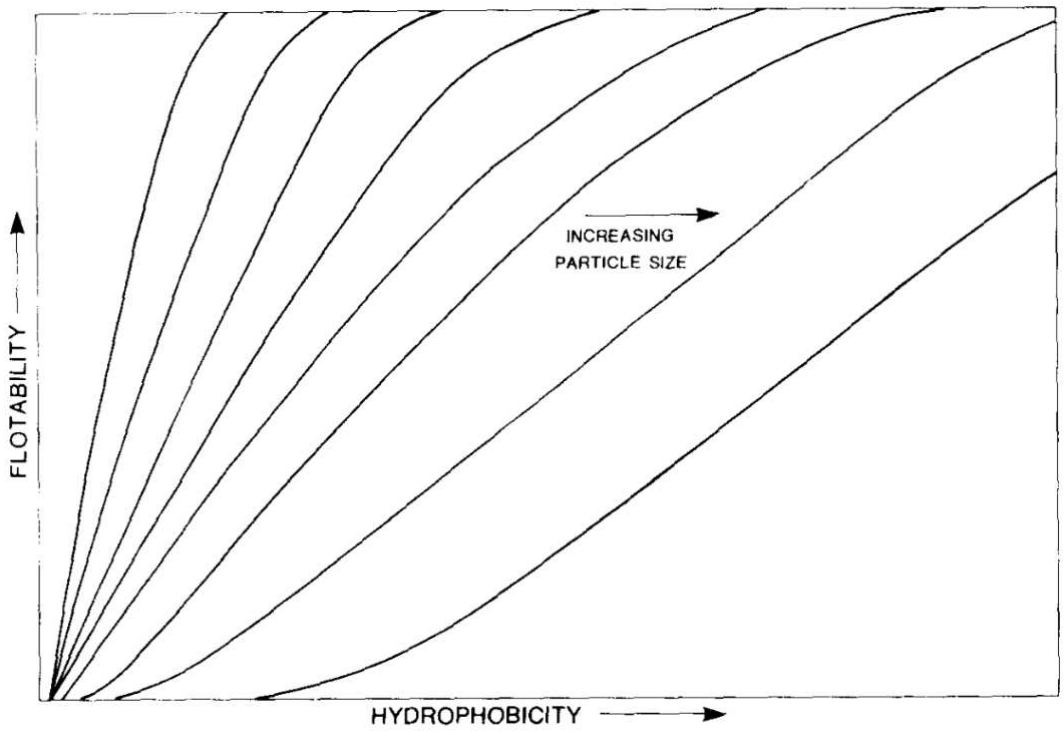

Source: Trahar (1981).

Efficient recovery of fine and ultrafine particles requires increasing collision energy within the flotation system. This can be achieved through two main strategies: enhancing collision probability or improving particle-bubble interactions efficiency. The first strategy involves agglomerating valuable solids or attaching them to hydrophobic coarse particles that acts as carriers. The use of smaller bubbles also enhance recovery by increasing bubble residence time, which is particularly effective in column flotation, where countercurrent flow improves selectivity. The second strategy involves using chemisorption collectors that promote fine particles aggregation, increasing attachment efficiency (FUERSTENAU, 1980; SANTANA, 2011; TRAHAR, 1981).

Selectivity in flotation is significantly affected by particle size due to mineral surface interactions with reagents. Fine and ultrafine particles have a high probability of attachment to bubbles, then their low mass results in long contact time and high adhesion efficiency. The increased surface area enhances reagent consumption, making desliming a common practice to reduce costs and prevent slime coating. However, desliming results in valuable mineral losses, driving research into improved flotation process for fine and ultrafine particles recovery. Various techniques have been explored, including the use of chemisorption collector, carrier

flotation, electrolytic flotation, selective flocculation, aggregation flotation, controlled dispersion flotation, column flotation, high intensity conditioning (FUERSTENAU, 1980).

Despite these advancements, industrial flotation systems remain predominantly designed to optimize the recovery of intermediate-sized particles, which possess favorable kinetic energy for efficient flotation. Consequently, the recovery of fine and ultrafine particles remains a significant challenge. Efficient flotation requires a precise balance between particle and bubble sizes to maximize particle-bubble interactions. However, conventional flotation cells often fail to produce an appropriate bubble size distribution for fine fractions, resulting in suboptimal recovery (RUBIO, 2013).

Bubble size plays a critical role in the flotation of fine and ultrafine particles, significantly influencing both recovery and selectivity. Large bubbles enhance recovery through entrainment but reduce selectivity and concentrate grade (e.g., P_2O_5) due to the unintended transport of gangue minerals. Conversely, smaller bubbles improve selectivity and grade by increasing particle-bubble sliding time and adhesion probability, though they may reduce recovery. REIS *et al.* (2023) demonstrated that bubbles in the 800-1000 µm range yielded the best flotation performance for fine, low grade phosphate particles. Bubble size can be controlled through frother addition or the use of specialized equipment, such as hydrodynamic cavitation systems, to generate very smaller bubbles. Notably, the application of micro and nano bubbles has demonstrated substantial potential for recovering ultrafine particles, as they bypass the collision-limited step and directly nucleate on hydrophobic surfaces, significantly improving flotation rates (WANG; LIU, 2021).

As illustrated in Figure 2.10, the one- and two-stage particle-bubble attachment models explain the advantages of micro and nano bubbles in flotation. The two-stage attachment mechanism offers both thermodynamic and hydrodynamic benefits over direct particle attachment to flotation-size bubbles. Initially, micro and nano bubbles attach more easily and rapidly to particle surfaces due to their smaller contact area, forming aggregates that increase the apparent particle size and enhance collision probability with larger bubbles. In the second stage, these tiny bubbles, being less hydrated than solid particles, facilitate interaction with flotation-size bubbles. Their coalescence leads to a greater reduction in system free energy compared to direct attachment while also accelerating liquid drainage. As a result, flotation efficiency improves, making the combination of micro, nano, and conventional flotation bubbles a promising approach for fine and ultrafine particle recovery (ZHOU *et al.,* 2020).

Figure 2.10 - One/two-stage attachment model

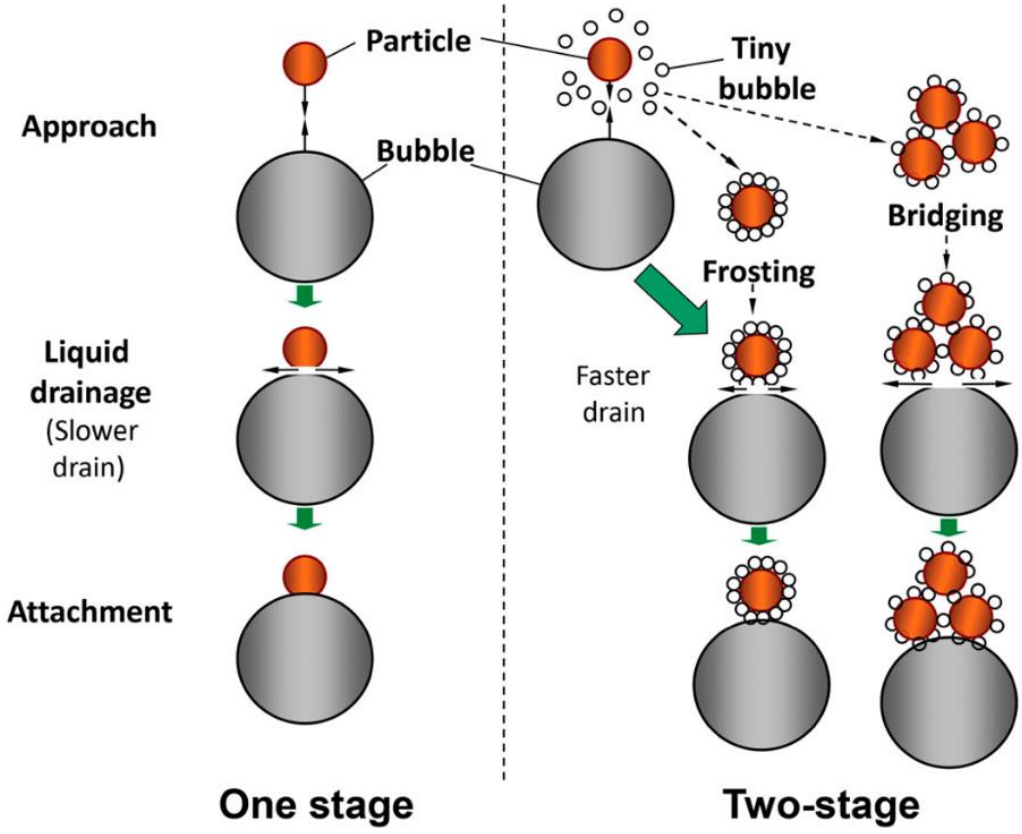

Source: Zhou *et al.* (2020).

Sun *et al.* (2006) also demonstrated that fine particles attach to cavitation-induced microbubbles, forming hydrophobic clusters that enhance attachment to flotation bubbles. This aggregation improves collision probability and attachment efficiency, leading to increased recovery. Hydrodynamic cavitation, a method for generating micro and nano bubbles, has shown significant potential for improving the recovery of fine and ultrafine minerals in flotation. Notably, the flotation kinetics of fine particles can be significantly enhanced by subjecting the feed slurry to prolonged high-energy conditioning, particularly through a high-intensity conditioning (HIC) stage before flotation. Critically, the micro and nano bubbles formed during HIC are retained throughout both the conditioning and subsequent flotation stages, sustaining their beneficial effects on particle-bubble interactions. However, the use of microbubbles or nanobubbles in the flotation of fine particles, aimed at increasing collision efficiency, also presents some disadvantages. Due to their low rising velocity, the flotation process requires a longer residence time in the flotation circuits. Additionally, the drag force exerted by very small bubbles may be insufficient to achieve good selectivity in the process.

High-intensity conditioning (HIC) has emerged as one of the most effective strategies for improving fine and ultrafine particle flotation. This process creates an optimal environment for the formation of small-sized bubbles through hydrodynamic cavitation. Cavitation bubbles and cavities are generated by a localized pressure drop in the liquid flow, which occurs due to high-intensity agitation that increases flow velocity and overcomes the attractive forces between water molecules. HIC enhances particle surface conditions, mitigates slime coatings, and promotes the formation of micro and nano bubbles, which accelerate particle-bubble attachment. HIC is conducted in an agitated tank, typically operating at speeds ranging between 800 and 3000 rpm (SUBRAHMANYAM; ERIC FORSSBERG, 1990). During this process, flotation reagents induce both physical and chemical changes on particle surfaces (TESTA, 2008). The observed recovery enhancement with HIC is attributed to surface cleaning, slime coating removal, and improved reagent distribution and diffusion in the pulp. Additionally, HIC promotes hydrodynamic cavitation through vigorous impeller rotation, producing micro and nano bubbles that remain stable throughout both the conditioning and subsequent flotation stages. These persistent bubbles continuously enhance collision efficiency and aggregate stability, thereby improving particle-bubble interactions. This sustained effect makes HIC particularly effective when combined with conventional flotation equipment, such as flotation columns (CAPPONI *et al.,* 2023; WANG; LIU, 2021).

The intense agitation in HIC provides sufficient energy to promote particle-bubbles aggregation, which improves flotation efficiency. Studies have shown that HIC promotes aggregate formation, significantly enhancing recovery and selectivity of ultrafine particles (CAPPONI *et al.,* 2023; ROSA, 1997; TESTA, 2008; WANG; LIU, 2021). The high-speed agitation induces hydrodynamic cavitation, where pressure fluctuations generate cavitation bubbles that serve as nuclei for aggregation. These micro and nano bubbles remain stable during conditioning and flotation, ensuring sustained improvements in particle-bubble attachment. Several factors influence aggregation in HIC, including particle size, surface charge, hydrophobicity, agitation time and velocity, and pulp solids concentration. These parameters impact collision probability, attachment efficiency, and aggregate stability. The maximum aggregated size and stability depend on hydrophobicity and turbulence levels. The geometry of the conditioning tank and impeller type also play critical roles. Cylindrical tanks with flat bottoms are commonly used, but square tanks can generate higher turbulence, improving particles dispersion. The inclusion of baffles enhances mixing efficiency; however, excessive baffles may localize the flow and reduce overall system performance (SUBRAHMANYAM; ERIC FORSSBERG, 1990). Rosa (1997) investigated the impact of high-intensity conditioning

(HIC) with different numbers of baffles (4, 2, and none) on the flotation of sulfidized lead and zinc ore. The results indicated that a higher number of baffles led to improved recovery. This study showed that the inclusion of baffles enhanced mixing efficiency, which in turn improved particle-bubble interactions and resulted in increased flotation recovery.

Impeller design significantly influences conditioning efficiency, with radial and axial impellers generating different flow patterns. Testa (2008) compared a four-bladed naval-type axial impeller with a Rushton-type radial impeller for HIC. The results showed that phosphate ore recovery was higher when a radial impeller was used, as it created greater turbulence, enhancing particle-bubble interactions and overall flotation performance. These findings reinforce the importance of adjusting conditioning parameters to improve the flotation efficiency of fine and ultrafine particles. Figure 2.11 presents a comparison of mixing conditions in different tank configurations: (I) unbaffled tanks, which exhibit a minimum shear rate, featuring (a) an axial impeller with three blades and (b) a radial impeller with six blades (Rushton); and (II) Baffled tanks, which generate a maximum shear rate, equipped with (a) a radial impeller with four blades and (b) an axial impeller with three blades (OLDSHUE, 1978 *apud* SUBRAHMANYAM; ERIC FORSSBERG, 1990).

Figure 2.11 - (I) Unbaffled tanks with minimum shear rate (II) Baffled tanks with maximum shear rate

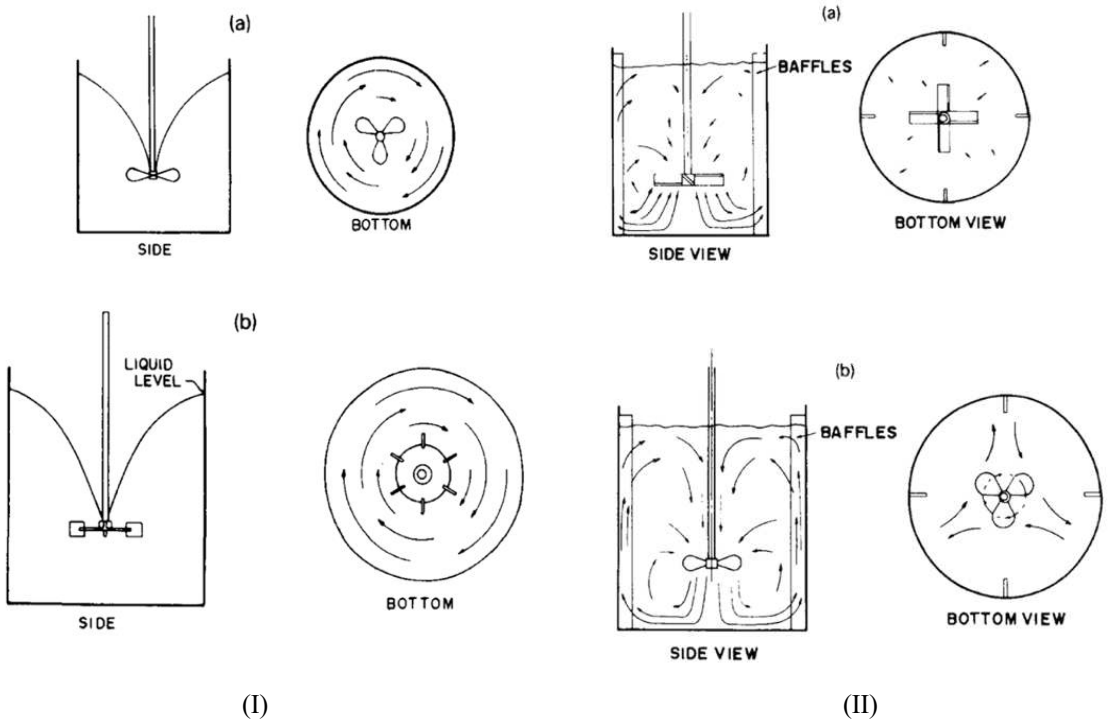

Source: Subrahmanyam; Eric Forssberg (1990) apud Oldshue (1978).

Sekhar *et al.* (2013) investigated the recovery of phosphate slime using a Denver cell, employing a two-step conditioning and flotation process. Initially, conditioning was conducted at 2200 rpm with a solid concentration of 18.82%, followed by dilution of the pulp to 9.41% solids. Flotation tests were then performed at impeller speeds of 1100 rpm and 1500 rpm to compare their effects on recovery. The results demonstrated that increasing the impeller speed during flotation significantly enhanced flotation performance. This integration of HIC and hydrodynamic cavitation significantly enhances flotation efficiency, providing a promising approach for recovering fine and ultrafine particles from tailings.

Further enhancing this process, micro and nano bubbles improve fine particle flotation by facilitating particle-bubble attachment, increasing flotation rates, and offering additional benefits such as higher contact angles, reduced slime coating, removal of oxidation layers, and lower reagent consumption. However, a notable disadvantage of using micro and nano bubbles is their tendency to increase water recovery, which leads to the entrainment of more gangue particles into the froth. This results in a dilution of the concentrate grade, a challenge that remains difficult to overcome in current micro and nano bubble flotation techniques (TRAHAR, 1976; WANG; LIU, 2021).

3. METHODOLOGY

Figure 3.1 presents the flowchart outlining the phases conducted in this study. In summary, two distinct investigations were carried out. The first study focused on the flotation of fine apatite ore, while the second examined ultrafine apatite ore flotation. The analyses were performed on two different samples obtained from separate phosphate ore reservoirs. A detailed description of each step is provided throughout this methodology section.

Figure 3.1 - Flowchart of the phases conducted in this study

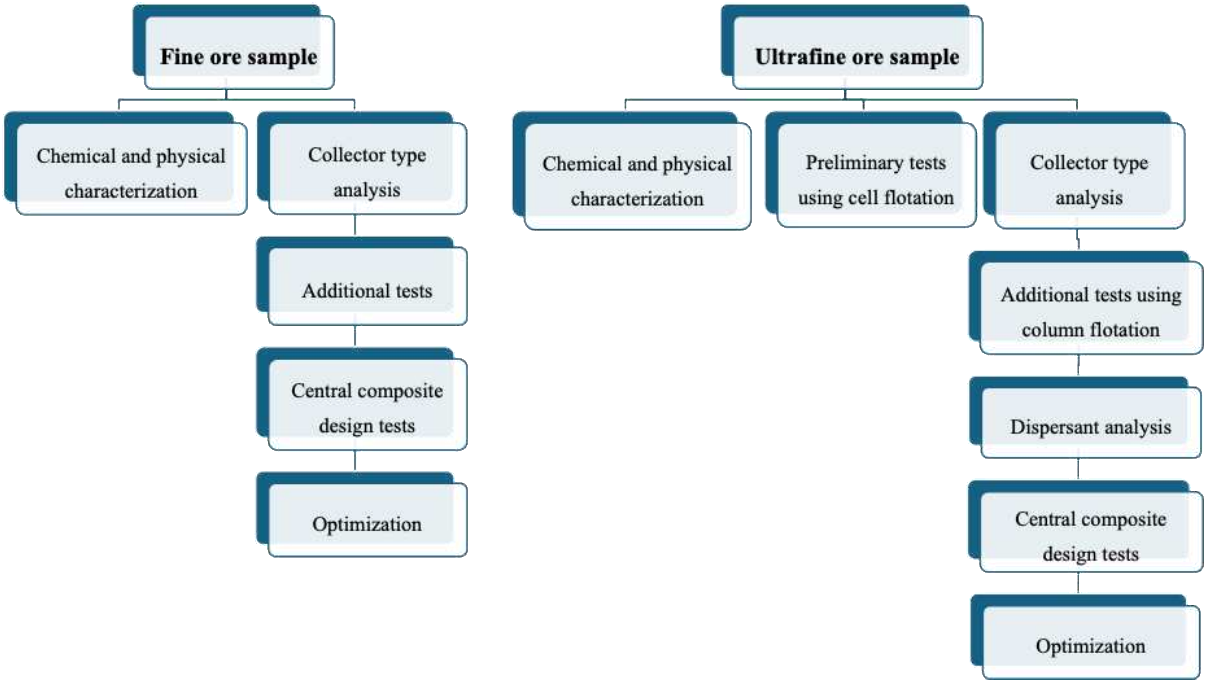

Source: Author (2025).

3.1. Characterization of ore samples

The representative tailings samples used in this study were collected from two production plants located in Catalão, Goiás, Brazil. Two distinct samples were analyzed: the first sample, obtained from Mosaic Fertilizers, consisted of dried tailings from the final flotation column's concentration circuit of fines (named as fine ore). The second sample, provided by CMOC International, comprised dried slimes generated during the desliming stage of the final pre-flotation process, which are currently deposited in a tailings pond (named as ultrafine ore). All dried samples were homogenized and prepared using a Jones-type sample splitter. Subsequently, the samples were subjected to particle size distribution analysis, as well as chemical and mineralogical characterization.

3.1.1. Particle size distribution

The particle size distribution (PSD) of the feed samples was determined using laser diffraction technology with a Malvern Mastersizer 2000® particle size analyser equipped with Hydro 2000 UM® at Faculty of Chemical Engineering of the Federal University of Uberlândia (FEQUI/UFU). Initially, a blank test was conducted using 500 mL of water and 20 mL of sodium hexametaphosphate (calgon) at a suspension concentration of 1g/L. Subsequently, the sample was added to the beaker, ensuring that the obscuration percentage remained within the range of 10% to 20%. To prevent particle agglomeration, ultrasonic dispersion was applied at a frequency of 7.0 Hz throughout the measurement process, and to avoid particle settling, the analysis was carried out under agitation with the rotation speed set to 3000 rpm. Five measurements were taken, each with a duration of five seconds.

The particle size distribution of the sample was analyzed using the equipment's proprietary software. The resulting size distribution data were then imported into STATISTICA® software (version 7.0) to estimate the model parameters and identify the best-fitting model for the experimental data.

3.1.2. Chemical and mineralogical characterization

The chemical composition of the flotation feed samples was obtained by X-ray fluorescence spectrometry (XRF - S8 Tiger,Bruker) at FEQUI/UFU. For the analysis, fused beads were prepared by melting 1g of concentrated ore sample with 10g of lithium tetraborate (Vulcan, Fluxana).

The mineralogical analysis of feed samples was obtained by x-ray diffraction (XRD) using Rigaky model Miniflex II with radiation source of CuKα (30 kV and 15 mA). The analysed ranged was of $5 \leq \theta \leq 80^{o}$ with 0.05^{o} of pace. The data was collected each one second. The crystalline phases present in the ore sample were identified using the JADE software, based on the Joint Committee on Powder Diffraction Standards (JCPDS) reference data.

3.2. Flotation reagents

The reagents play a fundamental role in modifying the surface properties of apatite and gangue minerals, rendering them hydrophobic and hydrophilic respectively. This modification enhances the selectivity of the flotation process. In Brazilian industries, vegetable oil soap is

traditionally used as collector in apatite flotation. However, fatty acids, such as those found in rice and soy oil soap, may not be highly effective for apatite flotation due to the tendency of calcite and dolomite to co-float with phosphate. Moreover, the selectivity and recovery of minerals in froth flotation are influenced by all reagents added into the flotation system (GORDEIJEV; HIRVA, 1999).

Therefore, this study also investigated alternative collectors, including Agem A3 from RJMG® Óleo Química and Flotigam 5806 from Clariant®. In all flotation tests, one of the collectors was used to enhance the hydrophobicity of apatite: rice oil soap (2.5 wt.%), Agem A3 (5 wt.%), and Flotigam 5806 (5 wt.%). Additionally, gelatinized cornstarch (3 wt.%) was introduced as a depressant to maintain the hydrophilicity nature of the gangue minerals. Furthermore, a sodium hydroxide (NaOH) solution (10 wt%) was utilized to adjust the pH of the pulp.

3.2.1. Rice oil saponification

The saponification reaction of rice oil was conducted as follows: Initially, 5.0 g of rice oil was weighed into a beaker. Then, 7.85 g of process water was measured into one beaker, and 180g of process water into another for dilution. Then, 7.15 g of a 10% NaOH solution was weighed. A stir bar was placed in the beaker with rice oil, which was then set on a magnetic stirrer. The 7.15 g of NaOH solution was combined with the 7.85 g of process water, and this beaker was also placed on a magnetic stirrer, but without the stir bar. Thermometers were immediately inserted into both beakers, and the solutions were heated to 70ºC. Once this temperature was reached, the NaOH and water solution was added to the rice oil beaker. The mixture was maintained at 70ºC and stirred at 1200 rpm for 15 minutes. After this, the heater was turned off, and the 180 g of dilution water was added while stirring continued for an additional 10 minutes. The final concentration of the collector was 2.5% by mass.

3.2.2. Agem A3 saponification

The saponification of Agem A3 collector by RJMG® was carried out as follows: First, 5.0 g of Agem A3 was weighed and placed in a beaker. Separately, 10g of deionized water was measured into a second beaker. Concurrently, 1.5 g of a 50% NaOH solution was weighed into a third beaker, and 83.5 g of deionized water was measured into another beaker for dilution. The mixture was stirred at 1200 rpm for 3 minutes. Subsequently, the NaOH solution was added

to the Agem A3's beaker, while maintaining continuous stirring for an additional 3 minutes. Following this, the dilution water was incorporated into the mixture and stirring continued for another 5 minutes. The final concentration of the Agem A3 collector was 5% by mass.

3.2.3. Flotigam 5806 saponification

The saponification of Flotigam 5806 collector by Clariant® was carried out as follows: First, 5.0 g of Flotigam was weighed and placed in a beaker. Separately, 20 g of deionized water was measured into a second beaker. Concurrently, 7.5 g of a 10% NaOH solution was weighed into a third beaker, and 66.8 g of deionized water was measured into another beaker for dilution. The mixture was stirred at 1200 rpm for 3 minutes. Subsequently, the NaOH solution was added to the Flotigam 5806 beaker, while maintaining continuous stirring for an additional 10 minutes. Following this, the dilution water was incorporated into the mixture and stirring continued for another 5 minutes. The final concentration of this collector was 5% by mass.

3.2.4. Cornstarch gelatinization

The depressant was prepared by gelatinizing cornstarch according to the following procedure: Initially, 5.0 g of cornstarch was weighed into a beaker, 45 g of processes water (tap water) was added to a second beaker, and 104.16 g of process water for dilution into a third beaker. Additionally, 12.5 g of 10% NaOH solution were prepared. The cornstarch was mixed with 45 g of process water and dissolved using an IKA LAborthechink RW 20 mechanical stirrer at minimum speed for 3 minutes to ensure a uniform solution. Subsequently, the NaOH solution was added to the mixture, and stirring continued at 1200 rpm for 10 minutes. The final mixture was diluted with 104.16 g of process water, resulting in a depressant with a final concentration of 3% by mass.

3.2.5. Dispersant

In this study, sodium silicate PA (Na_2SiO_3) was selected as the dispersant, incorporated during the first five minutes of the conditioning stage, in accordance with the experimental design. The addition of sodium silicate aimed to stabilize the slurry by preventing slime coating, thereby improving overall flotation efficiency and selectivity. The use of sodium silicate in

flotation systems is well-documented, as it facilitates the separation of fine particles by maintaining an optimal dispersion state, which is critical for the successful recovery of valuables minerals such as apatite (FILIPPOV *et al.,* 2014; SNOW; ZHANG; MILLER, 2004). Sodium silicate can act as both a dispersant and depressant for silicate gangue minerals, further enhancing the selectivity of the flotation process (ARANTES *et al.,* 2017; SILVA *et al.,* 2012).

3.3. Cell flotation test procedure

A flotation cell was employed in preliminary tests to achieve higher collision probability through increased turbulence during the flotation process. This approach aligns with the experimental methodology where preliminary rougher stage tests were conducted using ultrafine ore to evaluate the flotation performance in a CDC cell flotation system, Denver type as shown in Figure 3.2. The tests were carried out using a GFB-1000 EEPN model, part of the equipment available at the Laboratory of Mineral Processing and Mining (LaMPPMin) at the Federal University of Catalão (UFCAT). The experiments were performed in a 2 L flotation tank, where the pulp was conditioned at a constant stirring speed of 1400 rpm.

The pH of the pulp was adjusted to the desired level using a 10% NaOH solution, maintained for a 5-minute condition period. This was followed by the sequential addition of a depressant and collector, each introduced over a 5-minute interval. The target pH was consistently maintained throughout the conditioning process. Then, the air flowrate was initiated at 4 L/min, with the flotation process proceeding for 4.5 minutes. The flotation time was determined based on preliminary tests, with the shortest effective duration being selected for the best process efficiency.

Figure 3.2 - CDC cell flotation

Source: CDC (2025).

Upon completion of each test, the floated and non-floated products were carefully separated and subsequently dried in an oven. Table 3.1 shows the fixed operating conditions of cell flotation test.

Table 3.1 - Fixed conditions of cell flotation

Parameter	**Operational condition**
Conditioning time	5 min (each reagent)
Stirring speed in conditioning	1400 rpm
Stirring speed in flotation	1200 rpm
Air flowrate	4 L/min
Flotation time	4.5 min
Cell volume	2 L

Source: Author.

3.4. Ore conditioning for column flotation

3.4.1. High-intensity conditioning

Ore conditioning is a critical step prior to flotation, aimed at optimizing the interaction between mineral particles and reagents. This process enhances the hydrophobicity of apatite while maintaining the hydrophilicity of gangue minerals. The process begins with the addition of 340 g of dry ore to a PVC tank measuring 150 mm in diameter and 218 mm in heigh. Stirring was conducted at 1200 rpm using an IKA Labortechnick RW20 mixer equipped with a Rushton-type radial impeller (six blades; Figures 3.3 and 3.4), which was specifically selected for its demonstrated advantages in high-intensity conditioning applications. The Rushton design generates superior turbulent energy dissipation and mixing intensity compared to axial impellers, creating optimal hydrodynamic conditions for particle-reagent interaction (SUBRAHMANYAM; FORSSBERG, 1990; TESTA, 2008). The pH was adjusted and continuously monitored for 5 minutes, with or without the addition of a dispersant, in accordance with the experimental design.

Subsequently, the depressant was added to the suspension, and stirring continues for another 5 minutes, with continuous pH monitoring. The depressant selectively adsorbs onto the surfaces of gangue minerals, maintaining their hydrophilicity and reducing their affinity for the collector, which was a hydrophobic substance. This selective adsorption is critical for preventing gangue mineral from floating. Following this, the collector was introduced, and stirring continues for an additional 5 minutes, with further pH adjustments as needed. The

collector preferentially adsorbs onto the apatite surface, inducing hydrophobicity, which is essential for the efficient adhesion of apatite to air bubbles during flotation, thus ensuring selective recovery.

Figure 3.3 - Scheme of Roushton radial impeller with six blades

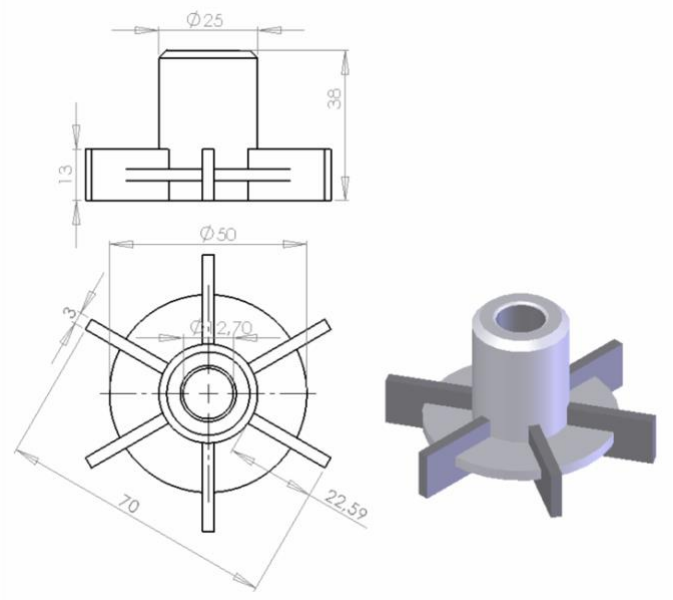

Source: Tabosa (2007).

Figure 3.4 - Roushton radial impeller with six blades

Source: Author (2025).

Finally, dilution water was added to the suspension to achieve 14% of solids percentage for flotation. The stirring rate was maintained at 1200 rpm for fine ore but reduced to 700 rpm

for ultrafine ore to prevent aggregate detachment. Throughout the conditioning process, the pH was maintained in accordance with the experimental design. Upon completion, the conditioning ore pulp was immediately transferred to the flotation column for subsequent processing.

3.4.2. Column flotation

The flotation tests were conducted in the acrylic column located in the Laboratory of Particulate System, part of the Chemical Engineering School at the Federal University of Uberlândia. Figures 3.5 and 3.6 illustrate the flotation unit, which consists of an acrylic column, divided into three sections. The first section is cylindrical, with a diameter of 4 cm and a length of 150 cm. The second section is a frusto-conical segment, 9.5 cm in height, and the third section is another cylindrical part with a diameter of 10 cm and a length of 12 cm.

Figure 3.5 - Design of experimental apparatus of column flotation

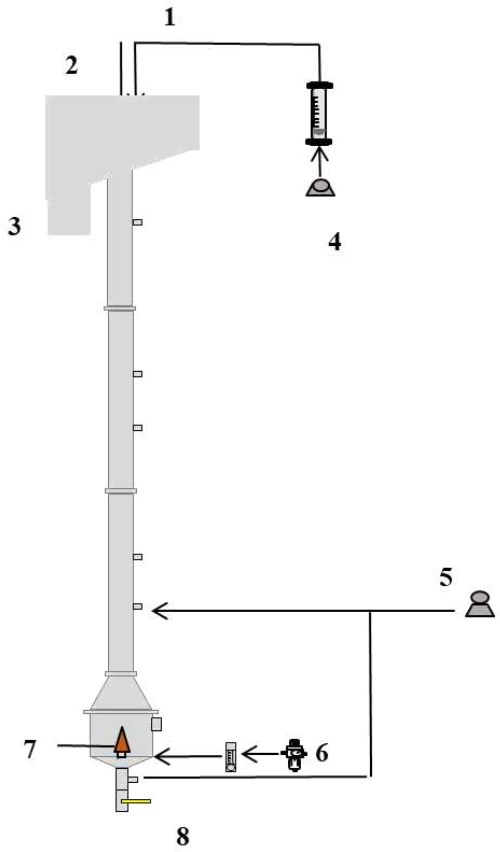

1- Wash water
2- Pulp feed
3- Float collection zone
4- Wash water line
5- Circulating load line
6- Compressed air line
7- Aerator
8- Tailing collection

Source: Mendes *et al.* (2024) (modified).

At the top of the column, a foam washer controlled by a peristaltic pump and a foam overflow tank were installed. At the bottom of the column, an aerator made of sintered bronze

was positioned. The aerator was connected to a compressed air line, with the airflow rate regulated by a rotameter. A circulating load was managed by a peristaltic pump, and the waste was collected via the reject outlet.

Figure 3.6 - Column flotation system

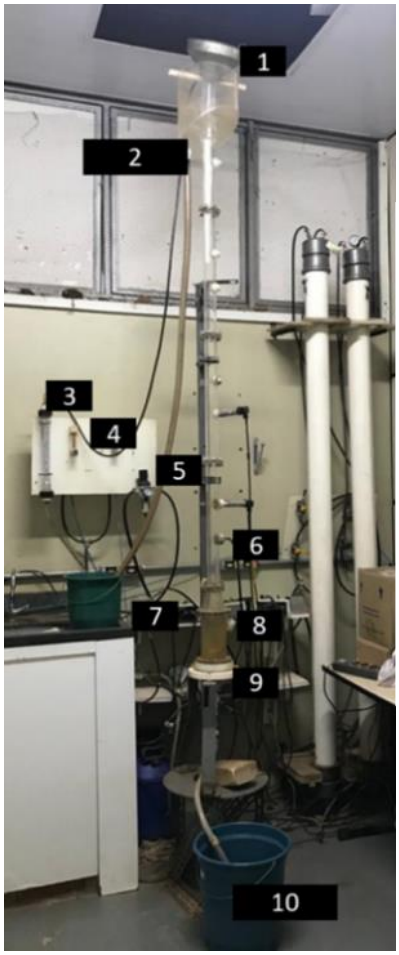

1- Wash water and pulp feed
2- Float collection zone
3- Wash water flow metre
4- Air flow metre
5- Compressed air line
6- Circulating load line
7- Peristaltic pumps of wash water feed
8- Peristaltic pump of recirculation feed
9- Aerator
10- Tailing collection

Source: Author (2025).

Batch flotation tests were conducted in the acrylic column previously described (Figure 3.6). The tests were performed with a circulating load (0.5 L/min) to ensure that the fed particles reached the collection zone. The flowrates of air (80 L/min), the wash water (0.15 L/min) and the circulating load, were initiated before the pulp was fed into the top of the column. The floating material was collected for 17 minutes. Table 3.2 shows the fixed operating conditions in the flotation tests.

These operating conditions were selected based on the best results from preliminary tests and previous work (OLIVEIRA, 2004; REIS,2015; SANTANA, 2011; SANTOS, 2010; SILVA, 2005).

Table 3.2 - Fixed conditions of column flotation

Parameter	Operational condition
Stirring speed in conditioning	1200 rpm
Mass of ore	340 g
Solid percentage in the column	14%
Air flowrate	80 L/min
Circulating load flowrate	0.5 L/min
Wash water flowrate	0.15 L/min
Air pressure in line	3 bar
Flotation time	17 min

Source: Author (2025).

3.5. Characterization of the products

After each flotation test, the floated and non-floated product were oven-dried at 105.0 ± 0.3°C for 24 h. Subsequently, the samples were weighed using an analytical balance with a precision of 1mg, and the chemical composition of each floated product was determined by X-ray fluorescence spectrometry (XRF) using S8 Tiger, Bruker spectrometer, as described in Section 3.1.2.

The quality of the apatite concentrate obtained from the flotation process was evaluated based on the P_2O_5 grade, apatite recovery, and flotation selectivity. The P_2O_5 grade was determined using X-ray fluorescence (XRF), as previously described. For the concentrate to be considered of high quality, the P_2O_5 grade must exceed 30% for fine ore and 24% for ultrafine ore. Apatite recovery for each flotation test was calculated using Equation (3.1).

$$R[\%] = \frac{M_c x_{ap,c}}{M_F x_{ap,F}} . 100 \quad (3.1)$$

where R denotes the recovery of apatite, M_F and M_c correspond to the masses [g] of the feed and the concentrate, respectively, while $x_{ap,F}$ and $x_{ap,c}$ correspond to the calcium oxide grade in the feed and the concentrate respectively. To ensure efficient beneficiation, the recovery rate must exceed 60% for fine ore and 40% for ultrafine ore (OLIVEIRA *et al.,* 2011; VALDERRAMA *et al.,* 2024). These criteria are essential for assessing the effectiveness of the flotation process and its ability to selectively concentrate apatite while minimizing the loss of valuable phosphate minerals.

The use of calcium oxide (CaO) for calculating apatite recovery is justified by the adsorption of the collector onto Ca^{2+} ions, which indirectly facilitates the collection of phosphorus within the apatite mineral. Previous geological studies (OLIVEIRA, 2004; SANTANA, 2011; SANTOS, 2010) have established a relationship between apatite grade and the calcium grade of the mineral deposit, as expressed by Equation (3.2). The CaO/P_2O_5 ratio is a critical indicator of recovery efficiency: a ratio significantly lower than the theoretical value suggests secondary phosphate recovery, while a higher ratio implies calcite recovery. To meet industry requirements, the ratio must remain close to 1.356, ensuring optimal selectivity for apatite flotation.

$$\frac{CaO\ grade}{P_2O_5\ grade} > 1.356 \tag{3.2}$$

The selectivity of the flotation process, particularly between apatite and the principal gangue minerals (Fe_2O_3 and SiO_2), was assessed through selectivity ratios calculated using Equation (3.3) and (3.4). These rations reflect the degree to which the P_2O_5 grade exceeds the grades of the main gangue minerals (Fe_2O_3 and SiO_2). A higher selectivity ratio signifies a more precise separation process (DERHY *et al.,* 2020; OLIVEIRA *et al.,* 2011).

$$SR_{Fe_2O_3} = \frac{P_2O_5 grade}{Fe_2O_3 grade} \tag{3.3}$$

$$SR_{SiO_2} = \frac{P_2O_5 grade}{SiO_2 grade} \tag{3.4}$$

3.6. Response index of flotation process (RI)

Rougher flotation is employed to recover the largest possible amount of valuable minerals (OEDIYANI *et al,* 2020). To evaluate the optimal conditions among the flotation tests, a flotation response index (RI) was developed. This RI measured the combined improvement in both P_2O_5 grade and apatite recovery. Given the greater importance of apatite recovery compared to P_2O_5 grade in the rougher flotation process, a weight of one was assigned to the P_2O_5 grade, while a weight of two was assigned to apatite recovery. The RI for fine and ultrafine ore were calculated using Equations (3.5) and (3.6), respectively.

$$RI_{fine} = \frac{P_2O_5\ grade}{30} + 2.\left(\frac{Apatite\ recovery}{60}\right) \quad (3.5)$$

$$RI_{ultrafine} = \frac{P_2O_5\ grade}{24} + 2.\left(\frac{Apatite\ recovery}{40}\right) \quad (3.6)$$

For fine ore, the RI was set to zero when the P_2O_5 grade was below 30% and apatite recovery was below 60%, as these values represent industry benchmarks. Similarly, for ultrafine ore, the RI was set to zero when the P_2O_5 grade was below 24% and apatite recovery below 40%. These thresholds reflect the minimum acceptable performance standards in the industry for effective flotation outcomes.

3.7. Experimental design

3.7.1. Fine ore

3.7.1.1. Collector type analysis of fine ore

A two-level factorial experimental design was implemented to systematically assess and compare the performance of different collectors, aiming to identify the optimal type for fine flotation. The investigated variables included the collector dosage (x_1), depressant dosage (x_2), and type of collector (x_3), as detailed in Table 3.3, which summarizes the experimental conditions and levels tested in both real and coded values (x_i).

Table 3.3 - Two-level factorial experimental design and codification of the variables

Test	**Collector dosage [ppm] (x_1)**	**Depressant dosage [ppm] (x_2)**	**Type of collector (x_3)**	x_1	x_2	x_3
1	70	700	Rice oil	-1	-1	-1
2	70	700	Agem A3	-1	-1	+1
3	110	700	Rice oil	+1	-1	-1
4	110	700	Agem A3	+1	-1	+1
5	70	900	Rice oil	-1	+1	-1
6	70	900	Agem A3	-1	+1	+1
7	110	900	Rice oil	+1	+1	-1
8	110	900	Agem A3	+1	+1	+1

Source: Author (2025).

Throughout this experimental phase, the pH and solid percentage during conditioning were maintained at fixed values of 12 and 40%, respectively, to ensure that the effects of collector and depressant could be isolated and accurately evaluated. These tests were conducted using a flotation column. Additionally, the system was operated without the addition of a dispersant to eliminate potential confounding factors. The fixed operating conditions of the column flotation are detailed in Table 3.2.

The flotation time was set at 17 minutes, and all tests were conducted in duplicate to ensure reproducibility. The average responses from these tests were calculated and used for analysis. The dosages of the collector and depressant were selected based on the optimal flotation conditions for fine ores identified by Reis *et al.* (2023), with an additional level included to extrapolate beyond these conditions. This experimental design was developed to evaluate the performance of different collectors under controlled conditions.

3.7.1.2. Additional tests for fines

After selecting rice oil as collector, additional tests were conducted to identify the best flotation conditioning parameters for maximizing the recovery and grade of fine particles. The experimental conditions tested during this phase is summarized in Table 3.4. These tests were performed using a flotation column to evaluate the system´s performance under controlled conditions. The primary objective of these preliminary tests was to determine the key variables and conditions that would be further investigated using a central composite design.

The additional tests examined the influence of five independent variables: (1) pH, (2) dosage levels of collector, (3) dosage levels of depressant, (4) solid concentration during conditioning, and (5) dispersant dosage. The dispersant dosage was determined based on the recommendations of Alsafasfeh and Alagha (2017). The solid concentration was set in accordance with the industry standards for conditioning fine ores. Additionally, alternative levels for these variables were explored to identify extreme conditions that could potentially enhance the performance of the flotation process. The fixed operation conditions of the column flotation are detailed in Table 3.2.

Table 3.4 - Additional test for fine particles

Test	pH	Collector dosage [ppm]	Depressant dosage [ppm]	Conditioning solid concentration [%]	Dispersant dosage [ppm]
3	12	110	700	40	0
1	12	70	700	40	0
9	12	30	700	40	0
7	12	110	900	40	0
5	12	70	900	40	0
10	12	30	900	40	0
11	12	110	900	40	250
12	12	110	900	40	2000
13	12	110	900	51	250
14	12	110	900	60	0
15	10	110	900	40	0
16	12	110	1100	40	0
17	12	150	900	40	0
18	10	150	900	40	0
19	10	400	400	40	0

Source: Author (2025).

3.7.1.3. Central composite design (CCD) for fines

A Central Composite Design (CCD) was implemented to systematically evaluate the effects of key variables on the flotation performance of fine particles. The variables investigated in this study included solid concentration during conditioning (x_5), collector dosage (x_1), depressant dosage (x_2), and pH (x_4). These parameters were selected based on their significant influence on the flotation process, as identified during preliminary tests. Table 3.5 present the experimental conditions studied and the corresponding nondimensionalizations of the variables (coded values).

The CCD was structured with an orthogonality factor of 1.48 to ensure better distribution of experimental points across the design space. Additionally, a single replicate conducted at the center point to assess experimental reproducibility and stability. All tests were conducted using a column flotation system, with the fixed operational condition of the column flotation detailed in Table 3.2. The codification of the variables, including their respective ranges and levels, is presented in Table 3.6.

Table 3.5 - Central composite design (CCD)

Test	Conditioning solid concentration [%] (x_5)	Collector dosage [ppm] (x_1)	Depressant dosage [ppm] (x_2)	pH (x_4)	x_5	x_1	x_2	x_4
20	40	350	300	10.00	-1	-1	-1	-1
21	40	350	300	11.50	-1	-1	-1	1
22	40	350	500	10.00	-1	-1	1	-1
23	40	350	500	11.50	-1	-1	1	1
24	40	450	300	10.00	-1	1	-1	-1
25	40	450	300	11.50	-1	1	-1	1
26	40	450	500	10.00	-1	1	1	-1
27	40	450	500	11.50	-1	1	1	1
28	60	350	300	10.00	1	-1	-1	-1
29	60	350	300	11.50	1	-1	-1	1
30	60	350	500	10.00	1	-1	1	-1
31	60	350	500	11.50	1	-1	1	1
32	60	450	300	10.00	1	1	-1	-1
33	60	450	300	11.50	1	1	-1	1
34	60	450	500	10.00	1	1	1	-1
35	60	450	500	11.50	1	1	1	1
36	35.17	400	400	10.80	-1.48	0	0	0
37	64.83	400	400	10.80	1.48	0	0	0
38	50	325.87	400	10.80	0	-1.48	0	0
39	50	474.13	400	10.80	0	1.48	0	0
40	50	400	251.74	10.80	0	0	-1.48	0
41	50	400	548.26	10.80	0	0	1.48	0
42	50	400	400	9.69	0	0	0	-1.48
43	50	400	400	11.91	0	0	0	1.48
44	50	400	400	10.80	0	0	0	0
45	50	400	400	10.80	0	0	0	0

Source: Author.

After analyzing the results obtained from the central composite design (CCD), a simultaneous optimization of multiple responses was performed using the desirability function methodology. This approach, widely recognized in multicriteria optimization, is particularly effective when multiple responses must be optimized concurrently under a single set of experimental conditions. When the optimal settings for each response are located in distinct regions of the experimental space, achieving a compromise becomes increasingly complex.

Modifications in one factor may improve a specific response while negatively affecting another, reinforcing the need for a balanced optimization strategy (BEZERRA *et al.,* 2008; DERRINGER; SUICH, 1980).

Table 3.6 - Variables codification and nondimensionalization

Variable	Experimental range					Nondimensionalization
	-α	-1	0	+1	+α	
Collector dosage	325.87	350	400	450	474.13	$x_1 = \frac{Collector\ dosage - 400}{50}$ (3.7)
Depressant dosage	251.74	300	400	500	548.26	$x_2 = \frac{Depressant\ dosage - 400}{100}$ (3.8)
pH	9.69	10	10.80	11.50	11.91	$x_4 = \frac{pH - 10.8}{0.75}$ (3.9)
Conditioning solid concentration	35.17	40	50	60	64.83	$x_5 = \frac{Solid\ concentration - 50}{10}$ (3.10)

Source: Author (2025).

The desirability function methodology addresses this complexity by transforming each predicted response (y_n) into an individual desirability index (d_n) which is normalized on a scale from 0 (entirely unsatisfactory) to 1 (fully satisfactory). These functions incorporate the performance criteria for each response, facilitating comparison across variables with different units or magnitudes. Equation (3.11) defines the individual desirability function used to maximize the predicted response models:

$$d_n = \begin{cases} 0 & if\ y_n \leq y_n^{min} \\ \left(\frac{y_n - y_n^{min}}{y_n^{max} - y_n^{min}}\right)^r & if\ y_n^{min} \leq y_n \leq y_n^{max} \\ 1 & if\ y_n \geq y_n^{max} \end{cases} \quad (3.11)$$

where y_n^{min} is the minimum acceptable value of y_n, y_n^{max} is the maximum value that is considered desirable, and r is a positive constant. The parameter r is a positive constant that defines the shape of the desirability function. When r=1, the desirability d_n increases linearly with the response y_n.

Subsequently, the individual desirability functions corresponding to each response are combined to calculate the overall desirability index D, as shown in Equation (3.12):

$$D = (d_1, d_2, \dots, d_n)^{1/n} \quad (3.12)$$

This index is calculated as the geometric mean of the individual desirability and ranges from 0 to 1, with higher values of D indicating more favorable and optimal system performance. The optimal operating conditions are determined by applying an algorithm that identifies the combination of factors that maximizes the overall desirability (BURATTI *et al.,* 2017 DERRINGER; SUICH, 1980; VIACAVA; ROURA; AGÜERO, 2015). The desirability calculations were carried out using the STATISTICA software. To validate the optimized models, experiments were conducted under the identified optimal conditions in triplicate. The average values were then compared with the predicted results to assess the accuracy and reliability of the models.

3.7.2. Ultrafine ore

3.7.2.1. Preliminary test of ultrafine ore using cell flotation

For the preliminary tests involving the flotation of ultrafine ore, Agem A3 was selected as the primary collector. The choice was based on its current application in the industry for the same type of ore, though for larger particles. Additionally, rice oil and Flotigam 5806 were tested as alternative collectors to evaluate their performance. Detailed specifications regarding the fixed conditions for these tests are shown in Table 3.1.

The primary objective of these preliminary tests was to identify the critical independent variables and conditions that would subsequently be explored through a central composite design. The experimental conditions applied in the preliminary flotation tests of the ultrafine ore, conducted in a mechanical cell, are presented in Table 3.7.

To this end, the tests investigated the impact of six independent variables: collector type, pH, collector dosage, depressant dosage, solid concentration during conditioning, and flotation solid concentration. These variables were selected based on their potential influence on the flotation performance of ultrafine ore derived from tailings.

Table 3.7 - Conditions of preliminary tests using cell flotation of ultrafine ore

Test	Collector type	Collector dosage [ppm]	Depressant dosage [ppm]	pH	Conditioning solid concentration [%]	Flotation solid concentration [%]
1	Agem A3	550	1200	12	52.78	38.78
2	Agem A3	110	1200	12	26.09	16.67
3	Agem A3	80	1400	12	21.05	11.43
4	Agem A3	80	1400	12	28.24	13.41
5	Agem A3	80	1400	12	31.78	17.35
6	Agem A3	80	2700	12	28.24	13.41
7	Agem A3	80	2700	9.5	28.24	13.41
8	Agem A3	80	3200	9.5	28.24	13.41
9	Agem A3	110	2700	9.5	28.24	13.41
10	Agem A3	110	3200	9.5	28.24	13.41
11	Agem A3	220	2700	9.5	28.24	13.41
12	Rice oil	220	2700	9.5	28.24	13.41
13	Flotigam 5806	220	2700	9.5	28.24	13.41
14	Agem A3	220	3200	9.5	28.24	13.41
15	Agem A3	80	2700	9	28.24	13.41
16	Agem A3	80	3200	9	28.24	13.41
17	Agem A3	80	3500	9	28.24	13.41
18	Agem A3	80	3700	9	28.24	13.41
19	Agem A3	80	3900	9	28.24	13.41
20	Agem A3	220	2700	9	28.24	13.41
21	Agem A3	220	3200	9	28.24	13.41
22	Agem A3	80	3500	9	30.68	14.84
23	Agem A3	80	3500	9	32.97	16.22
24	Agem A3	100	3500	9	32.97	16.22
25	Agem A3	100	3500	9	35.11	17.55
26	Agem A3	100	3500	9	37.11	18.85
27	Agem A3	100	3500	9	39.00	20.10
28	Agem A3	100	3500	9	40.78	21.32

Source: Author.

3.7.2.2. Collector analysis for ultrafine ore in column flotation

A two-level factorial experimental design was implemented to systematically evaluate the best collector type for ultrafine apatite flotation. The study investigated three critical

variables: collector dosage (x_1), depressant dosage (x_2) and collector type (x_3), as presented in Table 3.8. To isolate the effects of these variables, the pH and solid concentration during conditioning were maintained at fixed values of 12 and 40%, respectively. Furthermore, no dispersant was added to the system to eliminate potential confounding effects. The fixed operational conditions of the column flotation are detailed in Table 3.2

Table 3.8 - Two level factorial of ultrafine tailing ore

Test	**Collector dosage [ppm] (x_1)**	**Depressant dosage [ppm] (x_2)**	**Type of collector (x_3)**	x_1	x_2	x_3
29	50	700	Rice oil	-1	-1	-1
30	50	700	Agem A3	-1	-1	+1
31	110	700	Rice oil	+1	-1	-1
32	110	700	Agem A3	+1	-1	+1
33	50	900	Rice oil	-1	+1	-1
34	50	900	Agem A3	-1	+1	+1
35	110	900	Rice oil	+1	+1	-1
36	110	900	Agem A3	+1	+1	+1

Source: Author.

All tests were conducted using a column flotation system. To increase the reliability of the findings, each test was performed in duplicate, and the average responses were calculated and used for further analysis. The dosages of the collector and depressant were selected based on the optimal flotation conditions for fine ores identified by Reis *et al.* (2023), with an additional level incorporated to extend the investigations beyond these established conditions. This experimental design was developed to assess the performance of different collectors under controlled and standardized conditions.

3.7.2.3. Additional tests using column flotation

After identifying rice oil as the collector, additional tests were performed to evaluate the effect of five critical variables on ultrafine ore flotation performance. Table 3.9 presents the detailed experimental conditions analyzed during the additional tests. These variables included dispersant dosage, conditioning solid concentration, pH, collector and depressant dosages.

Table 3.9 - Additional tests conditions for ultrafine ore flotation

Test	Dispersant dosage[ppm]	Conditioning solid concentration [%]	pH	Collector dosage[ppm]	Depressant dosage[ppm]
31	0	40	12	110	700
37	250	40	12	110	700
38	2000	40	12	110	700
39	0	40	12	70	700
40	125	40	12	70	700
41	250	40	12	70	700
42	400	40	12	70	700
43	0	50	12	70	700
44	0	50	10	70	700
45	0	20	12	70	700
46	0	40	10	70	700
47	250	40	10	70	700
29	0	40	12	50	700
35	0	40	12	110	900
48	0	40	12	70	900
33	0	40	12	50	900
49	0	40	12	70	1100
50	0	40	12	70	1300
51	0	40	12	70	1500
52	0	40	12	70	1900
53	0	40	10	400	400
54	0	40	12	400	400
55	0	35	10	80	2618
56	0	35	12	80	2618
57	0	35	12	80	3000
58	250	35	12	80	2618
59	400	35	12	80	2618

Source: Author.

These tests aimed to identify the best ranges and conditions for the variables under investigation by assessing the impact of each variable on the P_2O_5 grade and apatite recovery. The results of these tests provided a foundation for the design of subsequent experiments. All tests were performed using a column flotation system, with the fixed operational conditions detailed in Table 3.2. Dispersant dosage was determined based on recommendations by Alsafasfeh and Alagha (2017), while the solid concentration during conditioning was set in

accordance with industry standards for fine ore processing. To explore potential improvements in flotation efficiency, additional levels of these variables were examined, including extreme conditions that could reveal new understanding into the process. The dosage of the collector and depressant, along with the pH levels, were extrapolated from the conditions established during the earlier analysis of collector type. This approach ensured consistency and comparability across all experimental phases.

During the additional experimental phase, Tests 60 and 61 was conducted under similar conditions to Test 41, except for conditioning time and agitation speed to examine the effects of conditioning time and agitation speed on the flotation efficiency of ultrafine ore. This replication aimed to assess whether adjustments to these specific parameters could improve the overall performance of the flotation process for ultrafine particle system. The specific conditions and parameter settings utilized in this analysis are presented in Table 3.10.

Table 3.10 - Specific conditions and parameters analyzing conditioning time and agitation speed

Test	Dispersant dosage [ppm]	Conditioning solid concentration [%]	pH	Collector dosage [ppm]	Depressant dosage [ppm]	Conditioning time for each reagent [min]	Conditioning stirring speed [rpm]
41	250	40.00	12	70	700	5	1200
60	250	40.00	12	70	700	10	1200
61	250	40.00	12	70	700	5	1500

Source: Author.

3.7.2.4. Evaluation of dispersant influence on ultrafine ore flotation in column flotation

This study aimed to enhance the understanding of how dispersant addition affects flotation performance by analyzing two key response variables: P_2O_5 grade and apatite recovery. The primary objective was to determine whether the use of a dispersant improves flotation efficiency or if better results could be achieved without its addition in the flotation of ultrafine ore. To systematically investigate this effect, a two-level factorial experimental design was implemented, focusing on three main process variables: collector dosage (x_1), depressant dosage (x_2), and dispersant dosage (x_6). The specific experimental conditions tested levels and variables codifications are detailed in Table 3.11.

Table 3.11 - Two factorial experimental design for dispersant analysis

Test	Collector dosage [ppm] (x_1)	Depressant dosage [ppm] (x_2)	Dispersant dosage [ppm] (x_6)	x_1	x_2	x_6
29	50	700	0	-1	-1	-1
62	50	700	250	-1	-1	+1
39	70	700	0	+1	-1	-1
41	70	700	250	+1	-1	+1
33	50	900	0	-1	+1	-1
63	50	900	250	-1	+1	+1
48	70	900	0	+1	+1	-1
64	70	900	250	+1	+1	+1

Source: Author.

To ensure a controlled evaluation, the pH and solid concentration during conditioning were maintained at fixed values of 12 and 40%, respectively. This approach allowed for an accurate assessment of the dispersant's influence while isolating the effects of the collector and depressant. All flotation experiments were conducted using a flotation column, with its fixed operational parameters comprehensively described in Table 3.2.

Each test was performed in duplicate to enhance the reliability of the results, and the average response values were calculated for subsequent analysis. The dosage levels of the dispersant, collector, and depressant were established based on preliminary investigations into ultrafine flotation utilizing a column flotation system. By conducting the experiments under controlled and reproducible conditions, the results are expected to provide evidence regarding the necessity of dispersant addition for the effective processing of ultrafine ore in flotation.

3.7.2.5. Central composite design of ultrafine ore

Based on the findings and analyses from previous phases of this study, which highlighted the significant influence of key variables on the flotation process, a Central Composite Design (CCD) was implemented to systematically investigate the effects of collector dosage (x_1) and depressant dosage (x_2) on the flotation performance of ultrafine particles. These previous phases, detailed in Sections 3.7.2.2 to 3.7.2.4, provided the foundation for determining the experimental conditions and parameter ranges, ensuring a comprehensive understanding of the flotation behavior of ultrafine particles.

The CCD was designed with a rotatability factor of 1.41 to ensure a uniform distribution of experimental points across the design space, thereby enhancing the robustness of the statistical analysis. To evaluate the reproducibility and stability of the experimental setup, a single replicate was conducted at the center point of the design. The codification of the variables, including their respective ranges and levels, is comprehensively outlined in Table 3.12. Additionally, Table 3.13 presents the experimental conditions studied, and the coded values of the variables.

Table 3.12 - Nondimensionalization of CCD variables of ultrafine tailing ore

Variable	**Experimental range**					**Nondimensionalization**
	-α	**-1**	**0**	**+1**	**+α**	
Collector dosage	22	30	50	70	78	$x_1 = \frac{Collector\ dosage - 50}{20}$ (3.13)
Depressant dosage	417	500	700	900	983	$x_2 = \frac{Depressant\ dosage - 700}{200}$ (3.14)

Source: Author.

Table 3.13 - CCD conditions of ultrafine ore flotation

Test	**Collector dosage [ppm] (x_2)**	**Depressor dosage [ppm] (x_3)**	x_1	x_2
65	30	500	-1	-1
66	30	900	-1	1
67	70	500	1	-1
64	70	900	1	1
68	22	700	-1.41	0
69	78	700	1.41	0
70	50	417	*0*	-1.41
71	50	983	0	1.41
72	50	700	0	-0
73	50	700	0	0

Source: Author.

All flotation tests were performed using a column flotation system with a fixed dispersant dosage of 250 ppm. The fixed operational parameters of the system are detailed in Table 3.2 of the Methodology. By conducting the experiments under controlled and reproducible conditions, this study aimed to provide deeper insights into the flotation

performance of ultra-fine particles and to identify the best conditions for their recovery. The results obtained from this experimental framework are expected to contribute significantly to the understanding and optimization of ultrafine particle flotation processes.

Following the analysis of the results obtained from the central composite design (CCD), the optimization of the ultrafine ore sample was conducted using the same methodology previously applied to the fine ore sample. Specifically, the desirability function approach was employed to facilitate the simultaneous optimization of multiple responses, as defined in Equations 3.11 and 3.12. This method converts each predicted response (y_n) into an individual desirability index (d_n) normalized on a scale from 0 to 1, thereby enabling the integration of responses with different units and magnitudes (BEZERRA *et al.,* 2008; BURATTI *et al.,* 2017; DERRINGER; SUICH, 1980; VIACAVA; ROURA; AGÜERO, 2015).

The overall desirability index was computed as the geometric mean of the individual desirability indices, and an optimization algorithm was applied to determine the optimal combination of variables that maximized this index. All calculations were performed using STATISTICA software.

To validate the optimized conditions, flotation tests were conducted in triplicate under the identified parameters. The average experimental results were then compared with the predicted values to assess the accuracy and reliability of the models.

4. RESULTS AND DISCUSSIONS

4.1. Feed samples characterization

4.1.1. Particle size distribution

Particle size distribution (PSD) of both ore samples was determined using laser diffraction technique with a Malvern Mastersizer® equipment. A sigmoidal model (Equation 1) was fitted to the experimental data of both samples, and the estimated parameters are presented in Table 4.1.

$$X = \frac{1}{1 + \left(\frac{d_{50}}{d}\right)^{p}} \quad (1)$$

Table 4.1 - Estimated parameters of particles size distribution

Sample	**Results of regression analysis**		
Fine ore	Fitted parameters	d_{50} [µm]	p
	Value	34.87	1.87
	Standard error	0.30	0.03
	R^2	0.999	
	Sauter mean diameter [µm]	17.98	
Ultrafine ore	Fitted parameters	d_{50} [µm]	p
	Value	4.29	1.45
	Standard error	0.07	0.03
	R^2	0.996	
	Sauter mean diameter [µm]	2.43	

Source: Author (2025).

The analysis revealed that 50% of the fine particles had diameter below 34.87µm, whereas for the ultrafine particles, this value was 4.29 µm. Figures 4.1 and 4.2 illustrate the PSD derived from experimental data and the sigmoidal model for the fine and ultrafine ore samples, respectively. These figures highlight a notable difference in PSD, d_{50} and Sauter mean diameter between the two samples. Furthermore, the d_{80} value for ultrafine particles is 11.91 µm, compared to 76.42 µm for fine particles. These results demonstrate a substantial variation in the size characteristics of the samples, which is expected to significantly influence their behavior during the flotation process.

Figure 4.1 - Particle size distribution of fine ore

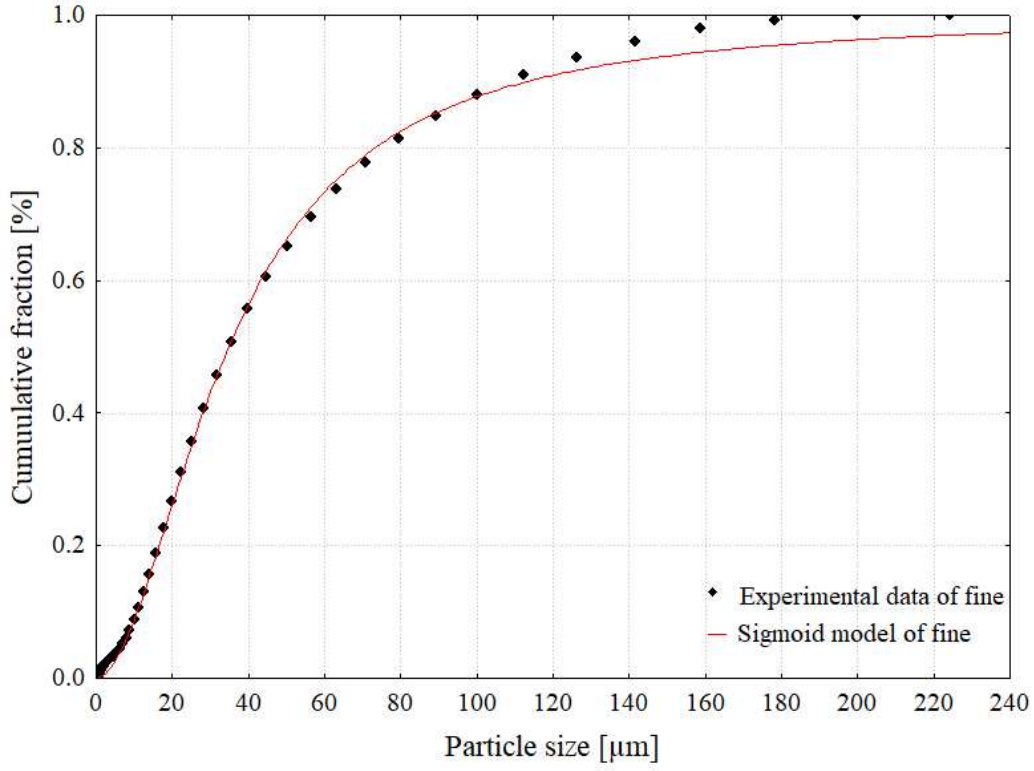

Source: Author (2025).

Figure 4.2 - Particle size distribution of ultrafine ore

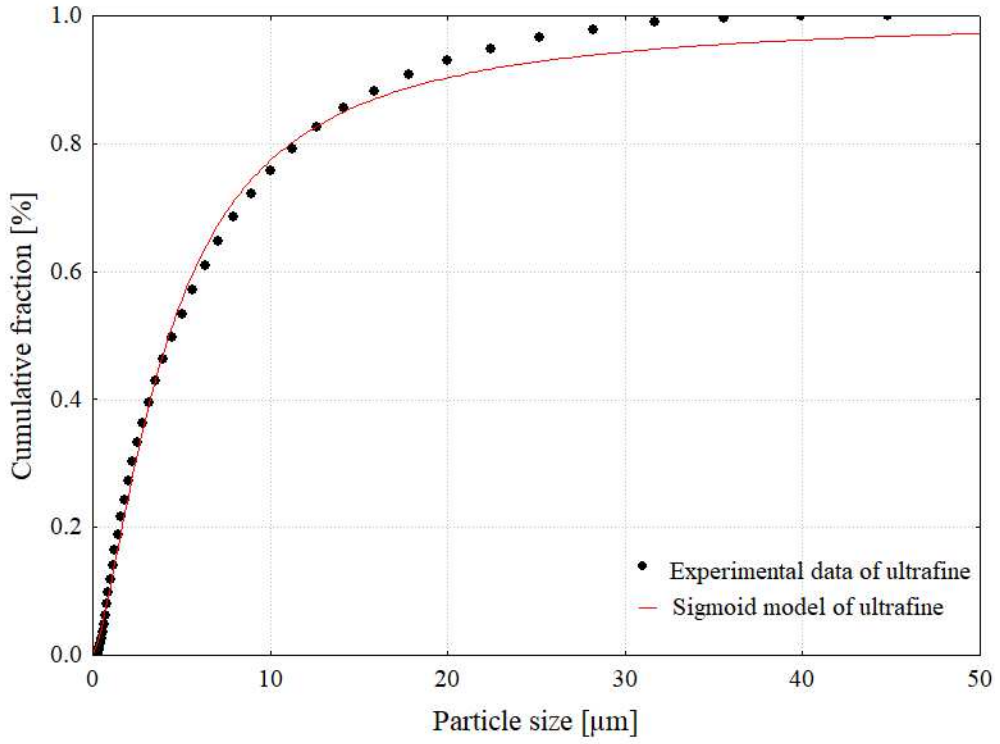

Source: Author (2025).

4.1.2. Chemical content and mineralogical analysis

To further characterize the feed material, the chemical composition of both fine and ultrafine ore feed samples was determined through X-ray fluorescence (XRF) analysis, as presented in Table 4.2.

Table 4.2 - Chemical composition of feed flotation samples

Sample		**Fine**	**Ultrafine**
Chemical composition [%]	P_2O_5	16.33	12.88
	CaO	21.07	16.38
	Fe_2O_3	19.77	34.86
	SiO_2	25.90	17.00
	TiO_2	8.45	1.74
	Al_2O_3	1.66	3.20
	CeO_2	1.41	2.11
	MgO	1.25	1.85
	MnO	0.66	2.39
	La_2O_3	0.56	0.68
	SrO	0.52	0.55
	ZrO_2	0.49	0.33
	BaO	0.42	2.99
	Nd_2O_3	0.41	0.45
	Nb_2O_5	0.32	0.82
	Pr_6O_{11}	0.17	0.30
	K_2O	0.16	0.10
	CuO	0.06	0.13
	ZnO	0.05	0.10
	NiO	0.04	0.09
	ThO_2	0.04	0.08
	SO_3	0.00	0.60
	Y_2O_3	0.00	0.03
	PbO	0.00	0.05
	LOI	0.14	0.28

Source: Author (2025).

The results indicate that the predominate gangue minerals in both ore samples are ferric oxide (Fe_2O_3) and the silicon dioxide (SiO_2). These findings align with the mineralogical

analysis, as the presence of goethite (source of Fe_2O_3) and quartz (source of SiO_2) in ultrafine ore sample corroborates the XRF data.

The mineralogical composition of the flotation feed samples was determined by X-ray diffraction (XRD) (see Figures I.1 and I.2 in Appendix I for the fine and ultrafine samples, respectively). The XRD analysis identified multiple minerals in each sample: the fine ore contained apatite ($Ca_5(PO_4)_3(F,Cl,OH)$), quartz (SiO_2), goethite ($FeO(OH)$), siderite ($FeCO_3$), hematite (Fe_2O_3), and anatase (TiO_2), while the ultrafine ore comprised apatite ($Ca_5(PO_4)_3(F,Cl,OH)$), quartz (SiO_2), calcite ($CaCO_3$), chlorite-serpentine $(Mg,Fe)_3Si_2O_5(OH)_4$, goethite ($FeO(OH)$), vermiculite $(Mg,Fe,Al)_3(Al,Si)_4O_{10}(OH)_2.4H_2O$, analcime ($NaAlSi_2O_6.H_2O$), hematite($Fe_2O_3$), and magnetite ($Fe_3O_4$). Notably, the presence of chlorite-serpentine, vermiculite, goethite, hematite, and magnetite in the ultrafine sample is of particular concern, as these minerals are prone to forming slime coatings. Such coatings adversely affect flotation performance by impeding reagent adsorption and diminishing apatite recovery (PAIVA; MONTE; GASPAR, 2011; SIS; CHANDER, 2003; YU et al., 2024). Characterizing these minerals provides critical insights into the ore's flotation behavior, enabling the development of targeted strategies to mitigate these challenges.

4.2. Flotation results of fine apatite ore derived from tailings

4.2.1. Collector type analysis for fine ore

A two-level factorial experimental design was implemented to systematically assess the optimal collector type for fine ore. The variables investigated in this study included collector dosage (x_1), depressant dosage (x_2), and type of collector (x_3). This design aimed to evaluate the performance of different collectors under controlled conditions, focusing on two vegetable oils-based collectors: rice oil, a conventional collector, and Agem A3, an alternative collector.

Rice oil is widely used in Brazil as cost-effective and efficient collector for the froth flotation of low-grade phosphate ores. Despite its advantages, the use of fatty acids as collectors often results in suboptimal flotation performance, particularly for fine ores. This is primarily due to their adsorption on calcium sites, which has been documented in literature. This lack of selectivity may compromise the overall efficiency of the flotation process (CAO, *et al.*, 2015; CARNEIRO *et al.,* 2023; RUAN *et al.*, 2019). To overcome this limitation, Agem A3 was tested as an alternative collector to evaluate its potential for improved selectivity and flotation efficiency.

Table 4.3 presents the flotation conditions and results obtained from the two-level factorial experimental design. Although, all tested conditions achieved P_2O_5 grade above 30%, apatite recovery was below 60%, resulting in an RI of zero for all conditions. The process demonstrated excellent reproducibility, with mean standard deviations of 0.468 for P_2O_5 grade and 1.388 for apatite recovery, and mean coefficients of variation of 0.013 and 0.031, respectively. Moreover, the CaO/P_2O_5 ratio in sample A3 remained practically constant, indicating the recovery of apatite.

Table 4.3 - Two-level factorial experimental design results

Test	**Collector dosage [ppm] (x_1)**	**Depressant dosage [ppm] (x_2)**	**Type of collector (x_3)**	**P_2O_5 grade [%] (y_g)**	**Apatite recovery [%] (y_r)**	$\frac{CaO}{P_2O_5}$
1	70	700	Rice oil	36.76	35.69	1.40
2	70	700	Agem A3	35.45	41.4	1.44
3	110	700	Rice oil	35.80	52.62	1.41
4	110	700	Agem A3	34.75	54.74	1.40
5	70	900	Rice oil	35.42	43.66	1.45
6	70	900	Agem A3	36.50	41.41	1.37
7	110	900	Rice oil	35.32	57.49	1.40
8	110	900	Agem A3	35.94	54.68	1.36

Source: Author (2025).

The experimental results formed the basis for statistical analysis. The independent variables were transformed into dimensionless variables as shown in Table 3.3 of Methodology Chapter. The statistically significant effects on P_2O_5 grade and apatite recovery, with p-value below 0.1, are presented in Table 4.4 The coefficient of determination (R^2) values was 0.910 for P_2O_5 grade and 0.988 for apatite recovery, indicating a strong correlation between the variables and the observed responses.

Table 4.4 - Statistical results: effects of the factors for the P_2O_5 grade and apatite recovery

Factor	**P_2O_5 grade**		**Apatite recovery**	
	Effect	**p-value**	**Effect**	**p-value**
Mean	35.74	0.00	47.71	0.00
x_1	-0.58	0.02	14.34	0.00
x_2	-	-	3.20	0.02
x_2x_3	1.01	0.00	-3.22	0.02

Source: Autor (2025).

Analysis of the significant factors affecting flotation performance revealed that P_2O_5 grade was primarily influenced by collector dosage (x_1) and the interaction between the collector type and depressant dosage (x_2x_3). For apatite recovery, the significant factors included collector dosage (x_1), depressant dosage (x_2), and the interaction between collector type and depressant dosage (x_2x_3). These results indicate that the dosages of the collector and depressant had a greater impact on flotation performance than the collector type. Furthermore, the effect of collector type was not statistically significant for either the P_2O_5 grade or apatite recovery when considered individually; it was significant only through its interaction with depressant dosage.

However, when analyzing selectivity, rice oil demonstrated superior performance compared to Agem A3, particularly in Fe_2O_3 removal, as it achieved higher selectivity ratio values at lower depressant dosages and maintained better SiO_2 removal across all tested conditions (Table 6.1 in Appendix II). Based on these findings, rice oil was selected as the collector for subsequent experiments due to its widespread use, cost-effectiveness and superior selectivity.

4.2.2. Additional tests for fine ore

After rice oil was chosen as a collector, additional tests were conducted to evaluate the impact of five key variables: pH, collector dosages, depressant dosages, solid concentration during conditioning, and dispersant dosages. The quality of the flotation products was assessed based on P_2O_5 grade, apatite recovery, and CaO/ P_2O_5 ratio in the floated product. As previously noted, the industrial specifications for fine ore flotation require a minimum P_2O_5 grade of 30% and apatite recovery rate of 60%. However, the previous results showed that achieving high values for both parameters simultaneously proved challenging under the tested conditions.

Table 4.5 presents the experimental conditions and results of the additional flotation tests, which were designed to identify the best conditions for subsequent Central Composite Design (CCD) studies. While all experiments achieved a P_2O_5 grade of at least 30% and CaO/P_2O_5 ratio were slightly above the target (1.356), apatite recovery reached the required industrial specifications only in Tests 17, 18, and 19. Among these, Test 19 yielded the highest response index (RI) of 3.86, with apatite recovery of 81.29% and P_2O_5 grade of 34.36%.

It was observed that reducing collector dosages led to higher P_2O_5 grade; however, this significantly decreased apatite recovery, particularly when compared to tests with 40% solid

concentration with the same depressant dosages. Conversely, increasing depressant dosages from 700 to 900, while maintaining other parameters constant, improved apatite recovery. This improvement may be attributed to enhanced froth stability and increased hydrodynamic entrainment, which the attachment of fine particles to bubbles could had been hindered, thereby promoting apatite recovery (FARROKHPAY; FILLIPOV; FORNASIERO, 2020;). However, when the depressant dosage was increased to 1100 ppm (Test 16), the P_2O_5 grade rose to 37.48%, which suggests that high-intensity conditioning may have generated micro- and nanobubbles, facilitating the formation of aggregates and their subsequent coalescence with air bubbles in the flotation column, promoting true flotation. However, apatite recovery declined substantially to 39.33%. This result suggests that very high depressant dosages can enhance P_2O_5 grade by effectively suppressing gangue mineral flotation but may also lead to a significant reduction in apatite recovery (SIS; CHANDER, 2003). This observation is further supported by the selectivity ratios SR_{Fe2O3} and SR_{SiO2} (see Table 6.2 in Appendix II), which indicate improved separation efficiency under these conditions.

Table 4.5 - Additional tests for fine ore

Test	pH	Collector dosage [ppm]	Depressant dosage [ppm]	Conditioning solid concentration [%]	Dispersant dosage [ppm]	P_2O_5 grade [%]	Apatite recovery [%]	$\frac{CaO}{P_2O_5}$	RI
3	12	110	700	40	0	35.80	52.62	1.41	0
1	12	70	700	40	0	36.76	35.69	1.40	0
9	12	30	700	40	0	37.24	20.79	1.41	0
7	12	110	900	40	0	35.32	57.49	1.40	0
5	12	70	900	40	0	35.42	43.66	1.45	0
10	12	30	900	40	0	36.62	25.11	1.42	0
11	12	110	900	40	250	36.35	49.30	1.43	0
12	12	110	900	40	2000	36.49	48.74	1.38	0
13	12	110	900	51	250	34.77	57.25	1.39	0
14	12	110	900	60	0	36.82	59.10	1.42	0
15	10	110	900	40	0	38.68	24.76	1.44	0
16	12	110	1100	40	0	37.48	39.33	1.45	0
17	12	150	900	40	0	34.80	64.39	1.41	3.31
18	10	150	900	40	0	34.66	72.46	1.45	3.57
19	10	400	400	40	0	34.36	81.29	1.39	3.86

Source: Author (2025).

To further improve flotation performance, Tests 11 and 12 were conducted to examine the effect of dispersant addition, compared to Test 7 (performed at the same conditions for other variables). While dispersant addition improved P_2O_5 grade, it also led to a nearly 10% reduction in apatite recovery. Additionally, Test 13, conducted under the same condition as Test 11 but with a higher solid concentration during conditioning (51%), almost achieved the minimum required apatite recovery (57.25%). However, this improvement was accompanied by a 1.58% decrease in P_2O_5 grade. Given the increase costs associated with dispersant use and its overall suboptimal flotation performance relative to Test 7, its application in fine flotation was considered unnecessary for subsequent experiments.

Test 14 was carried out in the same conditions of Test 7 to evaluate the effect of solid concentration during conditioning. The results indicated that 60% of solid concentrations (Test 14) improved all response metrics, thus enhancing flotation performance. This aligns with the literature suggesting that higher solid concentrations can promote greater recoveries while maintain concentrate quality (ALSAFASFEH; ALAGHA, 2017; TEAGUE; LOLLBACK, 2012). Based on these findings, the conditioning solid concentration was set withing a range of 40% to 60% for further studies.

To maximize flotation performance, experiments were conducted at pH levels of 10 (Test 15) and 12 (Test 7) to identify the most favorable pH range. The results indicated that pH 10 was more conducive to apatite flotation, as it promoted more effective collector adsorption onto the apatite surface (ALSAFASFEH; ALAGHA, 2017; VALDERRAMA *et al.*, 2024). Test 15 achieved the highest P_2O_5 grade (38.68%), however, it also resulted in a substantial reduction in apatite recovery by nearly 33%. Conversely, when a higher collector dosage was applied under the same conditions (Tests 17 and 18), pH 10 yielded improved flotation performance, achieving an apatite recovery of 72.46% while maintaining a stable P_2O_5 grade (Test 18). Thus, the pH range between 10 and 12 was selected for more investigations into its effect on fine ore flotation performance.

Based on the results of Tests 17 and 18, it was observed that a lower collector dosage and higher depressant dosage could be hinder the flotation performance. Consequently, the conditions were adjusted by significantly increasing the collector dosage (400 ppm), reducing the depressant dosage (400 ppm), maintaining a solid concentration of 40%, and setting the pH at 10. These adjustments resulted in Test 19, which achieved the highest performance among the preliminary experiments. This test provided a basis for establishing the variables and ranges for the subsequent CCD study. Moreover, it achieved a lower CaO/P_2O_5 ratio, which signifies that most of the calcium present is associated with apatite.

Notably from Tests 17 to 19, higher collector dosages led to increased apatite recovery but resulted in a reduction in P_2O_5 grade and selectivity ratios for both gangue minerals (see table 6.2 in Appendix II). This effect may be attributed to greater collector availability for selective adsorption onto the apatite surface, possibly combined with non-selective adsorption onto gangue minerals, which might dilute the concentrate (ELBENDARZ; ALEKSANDROVA; NIKOLAEVA, 2019). Furthermore, higher selectivity ratios were associated with significantly reduction of apatite recovery, falling below industrial requirements. These findings underscore the need to balance collector and depressant dosages, solid concentration during conditioning and pH settings, to improve flotation performance in terms of apatite recovery and P_2O_5 grade.

4.2.3. Central composite design for fine ore

After selecting all parameters based on previous tests, Table 4.6 presents the experimental conditions and corresponding results obtained from CCD tests for fine ore flotation. The variables analyzed included solid concentration during conditioning (x_5), collector dosage (x_1), depressant dosage (x_2) and pH (x_4). Central-point replication analysis demonstrated high reproducibility, yielding standard deviations of 0.075 (P_2O_5 grade) and 0.160 (apatite recovery), with corresponding coefficients of variation of 0.002 for both response variables.

The results indicate that most tests achieved P_2O_5 grades exceeding 30% and apatite recovery above 60%, except for Test 28, which yielded a P_2O_5 grade of 29.90%. All tests exhibited CaO/P_2O_5 ratios ranging from 1.38 to 1.45, consistent with phosphorus originating from apatite sources. To facilitate data interpretation, Figure 4.3 illustrates apatite recovery and P_2O_5 grade obtained from the CCD tests for fine ore. While P_2O_5 grades remained relatively stable across the tested conditions, apatite recovery exhibited greater variability. The highest flotation performance for fine ore was observed in the Test 39 which achieved a response index of 4.21, a P_2O_5 grade of 34.62% and an apatite recovery of 91.58%. This outcome was obtained with the highest collector dosage (474.13 ppm), while the other variables were maintained at the central point of the CCD.

The increase in collector dosage likely intensified the coating of the apatite surface, enhancing its hydrophobicity. Additionally, the formation of tiny bubbles during high-intensity conditioning may have promoted the creation of two-stage aggregates, which subsequently facilitated their coalescence with air bubbles in the flotation column. This process favored the

formation of aggregated particle-bubble structures, enhancing true flotation and mitigating the reduction in P_2O_5 grade (SANTOS, 2005; WANG; LIU, 2021).

Table 4.6 - Flotation results and corresponding conditions of CCD

Test	Conditioning solid concentration [%] (x_5)	Collector dosage [ppm] (x_1)	Depressant dosage [ppm] (x_2)	pH (x_4)	P_2O_5 grade [%] (y_g)	Apatite recovery [%] (y_r)	$\frac{CaO}{P_2O_5}$	RI
20	40	350	300	10.00	33.43	81.42	1.43	3.83
21	40	350	300	11.50	35.7	82.14	1.41	3.93
22	40	350	500	10.00	35.02	81.92	1.40	3.9
23	40	350	500	11.50	36.11	77.3	1.41	3.78
24	40	450	300	10.00	33.85	87.19	1.39	4.03
25	40	450	300	11.50	35.27	85.91	1.40	4.04
26	40	450	500	10.00	34.72	84.14	1.38	3.96
27	40	450	500	11.50	34.40	79.26	1.38	3.79
28	60	350	300	10.00	29.90	84.14	1.34	0
29	60	350	300	11.50	34.46	82.92	1.35	3.91
30	60	350	500	10.00	35.17	85.21	1.39	4.01
31	60	350	500	11.50	36.14	85.9	1.36	4.07
32	60	450	300	10.00	33.55	88.25	1.37	4.06
33	60	450	300	11.50	35.03	87.96	1.40	4.1
34	60	450	500	10.00	34.24	89.44	1.42	4.12
35	60	450	500	11.50	35.03	84.79	1.42	3.99
36	35.17	400	400	10.80	34.16	80.34	1.40	3.82
37	64.83	400	400	10.80	33.2	84.2	1.34	3.91
38	50	325.87	400	10.80	34.66	87.95	1.40	4.09
39	50	474.13	400	10.80	34.62	91.58	1.38	4.21
40	50	400	251.74	10.80	34.02	85.1	1.42	3.97
41	50	400	548.26	10.80	35.67	85.19	1.36	4.03
42	50	400	400	9.69	35.37	86.39	1.39	4.06
43	50	400	400	11.91	35.34	84.5	1.39	3.99
44	50	400	400	10.80	34.59	85.82	1.36	4.01
45	50	400	400	10.80	34.74	86.14	1.38	4.03

Source: Author (2025).

In contrast, the combination of high collector dosage and a pH of 10.8 likely reduced surface tension, as rice oil soap may act as a surfactant. This reduction in surface tension could have facilitated the formation of smaller and more stable bubbles, thereby potentially enhancing

flotation performance (MENDES *et al.*, 2024; VALDERRAMA *et al.*, 2024). Consequently, this process enhanced apatite recovery by also promoting non-selective mechanisms, such as mechanical entrapment and hydrodynamic entrainment, which are particularly prevalent in fine particles flotation systems (FENG; ALDRICH, 1999). However, despite the influence of these mechanisms, the depressant dosage and the solid concentration during conditioning were sufficient to improve selectivity, resulting in high apatite recovery without significantly compromising the P_2O_5 grade.

Figure 4.3 - Apatite recovery and P_2O_5 grade of CCD tests of fine ore

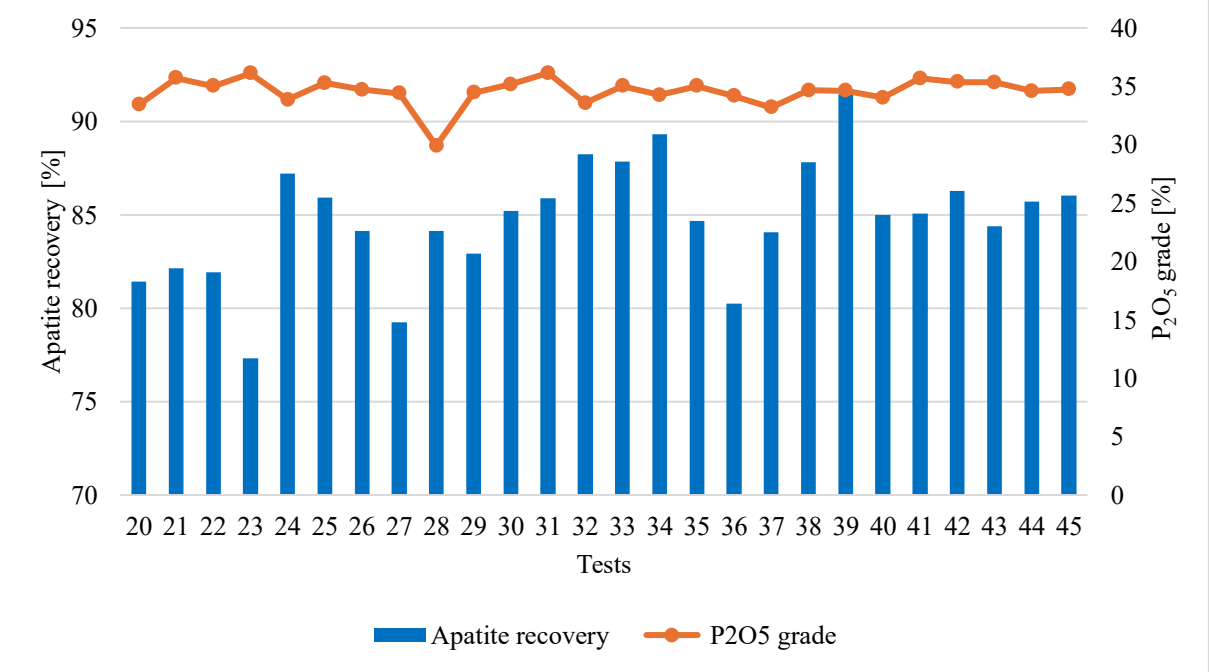

Source: Author (2025).

Although high apatite recoveries are often associated with entrainment, which can compromise selectivity (WANG *et al.,* 2016), effective flotation of fine particles requires a balance between true flotation and entrainment mechanisms to maximize both recovery and grade (GEORGE; NGUYEN; JAMESON, 2004; REIS *et al.*, 2019). In this study, the simultaneous occurrence of these mechanisms contributed to the favorable performance observed under the tested conditions. These results highlight the challenges associated with fine ore flotation and reinforce the necessity of balancing all parameters to optimize performance (Table 4.6).

To further analyze the influence of the studied variables, the effects of isolated and interactions terms were estimated using an ANOVA analysis. A significance level of 10% was

applied, and effects with p-values exceeding this threshold were excluded from the analysis. Table 4.7 shows the estimated effects and corresponding p-values of P_2O_5 grade and apatite recovery for fine ore.

Table 4.7 - Effects estimation and p-value of P_2O_5 grade for fine ore

Factor	P_2O_5 grade		Apatite recovery	
	Effect	**p-value**	**Effect**	**p-value**
Mean	34.687	0.00	86.559	0.000
x_1	-	-	3.076	0.000
x_2	1.360	0.000	-1.160	0.037
x_4	1.650	0.000	-1.798	0.003
x_5	-0.452	0.049	3.437	0.000
$x_1 . x_2$	-1.256	0.000	-1.424	0.025
$x_1 . x_4$	-0.912	0.002	-	-
$x_2 . x_4$	-1.120	0.000	-1.424	0.025
$x_2 . x_5$	0.480	0.064	2.014	0.003
x_1^2	0.036	0.011	2.625	0.003
x_2^2	-	-	-1.579	0.049
x_4^2	-	-	-1.306	0.096
x_5^2	-0.738	0.029	-4.195	0.000

Source: Author (2025).

It can be noted that the linear effects of depressant dosage (x_2) and pH (x_4), along with the interaction collector and depressant dosage ($x_1.x_2$), had the most significant influence on P_2O_5 grade. In contrast, the linear and quadratic effects of solid concentration during conditioning (x_5) and collector dosage (x_1), as well as the interaction between depressant dosage and solid concentration during conditioning ($x_2.x_5$) were the most significant factors affecting apatite recovery.

The empirical equations derived to describe the variation in P_2O_5 grade and apatite recovery in the concentrate as functions of the studied independent variables are presented in Equations 4.1 and 4.2 respectively. The parameters associated with individual variables, their interactions, and quadratic terms are expressed in a matrix system.

$$y_g = 34.687 + \underline{x}\,\underline{b}_g + \underline{x}\,\underline{B}_g\underline{x} \qquad R^2 = 0.914 \qquad (4.1)$$

$$\text{were: } \underline{b_g} = \begin{bmatrix} -0.226 \\ 0 \\ 0.680 \\ 0.825 \end{bmatrix} \text{ e } \underline{B_g} = \begin{bmatrix} -0.369 & 0 & 0.120 & 0 \\ 0 & 0.018 & -0.314 & -0.228 \\ 0.120 & -0.314 & 0 & -0.280 \\ 0 & -0.228 & -0.280 & 0 \end{bmatrix} \underline{x} = \begin{bmatrix} x_5 \\ x_1 \\ x_2 \\ x_4 \end{bmatrix}$$

$$y_r = 86.559 + \underline{x}\,\underline{b_r} + \underline{x}\,\underline{B_r}\,\underline{x} \qquad R^2 = 0.930 \qquad (4.2)$$

$$\text{were: } \underline{b_r} = \begin{bmatrix} 1.719 \\ 1.538 \\ -0.580 \\ -0.899 \end{bmatrix} \text{ e } \underline{B_r} = \begin{bmatrix} -2.097 & 0 & 0.503 & 0 \\ 0 & 1.312 & -0.356 & 0 \\ 0.503 & -0.356 & -0.789 & -0.356 \\ 0 & 0 & -0.356 & -0.653 \end{bmatrix} \underline{x} = \begin{bmatrix} x_5 \\ x_1 \\ x_2 \\ x_4 \end{bmatrix}$$

The coded equations are presented in Table 3.6 (Equations 3.6-3.10).

The analysis of the estimated equations parameters revealed that all variables influence the responses, regardless of their form—whether linear, quadratic, or interaction effects. To further elucidate the impact of operational variables P_2O_5 grade and apatite recovery, surface responses analyses were conducted. Figure 4.4 presents the surface response for (a) P_2O_5 grade and (b) apatite recovery as function of collector dosage (x_1) and solid concentration during conditioning (x_5), with other variables on central point.

Figure 4.4 - Response surface of solid concentration and collector dosage for a) P_2O_5 grade and b) apatite recovery

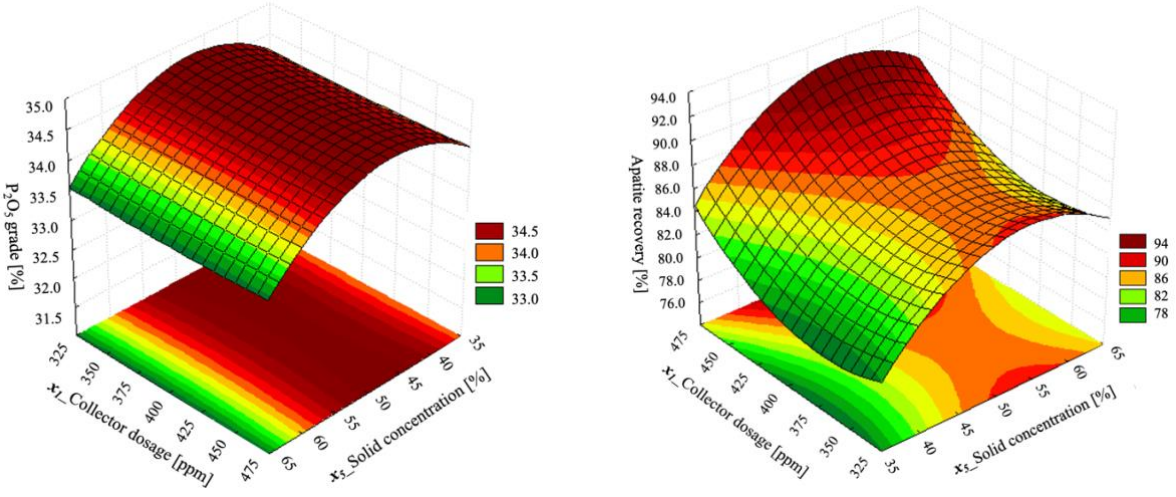

(a) (b)

Source: Author (2025).

The flotation of fine apatite tailings demonstrates a complex relationship between solid concentration, collector dosage, P_2O_5 grade, and apatite recovery. While a solid concentration

between 45% and 65% provided the greatest conditions for both responses, the influence of collector dosage was more intricate. Although high P_2O_5 grades were consistently achieved across all dosages, apatite recovery displayed two distinct regions of high performance: one below 325.87 ppm and another above 450 ppm both within the optimal solid concentration range.

The impact of solid concentration on flotation performance is well-documented in the literature. In phosphate flotation, conditioning at elevated solid concentrations is commonly employed. The present study's observations align with previous research. Teague and Lollback (2012) observed improved collector adsorption on phosphate surface at 75% solid during conditioning, which resulted in reduced silica activation and increased P_2O_5 recovery. While they found P_2O_5 grade was relatively unaffected by increasing the solid concentration from 50% to 75%, the improved recovery was attributed to the increase of collector concentration in the pulp, promoting chemisorption. They also suggested that denser pulp reduces the impact of dissolved Ca^{2+} and Mg^{2+}, minimizing quartz activation and reagent losses. Their experiments utilized a Denver flotation cell in a rougher-scavenger-cleaner circuit.

Similarly, Al-Thyabat, Yoon and Shin, (2011) also investigated the impact of solid concentration (20-40%) during conditioning on apatite flotation performance and reported similar trends. They also found that increasing solid concentration resulted in enhanced phosphate recovery (a 18% improvement in their study) which they attributed to increased collector concentration and decreased Ca^{2+} activity. Although P_2O_5 grade exhibited less sensitivity to variations in solid concentration, the overall flotation performance improved from the substantial increase in recovery without a concomitant reduction in grade. Al-Thyabat, Yoon and Shin, (2011) further suggested a link between solid concentration and collector dosage, observing that at high collector dosages, adsorption on phosphate involves both physisorption and chemisorption, while chemisorption prevails at lower dosages. This selective adsorption enhances apatite hydrophobicity, improving particle-bubble interactions and promoting aggregate formation, thus increasing both recovery and grade, which can be further enhanced when combined with high-intensity conditioning (HIC) (ALSAFASFEH; ALAGHA, 2017; WANG; LIU, 2021).

Despite these findings, the best solid concentration range identified in this study (45%-65%) is slightly lower than values reported in previous studies (75%). Statistical analysis confirmed the significant influence of solid concentration on apatite recovery. However, excessively high solids concentrations can hinder uniform reagent distribution due to increased pulp viscosity. This can lead to reduced collector adsorption onto the apatite surface and

consequently diminish flotation performance. Conversely, under low solid concentration conditioning, mineral particles are more widely dispersed, resulting in less stable particle-bubble aggregates (AL-THYABAT, YOON; SHIN, 2011, TEAGUE; LOLLBACK, 2012). This suggests that a balance is required, as both excessively high and very low solid concentration can be detrimental for fine particles flotation performance.

In flotation processes, it is generally observed that increasing collector dosage improves recovery, up to a certain limit, by enhancing adsorption, hydrophobicity, and particle-bubble aggregate stability (BRAVO *et al.*, 2005; OLIVEIRA *et al.*, 2005; OLIVEIRA, 2007; TEAGUE; LOLLBACK, 2012). However, this study revealed a more distinctive relationship. While high collector dosages, as expected, correlated with high recoveries, likely due to faster flotation kinetics (FENG; ALDRICH, 2004), unexpectedly high apatite recoveries were also observed at lower collector dosages. This result may be explained by fact that lower collector availability can lead to the formation of larger bubbles. This phenomenon aligns with the findings of Reis *et al.*, (2023), who reported that, although large bubbles might reduce the probability of particle-bubble collisions, they can simultaneously increase entrainment, indicating a potential shift in the dominant flotation mechanism. In this case, particle retention in the froth phase likely plays a significant role in the observed high recoveries. Moreover, the use of high-intensity conditioning could enhance collision probability, attachment efficiency, and the formation of particle-bubble aggregates, thereby improving overall flotation performance (SUN *et al.,* 2006). This observation highlights the importance of considering both collision probability and entrainment when interpreting flotation data.

Further analysis, as illustrated in Figure 4.5, examines the response surface for (a) P_2O_5 grade and (b) apatite recovery as function of depressant dosage(x_2) and pH (x_4), with other variables on central point. While all tested conditions met or exceeded industrial requirements for both responses, distinct trends emerged.

A region of lower apatite recovery was observed at depressant dosages above 548 ppm and pH values higher than 11.9. This aligns with findings from Cao *et al.*, (2015), who noted that high pH conditions, while potentially enhancing collector adsorption and reducing surface tension, can simultaneously decrease apatite hydrophobicity at pH 11.5, thus hindering recovery. Excess depressant may also contribute by adsorbing onto gangue minerals and non-selectively onto apatite (SANTANA *et al.*, 2011). This combined effect of high depressant dosage and high pH possibly creates a detrimental environment for apatite flotation.

Figure 4.5 - Response surface of depressant dosage and pH for a) P_2O_5 grade and b) apatite recovery

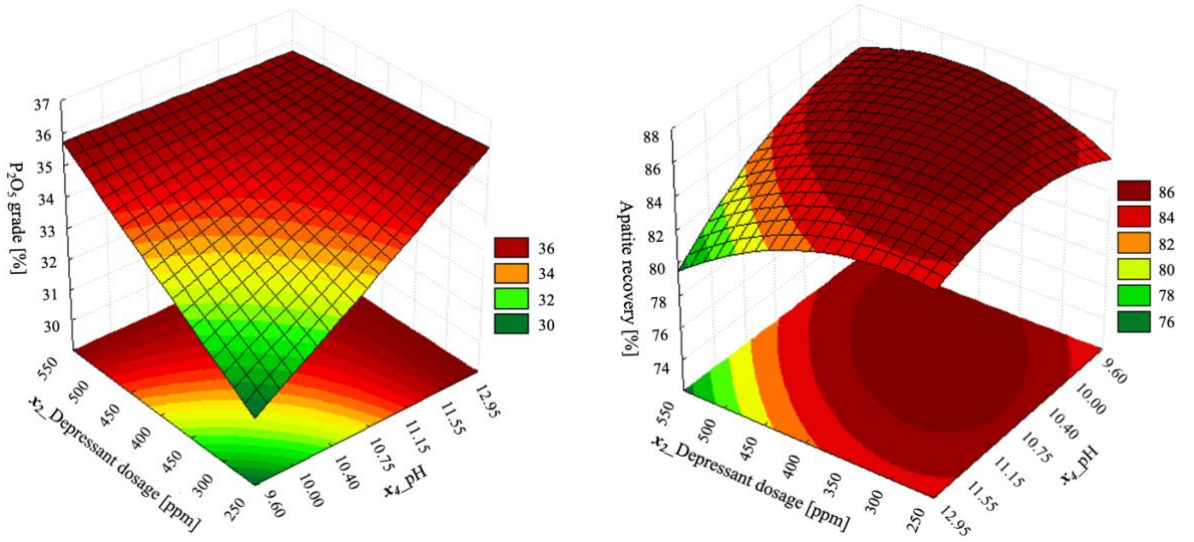

(a) (b)

Source: Author (2025).

However, the highest apatite recoveries were achieved within a pH range of 9.7 to 11.5 and a depressant dosage between 251.7 ppm and 450 ppm. Under these conditions, the depressant likely exhibits greater selectivity for gangue minerals, while pH range favors true flotation mechanisms by promoting more effective adsorption of the collector onto apatite surface, resulting in high P_2O_5 grade and apatite recovery (ALSAFASFEH; ALAGHA, 2017; VALDERRAMA *et al.*, 2024).

High P_2O_5 grades were observed under two distinct sets of conditions: depressant dosages above 548.26 ppm at pH levels below 10.8, and depressant dosage below 500 ppm at pH level above 11.7. In the first condition (high depressant/low pH), enhanced selectivity by suppressing gangue mineral flotation. This allows for more effective collector adsorption onto the apatite surface, improving the hydrophobicity without compromising depressant efficiency, resulting in a high P_2O_5 grade. However, this improvement was often accompanied by a decrease in apatite recovery, likely attributable to slower flotation kinetics under low pH. These observations corroborate previous findings (SANTANA *et al.*, 2011; SILVA *et al.*, 2019), which indicates that higher depressant dosages, while improving selectivity and P_2O_5 grade, can negatively impact recovery.

The second condition (low depressant/high pH) also yielded high P_2O_5 grades. Feng and Aldrich (2004) reported optimal apatite flotation results at pH 12.3, suggesting that elevated pH can enhanced flotation kinetics, likely through the formation of smaller, more stable bubbles.

At the same time, a lower depressant dosage in this high pH range was sufficient to depress gangue minerals while maintaining acceptable apatite recovery. High pH can influence mineral hydrophobicity and flotation kinetics. Hydroxyl ions may compete with depressant molecules for adsorption sites on mineral surfaces, potentially diminishing the effectiveness of starch depressant (MATIOLO *et al.*, 2017; SIS; CHANDER, 2003; TRAHAR, 1981).

Finally, in the flotation of fine ore, apatite recovery demonstrated greater variability across different operating conditions compared to P_2O_5 grade. This can reflect the complex interplay of collision, attachment and entrainment mechanisms. While high-intensity conditioning enhances collision and attachment, facilitating the formation of particle-bubble aggregates, entrainment can both promote and hinder the collection of these aggregates in the froth phase, thus influencing flotation performance. This finding highlights the importance of adjust correctly reagent dosing and flotation parameters to balance P_2O_5 grade and apatite recovery.

Following the evaluation of the central composite design (CCD) results, a multi-response optimization was conducted using the desirability function approach (BURATTI *et al.,* 2017; DERRINGER; SUICH, 1980; VIACAVA; ROURA; AGÜERO, 2015). The objective was to simultaneously maximize both apatite recovery and P_2O_5 grade while ensuring process efficiency and economic viability. This strategy is particularly relevant for tailings-derived apatite. Figure 4.6 presents the desirability profiles of the independent variables: solids concentration during conditioning (x_5), collector dosage (x_1), depressant dosage (x_2), and pH (x_4), using coded values associated with the maximization of P_2O_5 grade and apatite recovery. The optimal conditions identified by the desirability function, along with their corresponding decoded (actual) values, are provided in Table 4.8.

To validate the multi-response optimization results, confirmatory tests were conducted in triplicate using the optimal variable values. The predicted and experimental results, along with the standard deviation (SD) and coefficient of variation (CV) for each response, are summarized in Table 4.9. This table also reports the average CaO/P_2O_5 ratio of 1.37 for the optimized tests, confirming the apatite origin of the phosphorus, alongside the corresponding average selectivity ratios (SR Fe_2O_3 and SR SiO_2). The close agreement between predicted and experimental values underscores the robustness of the CCD model. The observed standard deviations were 0.474 for P_2O_5 grade and 0.974 for apatite recovery, indicating highly satisfactory consistency and reproducibility. Furthermore, the coefficient of variation (CV) for both responses remained below 5%, reinforcing the stability of the flotation process under the derived optimal conditions. Collectively, these results validate the desirability-based approach

and confirm that the optimized conditions consistently enhance flotation performance for the fine tailings-derived apatite sample.

Figure 4.6 - Desirability of fine ore

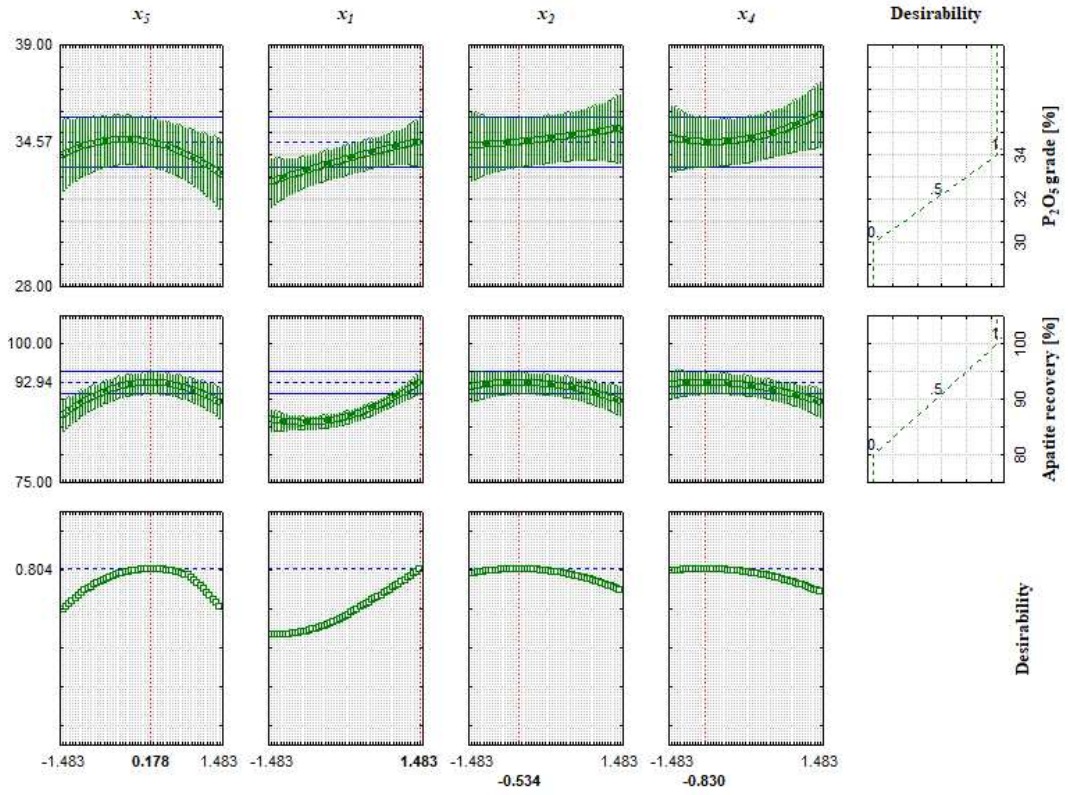

Source: Author (2025).

Table 4.8 - Coded and actual values of each variable at the optimal condition from desirability for fine ore

Variable	Coded value	Decoded value
Solid concentration during conditioning(x_5)	0.178	51.78 %
Collector dosage (x_1)	1.483	474.13 ppm
Depressant dosage (x_2)	-0.534	346.63 ppm
pH (x_4)	-0.830	10.18

Source: Author (2025).

Table 4.9 - Experimental and predicted response values of desirability optimization for fine ore

Response	Experimental result	Predicted result	Standard deviation	Coefficient of variation
P_2O_5 grade [%]	34.82	34.57	0.474	0.014
Apatite recovery [%]	92.16	92.94	0.974	0.011
CaO/P_2O_5	1.37	-	0.010	0.008
SR Fe_2O_3	8.41	-	0.502	0.060
SR SiO_2	5.71	-	0.269	0.047

Source: Author (2025).

4.3. Flotation results of ultrafine apatite ore derived from tailings

4.3.1. Preliminary test for ultrafine ore using cell flotation

The flotation of ultrafine tailings without desliming presented a considerable challenge. Preliminary cell flotation tests were conducted to identify critical variables and operating conditions for further investigation in the subsequent study phase. Table 4.10 presents the conditions and results of these preliminary tests.

The experimental findings revealed that none of the tested conditions simultaneously met the industrial requirements of achieving a P_2O_5 grade of at least 24% and a minimum apatite recovery of 40%. The best result was observed in Test 8, which reached a P_2O_5 grade of 17.46% and an apatite recovery of 40.56%. These results emphasize the complexity of achieving efficient flotation of ultrafine tailings without prior desliming in mechanical cell flotation. It was initially hypothesized that mechanical cell flotation might yield favorable results due to the mechanical energy input, which increases particle-bubble collision probability and could enhance stable aggregate formation). However, the observed outcomes contradicted this expectation, underscoring the limitations of mechanical energy alone in overcoming ultrafine particle challenges.

Flotation performance was found unsatisfactory in Tests 1 through 6, which were conducted at a high solid concertation during conditioning and a pH of 12. Despite achieving high apatite recovery, the P_2O_5 grade remained similar to that of the feed ore (12.88%), which suggests a possible predominance of non-true flotation mechanisms. Conversely, Tests 7 though 21, employing a conditioning solid concentration of 28.24% and flotation solid concentration of 13.41%, at pH values of 9.5 and 9, demonstrated improved performance. Under these conditions, the P_2O_5 grade increased, ranging from 15.55% to 17.46%. However, variations in the type of collector (Tests 11-13), as well as modifications in the dosages of both collector and depressant, had minimal impact on the P_2O_5 grade, although they significantly influenced apatite recovery rates. These findings suggest inadequate dispersion of ultrafine particles, which hindered the effective adhesion of collector to the apatite surface and the depressant to the gangue minerals. Consequently, this promoted the entrainment mechanism, reducing mineral separation efficiency (ELBENDARZ; ALEKSANDROVA; NIKOLAEVA, 2019; FARROKHPAY; FILLIPOV; FORNASIERO, 2020). This effect was more pronounced in Tests 22 to 28, which were conditioned at high solid concentrations. The increased pulp viscosity under these conditions likely facilitated the unintended entrainment of non-target minerals (ALSAFASFEH; ALAGHA, 2017).

Table 4.10 - Results and conditions of ultrafine tailings flotation using mechanical cell flotation

Test	Collector type	Collector dosage [ppm]	Depressant dosage [ppm]	pH	Conditioning solid concentration [%]	Flotation solids concentration [%]	P_2O_5 grade [%]	Apatite recovery [%]	$\frac{CaO}{P_2O_5}$
1	Agem A3	550	1200	12	52.78	38.78	12.92	92.47	1.30
2	Agem A3	110	1200	12	26.09	16.67	13.57	75.38	1.30
3	Agem A3	80	1400	12	21.05	11.43	13.84	75.46	1.32
4	Agem A3	80	1400	12	28.24	13.41	13.72	84.33	1.30
5	Agem A3	80	1400	12	31.78	17.35	13.99	86.45	1.32
6	Agem A3	80	2700	12	28.24	13.41	13.74	83.77	1.32
7	Agem A3	80	2700	9.5	28.24	13.41	15.55	25.18	1.28
8	Agem A3	80	3200	9.5	28.24	13.41	17.46	40.56	1.29
9	Agem A3	110	2700	9.5	28.24	13.41	17.09	42.81	1.32
10	Agem A3	110	3200	9.5	28.24	13.41	16.89	47.12	1.29
11	Agem A3	220	2700	9.5	28.24	13.41	16.47	71.95	1.31
12	Rice oil	220	2700	9.5	28.24	13.41	16.85	37.07	1.27
13	Flotigam	220	2700	9.5	28.24	13.41	17.08	69.00	1.34
14	Agem A3	220	3200	9.5	28.24	13.41	16.08	76.91	1.29
15	Agem A3	80	2700	9	28.24	13.41	16.12	27.67	1.29
16	Agem A3	80	3200	9	28.24	13.41	16.53	36.48	1.28
17	Agem A3	80	3500	9	28.24	13.41	16.92	43.44	1.32
18	Agem A3	80	3700	9	28.24	13.41	16.68	19.59	1.29
19	Agem A3	80	3900	9	28.24	13.41	-	-	-
20	Agem A3	220	2700	9	28.24	13.41	16.80	75.38	1.29
21	Agem A3	220	3200	9	28.24	13.41	16.31	75.92	1.30
22	Agem A3	80	3500	9	30.68	14.84	16.68	20.24	1.29
23	Agem A3	80	3500	9	32.97	16.22	14.20	15.79	1.22
24	Agem A3	100	3500	9	32.97	16.22	13.92	15.88	1.22
25	Agem A3	100	3500	9	35.11	17.55	14.03	17.95	1.20
26	Agem A3	100	3500	9	37.11	18.85	13.62	15.11	1.20
27	Agem A3	100	3500	9	39.00	20.10	13.26	14.83	1.22
28	Agem A3	100	3500	9	40.78	21.32	13.12	14.24	1.18

Source: Author (2025).

Despite extensive testing of various process variables, the results obtained using a mechanical flotation cell remained consistently unsatisfactory as evidenced by CaO/P_2O_5 ratio and the selectivity ratio of Fe_2O_3 and SiO_2 (see in Table 7.1 in Appendix II), in all conditions tested. These findings reinforce the inherent challenges associated with achieving efficient

flotation performance of ultrafine tailings ore, particularly without prior desliming. Given these limitations, further studies have focused on alternative flotation strategies, such as column flotation accompanied by high-intensity conditioning, to enhance separation efficiency and overcome the challenges posed by ultrafine particles recovery.

4.3.2. Experiments for ultrafine ore using column flotation

The recovery of fine and ultrafine particles through froth flotation presents considerable challenges due to their low mass and high surface area, which complicates particle-bubble interactions (RUBIO *et al*., 2007). As demonstrated in the previous section, conventional mechanical cells exhibited limited efficacy in recovering ultrafine particles under the conditions studied. In contrast, column flotation has increasingly replaced mechanical cells in phosphate concentration plants, offering several advantages. This technology enhances recovery efficiency through extended residence time and reduced turbulence, promoting the formation of stable particle-bubble aggregates (ARAUJO, VIANA, PERES, 2005; GUIMARÃES; PERES,2002; WANG; LIU, 2021). The low turbulence in column flotation increases the probability of stable aggregates reaching the froth phase, while the addition of wash water improves concentrate purity by removing entrained gangue minerals. These conditions not only reduce reagent consumption but also enhance selectivity, particularly for fine and ultrafine particles, by mitigating hydrodynamic entrainment (OEDIYANI *et al.,* 2020; OLIVEIRA *et al.,* 2011; WANG; LIU, 2021).

To further improve the recovery of fine and ultrafine particles, high-intensity conditioning (HIC) prior to column flotation can be applied. HIC promotes a two-stage attachment mechanism that provides both thermodynamic and hydrodynamic benefits. Initially, micro and nano bubbles attach rapidly to particle surfaces due to their small size, forming aggregates that increase the apparent particle size and enhance collision probability with larger bubbles. In the second stage, these micro and nano bubbles, being less hydrated than solid particles, facilitate interactions with flotation-size bubbles. Their coalescence results in a greater reduction in system free energy compared to direct attachment, while also accelerating liquid drainage, thereby improving flotation efficiency (ZHOU *et al.,* 2020). Additionally, HIC enhances particle-bubble interactions by removing surface contaminants, preventing slime coating, and improving reagent distribution and diffusion in the pulp. The intense agitation in HIC induces hydrodynamic cavitation, generating micro and nano bubbles that serve as aggregation nuclei, thereby increasing collision probability and attachment efficiency (SUN *et*

al., 2006; WANG; LIU, 2021). Thus, the integration of column flotation with high-intensity conditioning emerges as an effective strategy for ultrafine particle recovery, representing a superior alternative to mechanical flotation cells for subsequent experiments.

4.3.2.1. Collector type analysis in column flotation for ultrafine ore

Since preliminary tests using Agem A3, as collector, did not achieve the desired performance, a two-level factorial design was implemented to systematically evaluate collector efficiency and identify the best reagent for ultrafine ore flotation. Based on previous experiments conducted on fine ore, rice oil and Agem A3 were investigated as potential collectors for ultrafine particles. The experimental design included three independent variables: the collector dosage (x_1), the depressant dosage (x_2) and type of collector(x_3), enabling a comprehensive assessment of their impact on flotation performance. Consistent reproducibility was observed, with mean standard deviations of 0.430 (P_2O_5 grade) and 2.963 (apatite recovery), and coefficients of variation of 0.022 and 0.046, respectively. Table 4.11 shows the flotation conditions and corresponding results from the two-level factorial experimental design.

Table 4.11 - Flotation conditions and results of two-level factorial experimental design of ultrafine ore

Test	Collector dosage [ppm] (x_1)	Depressant dosage[ppm] (x_2)	Type of collector (x_3)	P_2O_5 grade [%]	Apatite recovery [%]	$\frac{CaO}{P_2O_5}$
29	50	700	Rice oil	24.5	41.68	1.40
30	50	700	Agem A3	19.94	60.98	1.33
31	110	700	Rice oil	20.22	55.29	1.36
32	110	700	Agem A3	17.6	65.6	1.33
33	50	900	Rice oil	23.61	42.11	1.40
34	50	900	Agem A3	19.45	63.00	1.33
35	110	900	Rice oil	18.51	63.17	1.33
36	110	900	Agem A3	16.98	70.59	1.31

Source: Author (2025).

According to industrial standards, the flotation concentrate must achieve a minimum P_2O_5 grade of 24%, an apatite recovery above 40%, and CaO/P_2O_5 ratio around 1.356. Although tested conditions yielded apatite recovery exceeding 40%, only Test 29 satisfied all industrial

criteria, achieving a concentrate with a P_2O_5 grade of 24.5%, apatite recovery of 41.68%, with CaO/ P_2O_5 ratio of 1.40. Consequently, Test 29 achieved a response index of 3.15, whereas all the remaining tests had a response index of zero.

The combined experimental data provided the foundation for a statistical assessment for this two-level factorial experimental design. In this analysis, the independent variables were converted into dimensionless forms, as shown in Table 3.8 in the Methodology Chapter. The statistically significant effects on P_2O_5 grade and apatite recovery, determined at a p-value below 0.1, are detailed in Table 4.12. The high coefficients of determination ($R^2 = 0.991$ for P_2O_5 grade and $R^2 = 0.995$ for apatite recovery) indicate a strong correlation between the selected variables and flotation performance.

Table 4.12 - Statistical results: effects of the factors of P_2O_5 grade and apatite recovery for ultrafine ore

Factor	**P_2O_5 grade**		**Apatite recovery**	
	Effect	**p-value**	**Effect**	**p-value**
Mean	20.101	0.000	57.911	0.000
x_1	-3.547	0.001	11.502	0.007
x_2	-0.927	0.043	3.612	0.063
x_3	-3.217	0.001	14.262	0.004
$x_1.x_2$	-	-	2.822	0.097
$x_1.x_3$	1.142	0.025	-5.397	0.029

Source: Author (2025).

The significantly factors influencing the P_2O_5 grade were the collector dosage (x_1), the depressant dosage (x_2), collector type (x_3) and the interaction between the collector dosage and collector type ($x_1.x_3$). Similarly, apatite recovery was affected by the same factors, although with opposite signals, along with an additional contribution from the interaction between collector dosage and depressor dosage ($x_1.x_2$). These opposite signs highlight the contrasting effects on both responses, which is an intrinsic characteristic of flotation processes. The results also indicated that the variables collector type and dosage had the most substantial effects on both P_2O_5 grade and apatite recovery.

As shown in Table 4.11, the collector type had a significant impact on both P_2O_5 grade and apatite recovery. Rice oil demonstrated greater selectivity than Agem A3, as evidenced by its compliant CaO/P_2O_5 ratio and superior selectivity ratios for both Fe_2O_3 and SiO_2 (see Table 7.2 in Appendix II), leading to higher P_2O_5 grades. However, this improvement in P_2O_5 grades was accompanied by a reduction in apatite recovery. The results suggest that rice oil enhanced

true flotation while minimizing hydrodynamic entrainment. In contrast, Agem A3, which exhibited lower selectivity, promoted greater apatite recovery through increased entrainment, resulting in slight variations in P_2O_5 grade. These observations indicate that while Agem A3 enhanced apatite recovery via entrainment, rice oil achieved superior performance in ultrafine apatite tailings flotation due to its higher selectivity and overall responses. Consequently, rice oil was selected as the collector for the subsequent studies.

4.3.2.2. Additional tests using column flotation for ultrafine ore

Following the selection of rice oil as the collector for ultrafine phosphate ore flotation, a series of additional experiments was conducted to evaluate the effects of five key parameters: dispersant dosage, conditioning solids concentration, pH, collector dosage, and depressant dosage. Table 4.13 presents the experimental conditions, and the corresponding results obtained from these additional column flotation tests. Flotation performance was assessed against industrial standards for ultrafine tailings flotation, which require a minimum of 24% P_2O_5 grade, an apatite recovery of 40%, and a CaO/ P_2O_5 ratio close to 1.356. Among all experiments, only Test 29 (previous set experiments) met these criteria, achieving a response index (RI) of 3.15 with 24.5% of P_2O_5 grade, an apatite recovery of 41.68% and a CaO/P_2O_5 ratio of 1.40.

Analysis of Tests 31 and 37-42 revealed the significant impact of dispersant dosage on flotation performance. The interaction between sodium silicate and calcium ions might be contributed to the decrease in apatite recovery (AL-THYABAT, 2009). This effect was particularly evident at high dispersant dosages (400 and 2000 ppm), where flotation efficiency declined, likely due to reduced collector adsorption on the apatite surface, therefore the sodium silicate effectively acted as a depressant (ARANTES *et al.,* 2017). In contrast, moderated dispersant dosages (125 and 250 ppm) appeared to enhance ultrafine particles dispersion, improving both apatite recovery and achieving compliance with the target CaO/P_2O_5 ratio specifications. These results suggest that dispersant effectiveness depends on its interaction with collector and depressant reagents, which are crucial for maximizing flotation performance by improving ultrafine particles dispersion (QI; KLAUBER; WARREN, 1993). Based on these observations, a more detailed investigation was conducted in the following section to assess the effect of dispersant with varying collector and depressant dosages.

Table 4.13 - Additional column flotation tests of ultrafine tailings ore

Test	Dispersant dosage [ppm]	Conditioning solid concentration [%]	pH	Collector dosage [ppm]	Depressant dosage [ppm]	P_2O_5 grade [%]	Apatite recovery [%]	$\frac{CaO}{P_2O_5}$
31	0	40	12	110	700	20.22	55.29	1.36
37	250	40	12	110	700	19.31	59.56	1.37
38	2000	40	12	110	700	17.3	44.89	1.30
39	0	40	12	70	700	19.75	49.44	1.35
40	125	40	12	70	700	20.61	50.96	1.43
41	250	40	12	70	700	20.67	51.46	1.38
42	400	40	12	70	700	19.73	40.93	1.24
43	0	50	12	70	700	-	-	-
44	0	50	10	70	700	16.82	6.07	1.28
45	0	20	12	70	700	-	-	-
46	0	40	10	70	700	17.82	7.52	1.31
47	250	40	10	70	700	17.49	5.60	1.31
29	0	40	12	50	700	24.5	41.68	1.40
35	0	40	12	110	900	18.51	63.17	1.33
48	0	40	12	70	900	20.16	50.10	1.34
33	0	40	12	50	900	23.61	42.11	1.40
49	0	40	12	70	1100	20.47	50.79	1.39
50	0	40	12	70	1300	20.66	53.38	1.39
51	0	40	12	70	1500	20.02	51.38	1.36
52	0	40	12	70	1900	19.66	52.94	1.40
53	0	40	10	400	400	15.07	68.14	1.31
54	0	40	12	400	400	15	92.63	1.33
55	0	35	10	80	2618	15.34	22.14	1.32
56	0	35	12	80	2618	19.5	54.23	1.35
57	0	35	12	80	3000	18.77	51.00	1.38
58	250	35	12	80	2618	19.09	50.81	1.37
59	400	35	12	80	2618	19.09	50.46	1.34

Source: Author (2025).

Optimizing solid concentration during conditioning is essential for effective particle-reagent interactions. Alsafasfeh and Alafha (2017) studied the effect of solid concentration, varying it among 20%, 40% and 60% using a Denver D-12 flotation cell. Their study, which also considered the influence of the collector, frother, and dispersant, concluded that higher solids concentrations resulted in the highest concentrate recovery and grade. Thus, maintaining

an adequate solid content promotes greater reagent adsorption onto the mineral surface, thereby enhancing flotation selectivity.

However, excessive solid concentration can increase pulp viscosity, promoting particle agglomeration and hindering the effective adsorption of collector and depressant onto minerals surface. In the case of ultrafine particles, this has a negative effect on recovery rates and overall flotation performance (TAO, 2005; LIU, 2020). Such effects were evident when comparing Tests 43 and 44 with Tests 39 and 46, respectively. In Test 43, conducted at 50% solids, flotation was inhibited due to high pulp viscosity combined with elevated pH. To mitigate this effect, Test 44 were conducted at pH 10, resulting in reduced viscosity. Despite this adjustment, the flotation response remained significatively below the required specifications for ultrafine tailings flotation.

Conversely, insufficient solid concentration during conditioning (Test 45) may have compromised apatite hydrophobicity and gangue mineral hydrophilicity due to the decrease on reagents adsorption efficiency (TEAGUE; LOLLBACK, 2012), further hindering flotation performance, as evidenced by the lack of flotation in Test 45. Based on these findings, a solid concentration of 40% was selected for further experiments, as it provided a balance between reagent adsorption efficiency and pulp viscosity.

Flotation performance was consistently superior at pH 12 compared to pH 10, with higher P_2O_5 grades and improved apatite recovery. Even with dispersant addition (Test 47), flotation at pH 10 yielded significantly lower recoveries. Lafhaj, Filippov and Filippova (2017) investigated the separation of calcite and apatite using oleic and linoleic acids, finding that calcite exhibited better floatability at lower pH levels, while apatite recovery was enhanced above pH 10. Their study showed that sodium linoleate outperformed oleic acid at higher pH, leading to superior apatite recovery. This effect was attributed to stronger linoleic acid interaction with calcium ions on the apatite surface and enhanced stability of its dimeric form at elevated pH, improving adsorption.

Rice oil, the collector used in the present work, is a vegetable-based oil composed predominantly of oleic, linoleic and linolenic acids, successfully employed in apatite flotation in Brazil (CAO *et al.,* 2015). Given its high oleic and linoleic content, rice oil has proven particularly effective under alkaline conditions, reinforcing its suitability as collector for apatite flotation, especially at high pH. These findings align with the study by Santana *et al.* (2012), which demonstrated that pH of 11.5 favored both flotation selectivity and apatite recovery for fine ore. Consequently, pH 12 was selected for subsequent experiments.

Further analysis revealed that lower collector dosages improved the P_2O_5 grade but were associated with reduced apatite recovery. When the depressant dosage was varied (Tests 39, 48-52) while remaining other parameters constant, it had a negligible impact on flotation performance. This suggests that within the tested range, depressant dosages had a limited effect on both P_2O_5 grade and apatite recovery. To maximize flotation performance, Tests 53 and 54 were conducted using conditions that had previously been successful for fine ore flotation in preliminary experiments. However, these conditions did not enhance ultrafine flotation performance; instead, they promoted non-selective reagent adsorption and entrainment, highlighting the distinct behavior of fine and ultrafine particles.

Tests 55 to 57 were designed based on the findings of Matiolo *et al.* (2019), who investigated the effectiveness of flotation circuits and column sizes for phosphate recovery from slimes with Sauter mean diameter (d_{32}) of 2.6 µm and 5 µm. In their study, the samples underwent desliming before flotation, after which they were floated using depressant dosages ranging from 2300 g/t to 3000 g/t, pH levels between 9.5 and 10.8, collector dosages of 70-130g/t, and conditioning at 35% solids in continuous flotation system. Their findings indicated that effective iron impurity control required depressant dosages up to 2200g/t, with a maximum of 3000 g/t achieving P_2O_5 grade higher than 30% and recovery rates ranging from 29% to 42%.

Based on these parameters, Tests 55 to 57 were conducted, but the results showed that neither the P_2O_5 grade nor apatite recovery met industrial specifications. To address this, additional Tests (58 and 59) were performed under the same conditions as Test 56, with the addition of dispersant. However, these modifications also failed to achieve the required specifications. The results indicate that the tested parameters (pH, depressant dosage, and dispersant addition) were insufficient to achieve significant flotation performance, likely due to the absence of desliming. This suggests that the lack of desliming significantly hindered optimal flotation performance.

Previous studies have highlighted the critical role of agitation speed and conditioning time in flotation performance. For instance, Subrahmanyam and Eric Forssberg (1990) reported that aggregate formation reached its maximum at 1200 rpm, which led to the selection of 1200 rpm and 1500 rpm as test speeds to investigate their effect on flotation recovery. Similarly, Oliveira *et al*. (2005) observed that both P_2O_5 grade and apatite recovery initially improved with longer conditioning times but declined after exceeding a specific threshold for intermediate particle. To explore this further, the conditioning time for each reagent was doubled to evaluate its impact on flotation outcomes. To determine the influence of these parameters on the ultrafine

tailings ore system in this study, Test 41 was replicated under the same conditions (Table 4.14), with adjustments made only to the agitation speed and conditioning time.

Table 4.14 - Conditions and results of agitation speed and conditioning time

Test	Conditioning time for each reagent [min]	Stirring speed [rpm]	P_2O_5 grade [%]	Apatite recovery [%]	$\frac{CaO}{P_2O_5}$
41	5	1200	21.26	48.59	1.38
60	10	1200	21.4	48.07	1.36
61	5	1500	21.67	48.96	1.38

Source: Author (2025).

The results indicated that neither the agitation speed nor the conditioning time significantly affected the P_2O_5 grade, apatite recovery, or CaO/P_2O_5 ratio. Therefore, the stirring speed was fixed at 1200 rpm and conditioning time of each reagent in 5 minutes subsequent experiments. Thereby simplifying the experimental design and enabling a more focus investigation of the variables that exert a pronounced influence on ultrafine ore flotation performance.

4.3.2.3. Dispersant analysis for ultrafine ore

To improve flotation performance and achieve the industrial requirements specifically, a P_2O_5 grade above 24%, apatite recovery exceeding 40%, and a CaO/P_2O_5 ratio close to 1.356 for ultrafine tailings ore, a two-factorial experiment design was implemented to evaluate the effect of dispersant addition. Table 4.15 presents the conditions and results, analyzing the influence of collector dosage (x_1), depressant dosage (x_2) and dispersant dosage (x_6). The process demonstrated high reproducibility, with mean standard deviations of 0.267 (P_2O_5 grade) and 0.809 (apatite recovery), and corresponding coefficients of variation of 0.012 and 0.017.

The addition of dispersant significantly enhanced ultrafine ore flotation, leading to improvements in both P_2O_5 grade and apatite recovery. The consistent CaO/P_2O_5 ratio confirmed the apatite origin of phosphorus. Notably, the sodium silicate dispersant also acts as a depressant for silicate gangue minerals, which were present according to the mineralogical analysis. This specific depressing action provides a clear justification for the markedly higher selectivity against SiO_2 (SR_{SiO2}).The selectivity ratios (SR_{Fe2O3} and SR_{SiO2}) confirmed the increased process selectivity in the presence of the dispersant. Among all the tested conditions,

Tests 29, 62, and 63 achieved the industrial requirements. Although Test 62 yielded the highest P_2O_5 grade (25.48%), the most favorable overall performance was observed in Test 63, which achieved a P_2O_5 grade of 24%, an apatite recovery of 45.87%, and an IR of 3.29. This test was conducted under conditions of lower collector dosage (50 ppm), the presence of dispersant (250 ppm), and the highest depressant dosage (900 ppm).

Table 4.15 - Two factorial experimental design of dispersant analysis.

Test	Collector dosage [ppm] (x_1)	Depressant dosage [ppm] (x_2)	Dispersant dosage [ppm] (x_6)	P_2O_5 grade [%]	Apatite recovery [%]	$\frac{CaO}{P_2O_5}$	SR Fe_2O_3 [%]	SR SiO_2 [%]	IR
29	50	700	0	24.50	41.68	1.40	1.29	3.54	3.10
62	50	700	250	25.48	43.52	1.38	1.41	4.08	3.24
39	70	700	0	19.75	49.44	1.39	0.80	1.80	0
41	70	700	250	20.67	51.46	1.38	0.85	2.00	0
33	50	900	0	23.61	42.11	1.40	1.18	2.98	0
63	50	900	250	24.00	45.87	1.39	1.19	3.10	3.29
48	70	900	0	20.16	50.10	1.34	0.81	1.81	0
64	70	900	250	20.73	53.97	1.37	0.86	1.98	0

Source: Author (2025).

The experimental data were statistically evaluated, with independent variables converted into dimensionless forms, as shown in Table 3.11 in the Methodology Chapter. Table 4.16 presents the effects and p-values of P_2O_5 grade and apatite recovery, which were statistically significant at a significance considering a significance level of 10% (R^2 =0.999 for both P_2O_5 grade and apatite recovery).

Table 4.16 - Effects and p-values of P_2O_5 grade and apatite recovery of CCD

Factor	P_2O_5 grade		Apatite recovery	
	Effect	p-value	Effect	p-value
Mean	22.362	0.000	47.269	0.000
x_1	-4.070	0.000	7.947	0.000
x_2	-0.475	0.010	1.487	0.000
x_6	0.715	0.004	2.872	0.000
x_1x_2	0.710	0.004	-	-
x_2x_6	-0.235	0.038	0.942	0.001

Source: Author (2025).

The significant factors influencing P_2O_5 grade and apatite recovery were collector dosage (x_1), depressant dosage (x_2), dispersant dosage (x_6) and the interactions dispersant and depressant dosage (x_2x_6). For P_2O_5 grade, the interaction between the collector and depressant dosage (x_1x_2) was also significant. Among these significant factors, collector dosage had the most pronounced effect on both responses, followed by dispersant dosage, which had a stronger effect on apatite recovery than on P_2O_5 grade. These results suggest that the dispersant may be induced electrostatic repulsion among ultrafine particles, promoting more selective adsorption of collector onto apatite and depressant onto gangue minerals. This mechanism enhanced selectivity, as evidenced by the increase in P_2O_5 grade and apatite recovery (MOLIFIE *et al.,* 2023).

The dispersant likely contributed to reducing ultrafine agglomerated particles, maintaining a more stable pulp suspension compared to the system without dispersant (FARROKHPAY; FILLIPOV; FORNASIERO, 2020; SAJJAD; OTSUKI, 2022). Furthermore, dispersant can reduce pulp viscosity, which is often increased by the presence of ultrafine particles. Lower viscosity can improve hydrodynamic conditions, enhancing particle-bubble interactions and thus flotation performance (ALSAFASFEH; ALAGHA, 2017).

Based on these results, sodium silicate, at a dosage of 250 ppm, was selected as dispersant for incorporation into the ultrafine tailings ore flotation system for subsequent CCD experiments. These findings underscore the importance of understanding the influence of dispersant in flotation performance, as well as the need to optimize collector and depressant dosages. These factors will be further explored in the next phase of the study to maximize flotation performance.

4.3.3. Central Composite Design for ultrafine ore

Based on previous tests conducted, Table 4.17 presents the experimental conditions and results obtained from central composite design (CCD) tests conducted on ultrafine tailings ore flotation. These tests specifically investigated the influence of collector dosage (x_1), and depressant dosages (x_2) on flotation performance.

The results demonstrated consistent reproducibility, with standard deviations of 0.130 (P_2O_5 grade) and 0.440 (apatite recovery), corresponding to coefficients of variation of 0.005 and 0.010, respectively. These statistical parameters were derived from central point replication analysis. While all tests yielded a CaO/ P_2O_5 ratio approximating the target value of 1.356 (consistent with apatite-derived phosphorus), satisfying both the industry-standard minimum

P_2O_5 grade of 24% and at least 40% apatite recovery proved more challenging; Tests 70-73 met these criteria. Figure 4.7 illustrates the apatite recovery and P_2O_5 grade results from the CCD tests to facilitate data interpretation.

Table 4.17 - Experimental conditions and results of the CCD applied to ultrafine ore flotation

Test	Collector dosage [ppm] (x_1)	Depressant dosage [ppm] (x_2)	P_2O_5 grade [%] (y_g)	Apatite recovery [%] (y_r)	$\frac{CaO}{P_2O_5}$	RI
65	30	500	28.42	29.43	1.43	0
66	30	900	28.47	30.03	1.37	0
67	70	500	21.98	48.65	1.37	0
64	70	900	20.73	53.97	1.36	0
68	22	700	29.86	22.23	1.40	0
69	78	700	20.38	53.59	1.36	0
70	50	417	24.34	42.21	1.40	3.12
71	50	983	24.35	41.66	1.39	3.10
72	50	700	25.35	43.08	1.38	3.14
73	50	700	25.61	43.96	1.40	3.27

Source: Author (2025).

Figure 4.7 - Apatite recovery and P_2O_5 grades of CCD tests results

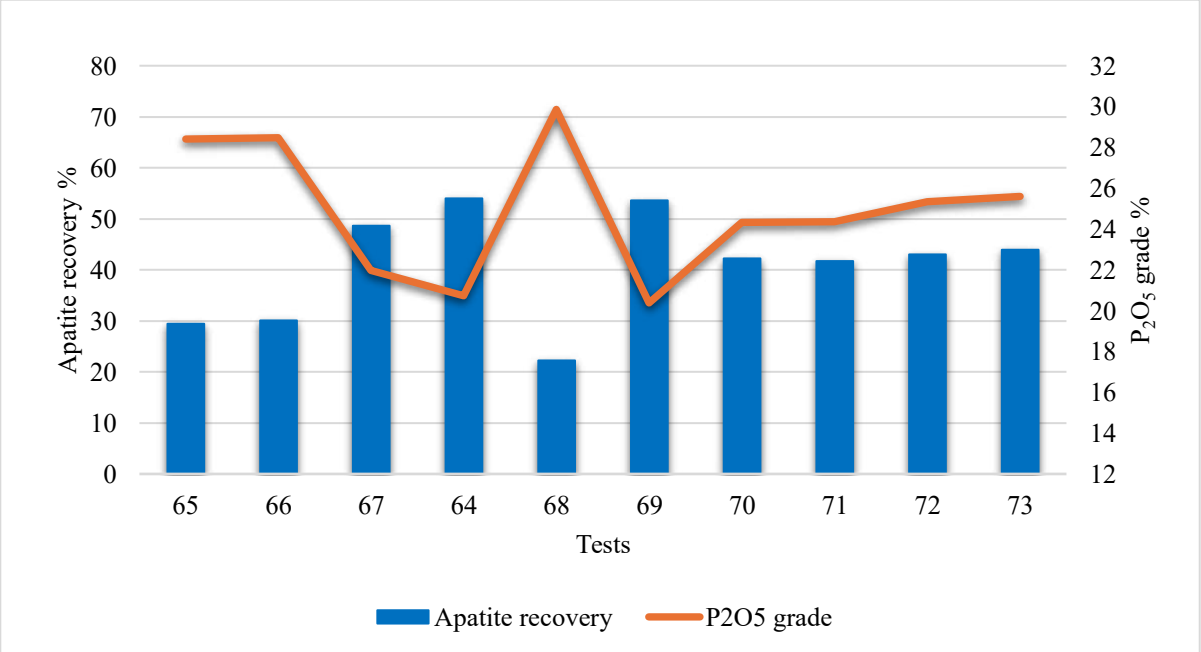

Source: Author (2025).

Both responses exhibited fluctuations across the tested conditions. The highest response index (RI) was observed in Tests 72 (3.14) and 73 (3.27), which corresponded to the central

point replicates with a collector dosage of 50 ppm and a depressant dosage of 700 ppm. However, the highest P_2O_5 grade (29.86%) was achieved in Test 68, corresponding to the lowest collector dosage (22 ppm) tested. This test, however, also yielded the lowest apatite recovery (22.23%).

The influence of the examined variables on the CCD experiments was assessed by estimating individual and interaction effects using an ANOVA. A significance level of 0.1 was applied, and parameters with p-values exceeding this threshold were excluded from the analysis. Table 4.18 shows the estimated effects and corresponding p-values for P_2O_5 grade and apatite recovery in the ultrafine tailing's ore flotation.

Table 4.18 - Estimation of effects and p-value of P_2O_5 grade for ultrafine ore

Factor	P_2O_5 grade		Apatite recovery	
	Effect	**p-value**	**Effect**	**p-value**
Mean	25.322	0.000	42.78	0.000
x_1	-6.897	0.000	21.388	0.000
x_1^2	-	-	-4.760	0.009
x_2^2	-0.933	0.013	-	-
x_1x_2	-0.650	0.088	-	-

Source: Author (2025).

The linear effect of collector dosage was the most significant factor influencing both P_2O_5 grade and apatite recovery. Conversely, depressant dosage had no significant effect on apatite recovery, nor did its quadratic term or its interaction with collector dosage. However, for P_2O_5 grade, the quadratic effect of depressant dosage and its interaction with collector dosage were statistically significant.

Equations 4.3 and 4.4 present the empirical models describing the variations in P_2O_5 grade and apatite recovery as function of the studied independent variables (collector and depressant dosages), respectively. The coefficients corresponding to isolated variables, interactions, and quadratic terms were represented within a matrix system.

$$y_g = 25.322 + \underline{x}\,\underline{b_g} + \underline{x}\,\underline{B_g}\underline{x} \qquad R^2 = 0.994 \qquad (4.3)$$

were: $\underline{b_g} = \begin{bmatrix} -3.448 \\ 0 \end{bmatrix}$ e $\underline{B_g} = \begin{bmatrix} 0 & -0.162 \\ -0.162 & -0.466 \end{bmatrix}$ $\underline{x} = \begin{bmatrix} x_1 \\ x_2 \end{bmatrix}$

$$y_r = 42.785 + \underline{x}\,\underline{b}_r + \underline{x}\,\underline{B}_r\underline{x} \qquad R^2 = 0.982 \qquad (4.4)$$

were: $\underline{b}_r = \begin{bmatrix} 10.939 \\ 0 \end{bmatrix}$ e $\underline{B}_r = \begin{bmatrix} -2.380 & 0 \\ 0 & 0 \end{bmatrix}$ $\underline{x} = \begin{bmatrix} x_1 \\ x_2 \end{bmatrix}$

The coded equations are presented in Table 3.12 (Equations 3.13 and 3.14).

Figure 4.8 illustrates the response surface for (a) P_2O_5 grade and (b) apatite recovery as function of collector dosage (x_1) and depressant dosage (x_2). The complexity of these variables makes it difficult to simultaneously maximize both P_2O_5 grade and apatite recovery, as the conditions that favor one often hinder the other.

Figure 4.8 - Surface response for (a) P_2O_5 grade and (b) apatite recovery as function of solid concentration during conditioning (x_1) and collector dosage (x_2)

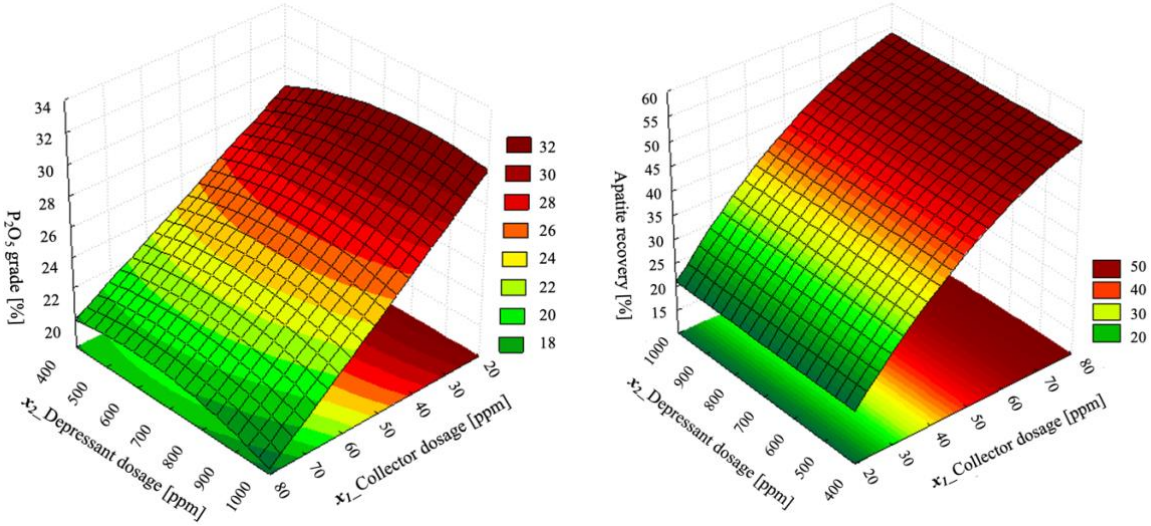

(a) (b)

Source: Author (2025).

The results indicate that increasing collector dosage leads to a decrease in P_2O_5 grade, which can be attributed to the adsorption mechanisms of the collector on phosphate minerals. At low dosages, the observed enhancement in apatite hydrophobicity, leading to a higher P_2O_5 grade (as in Test 68, Figure 4.7, with a grade of 29.86%), is consistent with a potential chemisorption mechanism. In contrast, at high dosages, the increased collector consumption and subsequent decrease in concentrate grade suggest that non-selective adsorption on gangue minerals may be occurring, potentially through mechanisms such as physisorption and possibly chemisorption. The region of highest P_2O_5 grade were observed with collector dosage below 22 ppm and depressant dosages above 500 ppm, consistent with the findings of Al-Thyabat; Yoon

and Shin (2011). Trahar (1981), observed that smaller particle sizes require lower collector dosages, due to their high surface area, favoring selective adsorption and true flotation (ALSAFASFEH; ALAGHA, 2017).

Apatite recovery, in contrast, is more pronounced at high collector dosages, a common trend in flotation due to enhanced particle hydrophobicity. Nonetheless, this also leads to non-selective gangue adsorption, potentially promoting entrainment (GEORGE; NGUYEN; JAMESON, 2004). Figure 4.8(b) shows that maximum recovery occurred at collector dosages above 78 ppm. However, this also compromised selectivity, as increased entrainment of gangue minerals reduces P_2O_5 grade. These findings highlight the critical influence of collector dosage on flotation performance, with a more pronounced effect on apatite recovery than on P_2O_5 grade, consistent with Oliveira *et al.* (2005). While higher collector dosages can generally improve recovery through enhanced adsorption, hydrophobicity, and particle-bubble stability (BRAVO *et al.,* 2005; MATIOLO *et al.,* 2019; OLIVEIRA *et al.,* 2005; OLIVEIRA, 2007; TEAGUE; LOLLBACK, 2012; YU *et al.,* 2024), ultrafine particles present significant challenges. Their low mass and small size reduce collision and attachment probabilities, resulting in poor flotation kinetics, while their susceptibility to entrainment further complicates selectivity (ELBENDARZ; ALEKSANDROVA; NIKOLAEVA, 2019; FARROKHPAY; FILIPPOV; FORNASIERO, 2020; WANG; LIU, 2021).

Interestingly, for the range used in this experimental design, depressant dosage did not significantly influence recovery rates, contrasting with expectations that excessive depressant concentration would suppress the flotation of both valuable and gangue minerals. This behavior is attributed to the adsorption mechanisms of starch, which can interact with apatite surfaces through both physical and chemical mechanisms (ARAUJO, 1988; BAI *et al.,* 2019; TOHRY *et al.,* 2021). Additionally, starch adsorption on both apatite and gangue minerals reduces flotation selectivity. The challenges posed by ultrafine particles, including their low mass and momentum, exacerbate this effect, requiring extended residence times for recovery. Furthermore, the entrainment of fine gangue particles into the froth layer dilutes the concentrate, contributing to lower recovery efficiencies. However, when used in combination with ionic collectors, starch can promote excessive froth formation. This leads to increased froth stability, which may ultimately reduce flotation efficiency (GUIMARÃES; ARAUJO; PERES, 2005; PAVLOVIĆ; BRANDÃO, 2003).

Despite these challenges, a collector dosage of 50 ppm provided a reasonable compromise, achieving the minimum industrial requirements of 24% P_2O_5 grade and 40% apatite recovery. These results emphasize the critical role of particle size in flotation

performance. As demonstrated by Pease *et al.* (2010), flotation efficiency is higher when applied to narrow size distributions. Particles of 5 μm exhibit entirely different hydrodynamics and possess ten times the surface area per unit weight compared to 50 μm particles. This increased surface area significantly raises reagent consumption, making desliming a common practice to reduce costs and prevent slime coating (MATIOLO *et al.,* 2019). However, desliming also results in valuable mineral losses, driving research into improved flotation processes for fine and ultrafine particle recovery.

Recovering ultrafine particles, which in this study had a Sauter mean diameter of 2.43 μm, without prior desliming increases susceptibility to slime coating, a major challenge due to particle agglomeration and increased pulp viscosity. To address this issue, high-intensity conditioning (HIC) was employed, incorporating sodium silicate as a dispersant to reduce pulp viscosity and improve particles dispersion. Flotation experiments were conducted at pH 12, where the dominant silicate species, $SiO(OH)_3^-$, adsorbs onto mineral surfaces, generating electrostatic repulsion between particles and thus reducing aggregation and enhances pulp stability. Furthermore, the depressant properties of sodium silicate may be diminished at this high pH (MOLIFIE *et al.,* 2023), while its ability to increase the negative charge on particle surfaces further minimizing slime coating (FARROKHPAY; FILLIPOV; FORNASIERO*,* 2020). Additionally, HIC likely facilitated the formation of micro and nanobubbles, promoting the two-stage attachment mechanism described by Zhou *et al*. (2020). The coalescence of these bubbles enhanced collision probability and attachment efficiency, leading to improved flotation performance, as observed in Tests 70 through 73. The enhanced dispersion and reduction in initially agglomerated particles further demonstrate the effectiveness of the HIC method combined with a dispersant, which promotes the formation of particle-bubble aggregate. This approach, followed by column flotation, significantly improves ultrafine apatite recovery.

Subrahmanyam and Eric Forssberg (1990) observed that higher agitation overcame the energy barriers between particles due to electrostatic repulsion, van der Waals forces, and specific chemical interactions, enabling particles collision and subsequent attachment via hydrophobic association. They observed that flocculation was maximum at 1200 rpm while no aggregate formation occurred at a low shear rate of 400 rpm. However, for ultrafine particles as 2 μm of synthetic PbS, prolonged stirring can lead to both the formation and disruption of aggregates due to their extremely small size, as noted by Fuerstenau, Hanson and Li (1988). This phenomenon may explain the reduced apatite recovery observed in this study. On the other hand, increasing residence time, combined with optimized collector dosage, could improve

flotation performance by allowing the froth to drain more effectively, which could decrease entrainment and further enhance recovery.

The presented findings reinforce the critical need for parameter optimization in ultrafine apatite tailings flotation. This study validates the potential of these tailings as a valuable secondary resource, offering solutions to reduce tailings storage, environmental impact, and improve resource efficiency. Combining mineral recovery with responsible environmental management can lead to cost-effective and sustainable beneficiation practices, contributing significantly to both scientific knowledge and industry advancement.

Building upon the methodological framework established for fine particle processing, a parallel multi-response optimization study was conducted for ultrafine ore using the desirability function approach following central composite design (CCD) evaluation (BURATTI *et al.,* 2017; DERRINGER; SUICH, 1980; VIACAVA; ROURA; AGÜERO, 2015). The optimization targeted simultaneous maximization of both apatite recovery and P_2O_5 grade while maintaining process efficiency and economic feasibility - critical considerations for ultrafine particle beneficiation from tailings sources. The desirability profiles (Figure 4.9) illustrate the response surfaces for key operational parameters: collector dosage (x_1) and depressant dosage (x_2), analyzed using coded values to identify optimal conditions for P_2O_5 grade and apatite recovery maximization.

Figure 4.9 - Desirability of ultrafine ore

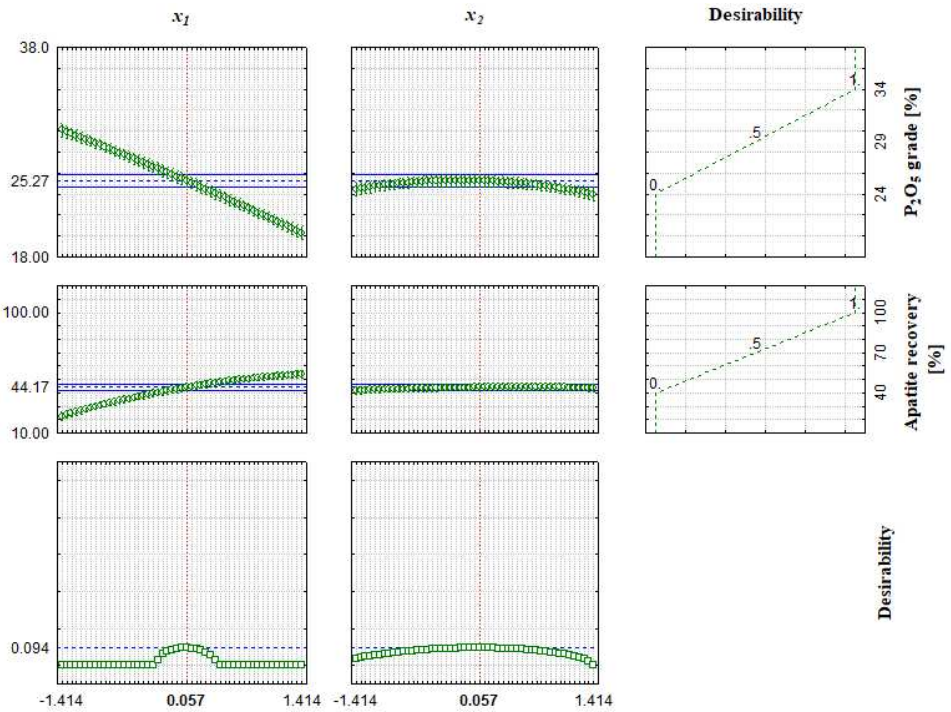

Source: Author (2025).

Table 4.19 presents both the coded optimal values identified through desirability function analysis and their corresponding actual (decoded) values.

Table 4.19 - Coded and actual values of each variable at the optimal condition from desirability for ultrafine ore.

Variable	Coded value	Decoded value
Collector dosage (x_1)	0.057	52.83 ppm
Depressant dosage (x_2)	0.057	711.31 ppm

Source: Author (2025).

Experimental validation was performed through triplicate confirmatory tests under the determined optimal conditions. As detailed in Table 4.20, the close correlation between predicted and experimental results (with standard deviations of 0.566 for P_2O_5 grade and 0.962 for recovery) confirms the model's predictive accuracy. This table also presents the average CaO/P_2O_5 ratio of 1.39 for the optimized tests, confirming the apatite origin of the phosphorus, along with the corresponding average selectivity ratios (SR Fe_2O_3 and SR SiO_2). The exceptional reproducibility is further evidenced by coefficient of variation (CV) values consistently below 5% for P_2O_5 grade, apatite recovery and CaO/P_2O_5 responses, demonstrating notable process stability.

Table 4.20 - Experimental and predicted response values of desirability optimization for ultrafine ore.

Response	Experimental result	Predicted result	Standard deviation	Coefficient of variation
P_2O_5 grade [%]	26.10	25.27	0.566	0.022
Apatite recovery [%]	43.94	44.17	0.962	0.022
CaO/P_2O_5	1.39	-	0.003	0.002
SR Fe_2O_3	1.66	-	0.308	0.186
SR SiO2	5.73	-	0.795	0.139

Source: Author (2025).

These comprehensive results not only validate the effectiveness of the desirability function approach for ultrafine apatite systems but also confirm the practical applicability of the optimized parameters. The low observed deviations between predicted and actual performance metrics underscore the robustness of this optimization strategy for enhancing flotation efficiency in challenging ultrafine tailings processing applications.

5. CONCLUSIONS

Based on the results of this study on the flotation of fine and ultrafine apatite tailings, it can be concluded that the flotation of deslimed fine ore tailings demonstrated significantly better performance compared to ultrafine, non-deslimed ore tailings. The flotation tests highlighted the critical role of collector selection in achieving efficient separation and apatite recovery. Rice oil was found to be more effective than Agem A3, providing superior selectivity, which enhanced true flotation and minimized gangue entrainment.

For flotation of fine apatite tailings:

The flotation of deslimed fine ore tailings demonstrated significant improvements in performance through the analysis of key variables: solid concentration during conditioning, collector dosage, depressant dosage, pH, and dispersant dosage. Although dispersant dosage was evaluated as part of the study, its use was found to be unnecessary for the fine ore flotation system. The optimal conditions were identified, conducted with 51.48% solid concentration during conditioning, a collector dosage of 474.13 ppm (the highest dosage tested), a depressant dosage of 346.63 ppm, and a pH of 10.18, yielded the best response. This condition successfully reached the industrial specifications, achieving 34.82% of P_2O_5 grade and 92.16% of apatite recovery.

The analysis of individual variables revealed that greater performance was achieved within the following ranges: solid concentration during conditioning between 45%-65%, collector dosage above 450 ppm, depressant dosage between 251.7-450 ppm, and pH between 9.7-11.9.

Ultimately, this study demonstrates the feasibility of improving the flotation performance of fine ore tailings, significantly reducing the volume of material sent to slime ponds. The integration of high-intensity conditioning followed by column flotation enabled the achievement of satisfactory performance, enhancing both recovery and grade. By enhancing resource recovery and minimizing environmental impact, these findings support a more sustainable and eco-friendly mineral processing approach.

For flotation of ultrafine apatite tailing:

The flotation of ultrafine apatite tailings presents significant challenges due to the very small particle size, which adversely affects both recovery and selectivity. Notably, this ultrafine

ore did not undergo desliming, a common practice in flotation processes, which further complicates the separation efficiency. Initial cell flotation tests confirmed these inherent difficulties, as none of the tested conditions simultaneously achieved the required P_2O_5 grade (24%) and minimum apatite recovery (40%). These results can be attributed to differences in mineralogical composition, which also influenced reagent dosage requirements. Given these limitations, optimization through alternative strategies became essential, leading to the adoption of column flotation combined with high-intensity conditioning (HIC).

The optimal condition for ultrafine ore flotation was achieved with a collector dosage of 52.83 ppm, a depressant dosage of 711.31 ppm, 40% solid concentration during conditioning, pH 12, and 250 ppm sodium silicate as a dispersant. This combination yielded the best results, with a P_2O_5 grade of 26.10% and an apatite recovery of 43.94%, meeting industrial requirements. Notably, increasing collector dosage improved recovery but reduced the P_2O_5 grade due to non-selective adsorption, underscoring the need for precise dosage control. Furthermore, while the depressant dosage had a limited effect on recovery, it was still an important parameter for analysis.

HIC proved effective in mitigating slime coating, enhancing particle-bubble interactions, and improving collision probability and attachment efficiency. In conclusion, this study demonstrates the feasibility of recovering ultrafine apatite from tailings using the proposed flotation strategies, even without the desliming process. The integration of HIC, followed by column flotation, can achieve acceptable concentrate grades and apatite recovery. These findings not only advance sustainable beneficiation practices but also provide a foundation for further research, including continuous process optimization and pilot-scale trials to validate industrial applicability. Collectively, this work contributes to advancing sustainable beneficiation practices, reducing tailings disposal, and enhancing resource efficiency in phosphate processing.

5.1. FUTURE WORKS

As future work, the following aspects are suggested:

- Investigating the effect of pulp rheology on flotation performance, particularly its influence on particle-bubble collision and attachment efficiency;
- Increasing the residence time to enhance the flotation performance of ultrafine ore;
- Analyzing the effect of column height on the flotation efficiency of ultrafine particles;

- Investigating alternative dispersants and their impact on selectivity and recovery;
- Evaluating the influence of microbubble and nanobubble technology to improve fine and ultrafine particle flotation;
- Evaluating the effect of water quality on the flotation performance of ultrafine ore.

REFERENCES

AARAB, I.; DERQAOUI, D.; AMARI, K. E.; YAACOUBI, A.; ABIDI, A.; ETAHIRI, A.; BAÇAOUI, A.Influence of surface dissolution on reagents' adsorption on low-grade phosphate ore and its flotation selectivity. **Colloids and Surfaces A: Physicochemical and Engineering Aspects,** v. 631, 127700, 2021.DOI: https://doi.org/10.1016/j.colsurfa.2021.127700

AHMED, H. A. Optimization of desliming prior to phosphate ore upgrading by flotation. **Physicochemical Problems of Mineral Processing**, v. 41, p. 79-88, 2007.

ALEKSANDROVA, T. N.; ELBENDARI, A. M. Increasing the efficiency of phosphate ore processing using flotation method. **Journal of Mining Institute**, v. 248, p. 260-271, 2021. DOI: https://doi.org/10.31897/PMI.2021.2.10

ALSAFASFEH, A.; ALAGHA, L. Recovery of phosphate minerals from plant tailings using direct froth flotation. **Minerals**, v. 7, n. 8, 12 ago. 2017. DOI: https://doi.org/10.3390/min7080145

ALSAFASFEH, A.; ALAGHA, L.; ALZIDANEEN, A.; NADENDLA, V. S. S. Optimization of flotation efficiency of phosphate minerals in mine tailings using polymeric depressants: Experiments and machine learning. **Physicochemical Problems of Mineral Processing**, v. 58, n. 4, 2022. DOI: https://doi.org/10.37190/PPMP/150477

AL-THYABAT, S. Empirical evaluation of the role of sodium silicate on the separation of silica from Jordanian siliceous phosphate. **Separation and Purification Technology**, v. 67, n. 3, p. 289-294, 2009. DOI: https://doi.org/10.1016/j.seppur.2009.03.034

AL-THYABAT, S.; YOON, R. H.; SHIN, D. Floatability of fine phosphate in a batch column flotation cell. **Minerals and Metallurgical Processing**, v. 28, n. 2, p. 110, 2011. https://doi.org/10.1007/BF03402396

ANSARI, M. I. Fine particle processing – A difficult problem for mineral engineers. *In:* PROCEEDINGS: PROF.97. Jamshedpur: NML, p. 93-102, 1997.

AQUINO, J. A.; OLIVEIRA, M. L. M.; FERNANDES, M. D. Flotação em Coluna. In: LUZ, A. B.; SAMPAIO, J. A.; FRANÇA, S. C. A. **Tratamento de Minérios.** 5 ed. Rio de Janeiro, CETEM/MCT, 2010, p. 517-558.

ARAÚJO, A. **Starch modification of the flocculation and flotation of apatite.** 1988. Thesis (Doctor of Mining Engineerig) – University of British Columbia, Vancouver, 1988.

ARAÚJO, A. C.; VIANA, P. R. M.; PERES, A. E. C. Flotation machines in Brazil—columns versus mechanical cells. *In:* CENTENARY OF FLOTATION SYMPOSIUM. BRISBANE, QLD, 6–9. AusIMM, Melbourne, p. 187–192, 2005.

ARANTES, R. S.; SOUZA, T. F.; LIMA, R. M. F. Influência do módulo do silicato de sódio na flotação de minério de ferro: Estudos fundamentais. **Tecnologia em Metalurgia, Materiais e Mineração,** v. 14, n. 1, p. 39-45, 2017. DOI: http://dx.doi.org/10.4322/2176-1523.1161.

AVELAR, A. N. **Caracterização dos minerais dos grupos da apatita e carbonatos no minério sílico-carbonatado de Catalão, GO, e sua relevância no processo de flotação**. Tese (Doutorado em Engenharia de Minas), UFMG, Belo Horizonte, 2018.

BAI, S.; DING, Z.; FU, X.; LI, C.; LV, C.; WEN, C. Investigations on Soluble Starch as the Depressant of Hematite during Flotation Separation of Apatite. **Physicochemical Problems of Mineral Processing**, v. 55, 2019. DOI: https://doi.org/10.5277/ppmp18108.

BENÍCIO, L. P. Overview of the use of phosphate fertilizers in Brazil, a review. **Agri-Environmental Sciences**, v. 8, n. 2, 2022. DOI: https://doi.org/10.36725/agries.v8i2.7761.

BEZERRA, M. A.; SANTELLI, R. E.; OLIVEIRA, E. P.; VILLAR, L. S.; ESCALEIRA, L. A. Response surface methodology (RSM) as a tool for optimization in analytical chemistry. **Talanta**, v. 76, n. 5, p. 965–977, 2008. DOI: https://doi.org/10.1016/j.talanta.2008.05.019.

BORROW, D. J.; VAN NETTEN, K.; GALVIN, K. P. Ultrafine Particle Recovery Using Thin Permeable Films. **Frontiers in Chemistry**, v. 6, 220, 2018. DOI: 10.3389/fchem.2018.00220.

BRABCOVÁ, Z.; KARAPANTISIOS, T.; KOSTOGLOU, M.; BASAROVÁ, P.; MATIS, K. Bubble-particle collision interaction in flotation systems. **Colloids and Surfaces A:**

Physicochemical and Engineering Aspects, v. 473, p. 95-103, 2015. DOI: https://doi.org/10.1016/j.colsurfa.2014.11.040.

BRAVO, S. V. C.; MONTE, M. B. M.; TOREM, M. L.; DUTRA, A. J. B.; TONDO, L. A. The influence of size and collector on the flotation of a very low grade auriferous ore. **Minerals Engineering**, v. 18, p. 459-461, 2005.

BULATOVIC, S. M. **Handbook of flotation reagents: chemistry, theory and practice: flotation of sulfide ores.** 1. ed. Amsterdam: Elsevier Science, 2007. v. 1. 458 p.

BURATTI, C.; BARBANERA, M.; LASCARO, E.; COTANA, F. Optimization of torrefaction conditions of coffee industry residues using desirability function approach. **Waste Management**, v. 73, p. 523–534, 2018. DOI: https://doi.org/10.1016/j.wasman.2017.04.012.

CAO, Q.; CHENG, J.; WEN, S.; LI, C.; BAI, S.; LIU, D. A mixed collector system for phosphate flotation. Minerals **Engineering,** v. 78, p. 114–121, 2015. DOI: https://doi.org/10.1016/j.mineng.2015.04.020.

CAPPONI, F. **Avanços na recuperação de finos de minérios pelo processo de flotação "extensora", o caso da mina de Chuquicamata**. Dissertação (Mestrado em Engenharia de Minas) – Universidade Federal do Rio Grande do Sul, Porto Alegre, 2005.

CAPPONI, F.; AZEVEDO, A.; OLIVEIRA, H.; RUBIO, J. Column rougher flotation of fine niobium-bearing particles assisted with micro and nanobubbles. **Minerals Engineering**, v. 199, 2023.

CARNEIRO, A. A.; SANTOS, A. M. A.; OLIVEIRA, M. S.; GUIMARÃES JUNIOR, M.; ALVES, J. V. S. Avaliação de diferentes polissacarídeos como depressores na flotação aniônica direta de minério fosfático ultrafino. *In:* XXVIII ENCONTRO NACIONAL DE TRATAMENTO DE MINÉRIOS E METALURGIA EXTRATIVA, Belo Horizonte, 4 a 8 de Novembro de 2019.

CARNEIRO, A.; OLIVEIRA, M.; SOUZA, C.; PAIM, T.; CRUZ, A.; ALVES, J. V.; GUIMARÃES JUNIOR, M. Flotação reativa como alternativa sustentável para remoção de ganga carbonática presente em minérios fosfáticos. **Matéria**, v. 28, n. 1, p. 1-9, 2023. DOI: https://doi.org/10.1590/1517-7076-RMAT-2022-0327

CARVALHO, J. A. E.; BRANDÃO, P. R. G.; HENRIQUES, A. B.; OLIVEIRA, P. S.; CANÇADO, R. Z. L.; SILVA, G. R. Selective flotation of apatite from micaceous minerals using patauá palm tree oil collector. **Minerals Engineering**, v. 156, 2020. DOI: https://doi.org/10.1016/j.mineng.2020.106474.

CARVALHO, M. R. **Interferência de cátions Ca^{2+} nas etapas de deslamagem e flotação de minério de ferro.** Dissertação (Mestrado em Engenharia de Minas) – PPG-EM, Universidade Federal de Ouro Preto, Ouro Preto, 2003.

CDC. About us. C.D.C Equipamentos Industriais Ltda [1994]. Disponível em: https:// cdc.ind.br/equipamentos/equipamentos-de-laboratorio/. Acesso em 15 jan. 2024.

CHAVES, A. P.; LEAL FILHO, L. S. B.; BRAGA, P. G. A. Flotação. In: LUZ, A. B.; SAMPAIO, J. A.; FRANÇA, S. C. A. **Tratamento de Minérios.** 5 ed. Rio de Janeiro, CETEM/MCT, 2010, p. 465-516.

CHAVES, A. P.; RODRIGUES, W. J. Máquinas de flotação. In: CHAVES, A. P. Coleção **Teoria e Prática do Tratamento de Minério: A Flotação no Brasil**. São Paulo, Oficina de Textos, 3 ed., 2013, p. 40-64.

CHENG, G. et al. A study of Bubble-particle interactions in a column flotation process. **Physicochemical Problems of Mineral Processing**, v. 53, n. 1, p. 17–33, 2017. DOI: 10.5277/ppmp170102

CHULA, A. M. D. **Caracterização mineralógica do minério fosfático da mina de Tapira-MG**. Tese (Doutorado em Engenharia de Minas) – Universidade Federal de Minas Gerais, Belo Horizonte, 2004.

COLLINS, G. L.; JAMESON, G. L. Experiments on the flotation of fine particles. The influence of particles size and charge. **Chemical Engineering Science**, v. 31, p. 985-991, 1976. DOI: https://doi.org/10.1016/0009-2509(76)87019-4

DABBEBI, R.; PERUMAL, P.; MOUKANNA, S. Management and valorization of phosphate beneficiation slime: a critical review. **International Journal of Environmental Science and Technology,** v. 20, p. 11763-11776, 2023.

DAI, Z.; FORNASIERO, D.; RALSTON, J. Particle–bubble attachment in mineral flotation. **Journal of Colloid and Interface Science**, v. 217, p. 70–76, 1999. DOI: https://doi.org/10.1006/jcis.1999.6319

DEMUNER, L. R. **Estudo da influência do holdup do ar na flotação em coluna para diferentes granulometrias de minério fosfático.** Dissertação (Mestrado em Engenharia Química), Universidade Federal de Uberlândia, Uberlândia, 2019.

DERHY, M.; TAHA, Y.; HAKKOU, R.; BENZAAZOUA, M. Review of the main factors affecting the flotation of phosphate ores. **Minerals**, v. 10, n. 12, p. 1-22, 2020. DOI: https://doi.org/10.3390/min10121109.

DERRINGER, G.; SUICH, R. Simultaneous Optimization of Several Response Variables. **Journal of Quality Technology** 12, 214–219, 1980. DOI: https://doi.org/10.1080/00224065.1980.11980968

DOBBY, G.; FINCH, J. Particle size dependence in flotation derived from a fundamental model of the capture process. **International Journal of Mineral Processing**, v. 21, p. 241–260, 1987. DOI: https://doi.org/10.1016/0301-7516(87)90057-3

DONG, L.; WEI, Q.; JIAO, F.; QIN, W. Utilization of polyepoxysuccinic acid as the green selective depressant for the clean flotation of phosphate ores. **Journal of Cleaner Production,** v. 282, 124532, 2021. DOI: https://doi.org/10.1016/j.jclepro.2020.124532.

ELBENDARZ, A.; ALEKSANDROVA, T.; NIKOLAEVA, N. Influence of operating parameters on the flotation of the Khibiny Apatite-Nepheline Deposits. **Journal of Materials Research and Technology**, v. 8, issue 6, p. 5080-5090, 2019. DOI: https://doi.org/10.1016/j.jmrt.2019.08.027

FARROKHPAY, S.; FILIPPOV, L.; FORNASIERO, D. Flotation of Fine Particles: A Review. **Mineral Processing and Extractive Metallurgy Review**, v. 42, n. 7, p. 473–483, 2020. DOI: https://doi.org/10.1080/08827508.2020.1793140.

FENG, D.; ALDRICH, C. Effect of particle size on flotation performance of complex sulphide ores. **Minerals Engineering**, v. 12, n. 7, p. 721-731, 1999. DOI: https://doi.org/10.1016/S0892-6875(99)00059-X

FILIPPOVA, I. V.; FILIPPOV, L. O.; DUVERGER, A.; SEVEROV, V. V. Synergetic effect of a mixture of anionic and nonionic reagents: Ca mineral contrast separation by flotation at neutral pH. **Minerals Engineering**, v. 66-68, p. 135-144, 2014. DOI: https://doi.org/10.1016/j.mineng.2014.05.009.

FUERSTENAU, D. W. Fine particle flotation. *In:* FINE PARTICLE PROCESSING, PROCEEDINGS INTERNATIONAL SYMPOSIUM, v. 1, p. 669–70, 1980.

FUERSTENAU, D. W.; HANSON, C.; LI, J. S. Shear flocculation and carrier flotation of fine hematite. *In:* PROCEEDINGS OF METALLURGICAL SOCIETY OF CANADIAN INSTITUTE OF MINING AND METALLURGY, PRODUCTION AND PROCESSING OF FINE PARTICLES, Pergamon, 1988. p. 329-335. DOI: https://doi.org/10.1016/B978-0-08-036448-3.50039-6.

GEORGE, P.; NGUYEN, A. V.; JAMESON, G. J. Assessment of true flotation and entrainment in the flotation of submicron particles by fine bubbles. Minerals Engineering, v. 17, p. 847-853, 2004. DOI: https://doi.org/10.1016/j.mineng.2004.02.002

GORDEIJEV, J.; HIRVA, P. Theoretical studies on the interaction of oleoyl sarcosine with the surface of apatite. Surface Science, v. 440, p. 321-326, 1999. DOI: https://doi.org/10.1016/S0039-6028(99)00810-9.

GOUVEIA, D. S. **Obtenção de pós nanométricos de hidroxiapatita utilizando ultra-som**. Tese (Doutorado em ciências da área de tecnologia nuclear – materiais), USP, São Paulo, 2008.

GUIMARÃES, R. C. **Separação de barita em minério fosfático através da flotação em coluna**. Dissertação (Mestrado) – Universidade de São Paulo, São Paulo, 1995.

GUIMARÃES, R. C.; ARAUJO, A. C.; PERES, A. E. C. Reagents in igneous phosphate ores flotation. **Minerals Engineering**, v. 18, n. 2, p. 199-204, 2005. DOI: https://doi.org/10.1016/j.mineng.2004.08.022.

GUIMARÃES, R. C.; PERES, A. E. C. Experiência brasileira de produção de concentrado fosfático a partir de lamas. *In:* PROCEEDINGS OF THE XIX ENCONTRO NACIONAL DE TRATAMENTO DE MINÉRIOS E METALURGIA EXTRATIVA, Recife, Brasil, 26–29, 2002. v. I, p. 247–253.

GUO, F.; LI, J. Separation strategies for Jordanian phosphate rock with siliceous and calcareous gangues. **International Journal of Mineral Processing**, v. 97, n. 1-4, p. 74-78, 2010. DOI: https://doi.org/10.1016/j.minpro.2010.08.006.

HADLER, K.; AKTAS, Z.; CILLIERS, J. J. The effects of frother and collector distribution on flotation performance. **Minerals Engineering**, v. 18, n. 2, p. 171-177, 2005. DOI: https://doi.org/10.1016/j.mineng.2004.09.014.

HEWITT, D.; FORNASIERO, D.; RALSTON, J. Bubble–particle attachment. Journal of the Chemical Society, Faraday Transactions, v. 91, p. 1997–2001, 1995. DOI: https://doi.org/10.1039/FT9959101997

IFA - International Fertilizer Association [1927]. Disponível em: https://www.ifastat.org/ databases/ graph/1_1?utm_source=chatgpt.com. Acesso em 15 set. 2024.

JENA, M. S.; BISWAL, S. K.; DAS, S. P.; REDDY, P. S. R. Comparative study of the performance of conventional and column flotation when treating coking coal fines. **Fuel Processing Technology**, v. 89, p. 1409–1415, 2008.

JIANG, H.; YANG, H.; XING, Y.; CAO, Y.; GUI, X. The effect of impeller speeds on the nanobubbles flotation efficiency of ultrafine coal particles. **Powder Technology**, v. 449, 120431, 2024. DOI: https://doi.org/10.1016/j.powtec.2024.120431.

KUPKA, N.; RUDOLPH, M. Froth flotation of scheelite – A review. **International Journal of Mining Science and Technology,** v. 28, n. 3, p. 373-384, 2018. DOI: https://doi.org/10.1016/j.ijmst.2017.12.001

LAFHJ, Z.; FILIPPOV, L.; FILIPPOVA, I. V. Improvement of calcium mineral separation contrast using anionic reagents: electrokinetics properties and flotation. **Journal of Physics: Conference Series**, v. 879, 012012, 2017. DOI: 10.1088/1742-6596/879/1/012012

LASKOWSKI, J. S.; LIU, Q.; O'CONNOR, C. T. Current understanding of the mechanism of polysaccharide adsorption at the mineral/aqueous solution interface. **International Journal of Mineral Processing,** v. 84, n. 1-4, p. 59-68, 2007. DOI: https://doi.org/10.1016/j.minpro.2007.03.006.

LAPIDO-LOUREIRO, F. E. V.; MELAMED, R. **O fósforo na agricultura brasileira: uma abordagem minero-metalúrgica.** Série Estudos e Documentos, n. 67. Rio de Janeiro: CETEM/MCT, 2006.

LEJA, J. **Surface chemistry of froth flotation**. New York: Plenum Press, 1982.

LIU, C.; ZHANG, W.; LI, H. Selective flotation of apatite from calcite using 2-phosphonobutane-1,2,4-tricarboxylic acid as depressant. **Minerals Engineering**, v. 136, p. 62–65, 2019. DOI: https://doi.org/10.1016/j.mineng.2019.03.003.

LIU, Y.; TAO, X.; JIANG, H.; CHEN, R. Intensification of fine apatite flotation with microbubble generation and inclined plates in the flotation column. **Chemical Engineering and Processing – Process Intensification,** v. 158, 108133, 2020. DOI: https://doi.org/10.1016/j.cep.2020.108133.

MATIOLO, E. **Avanços no desenvolvimento da coluna de três produtos – C3P fundamentos e aplicações.** Tese (Doutorado em Engenharia de Minas, Metalurgica e de Materiais), Universidade Federal de Porto Alegre, Porto Alegre, 2008.

MATIOLO, E.; COUTO, H. J. B.; TEIXEIRA, M. F. L.; FREITAS, A. S.; ALMEIDA, R. N. Recovery of Apatite from Slimes of A Brazilian Phosphate Ore. **Journal of Wuhan Institute of Technology,** v. 39, n. 6, 2017.

MATIOLO, E.; COUTO, H. J. B.; TEIXEIRA, M. F. L.; FREITAS, A. S.; ALMEIDA, R. N. A comparative study of different columns sizes for ultrafine apatite flotation. **Minerals,** v. 9, n. 7, 2019. DOI: https://doi.org/10.3390/min9070391.

MARTINS, M. **Molhabilidade de apatita e sua influência na flotação**. Tese (Doutorado em Engenharia Mineral), Universidade de São Paulo, São Paulo, 2009.

MENDES, T. F.; REIS, A. S.; SILVA, A. C.; BARROZO, M. A. S. Analysis of the Effect of Surfactants on the Performance of Apatite Column Flotation. **Minerals**, v. 14, n. 8, 840, 2024. DOI: https://doi.org/10.3390/min14080840.

MONTE, M. B. M.; PERES, A. E. C. Química de superfície na flotação. In: LUZ, A. B.; SAMPAIO, J. A.; FRANÇA, S. C. A. **Tratamento de minérios**. 5. ed. Rio de Janeiro: CETEM/MCT, 2010. p. 399-457.

MOLIFIE, A.; BECKER, M.; GELDENHUYS, S.; MCFADZEAN, B. Investigating the reasons for the improvement in flotation grade and recovery of an altered PGE ore when using sodium silicate. **Minerals Engineering**, v. 195, 108024, 2023. DOI: https://doi.org/10.1016/j.mineng.2023.108024.

NGUYEN, A. V.; EVANS, G. M. Movement of fine particles on an air bubble surface studied using high-speed video microscopy. **Journal of Colloid and Interface Science**, v. 273, n. 1, p. 271-277, 2004. DOI: https://doi.org/10.1016/j.jcis.2003.12.066.

NUNES, J. A. S. **Estudo de recuperação de chumbo de escória metalúrgica por flotação**. Tese (Doutorado em Engenharia Química), UFPE, 2015.

OEDIYANI, S.; MUTTAQUIN, A.; HARYONO, D.; SUWANDANA, R. F. Metallurgical performance of column and mechanical flotation as a rougher circuit in sphalerite ore flotation with %solid and frother dose variation. *In:* IOP CONFERENCE SERIES: MATERIAL SCIENCE AND ENGINEERING**,** v. 909, 012010, 2020. DOI: https://doi.org/10.1088/1757-899X/909/1/012010.

OLIVEIRA, M. S. **Flotação em coluna do rejeito remoído do processo de concentração da apatita.** Dissertação (Mestrado em Engenharia Química), PPG-EQ/UFU, Uberlândia, 2004.

OLIVEIRA, M. S.; ATAÍDE, C. H.; BARROZO, M. A. S. Selectivity in phosphate column flotation. **Minerals Engineering**, v. 20, n. 2, p. 197-199, 2007. DOI: https://doi.org/10.1016/j.mineng.2006.09.004.

OLIVEIRA, M. S.; Cioqueta, D. R.; Sallum, M.; Miro, R.; Guimarães, R. C.; Ataíde, C. H.; Barrozo, M. A. S. A study of the rejects recovery in a column flotation. **Materials Science Forum**, v. 498-499, p. 278-284, 2005. DOI: https://doi.org/10.4028/www.scientific.net/MSF.498-499.278.

OLIVEIRA, M. S.; SANTANA, R. C.; ATAÍDE, C. H.; BARROSO, M. A. S. Recovery of apatite from flotation tailings. **Separation and Purification Technology**, v. 79, n. 1, p. 79–84, 2011. DOI: https://doi.org/10.1016/j.seppur.2011.03.015

PASCOE, R. D.; DOHERTY, E. Shear flocculation and flotation of hematite using sodium oleate. **International Journal of Mineral Processing,** v. 51, n. 1-4, p. 269-282, 1997. DOI: https://doi.org/10.1016/S0301-7516(97)00033-1.

PAVLOVIC, S.; BRANDÃO, P. R. G. Adsorption of starch, amylose, amylopectin and glucose monomer and their effect on the flotation of hematite and quartz. **Minerals Engineering**, v. 16, n. 11, p. 1117-1122, 2003. DOI: https://doi.org/10.1016/j.mineng.2003.06.011.

PEASE, J. D.; CURRY, D. C.; YOUNG, M. F. Designing flotation circuits for high fines recovery. **Minerals Engineering**, v. 19, p. 831-840, 2006. DOI: https://doi.org/10.1016/j.mineng.2005.09.056

PEASE, J. D.; YOUNG, M. F.; CURRY, D.; JOHNSON, N. W. Improving fines recovery by grinding finer. **Mineral Processing and Extractive Metallurgy,** v. 119, n. 4, p. 216-222, 2010. DOI: https://doi.org/10.1179/037195510X12816242170852.

PENNA, R.; OLIVEIRA, M. L. M.; VALADÃO, G. E. S.; PERES, A. E. C. Estudo comparativo entre dois sistemas de aeração de coluna de flotação. **REM: Revista Escola de Minas**, v. 56, n. 3, 2003. DOI: https://doi.org/10.1590/S0370-44672003000300009.

PAIVA, P. P. R.; MONTE, M. B. M.; GASPAR, J. C. Concentration by apatite flotation originating from carbonatically affiliated rocks. **REM: Revista Escola de Minas,** v. 64, n. 1, p. 116, 2011. DOI: https://doi.org/10.1590/S0370-44672011000100015.

PERES, A. E. C.; ARAUJO, A. C. A flotação como operação unitária no tratamento de minérios. In: CHAVES, A. P. **Coleção Teoria e Prática do Tratamento de Minério: A Flotação no Brasil**. São Paulo, Oficina de Textos, 3 ed., 2013. p. 9-39.

QI, G. W.; KLAUBER, C.; WARREN, L. J. Mechanism of action of sodium silicate in the flotation of apatite from hematite. **International Journal of Mineral Processing**, v. 39, n. 3-4, p. 251-273, 1993. DOI: https://doi.org/10.1016/0301-7516(93)90019-7.

RAMOS, K. S. **Flotação metafosforito silicatado de Lagamar/MG**. Dissertação (Mestrado em Engenharia de Minas), Universidade Federal de Ouro Preto, Ouro Preto, 2018.

REIS, A. S. **Estudo da geração de bolhas de diversos tamanhos em coluna de flotação**. Dissertação (Mestrado em Engenharia Química), Universidade Federal de Uberlândia, Uberlândia, 2015.

REIS, A. S. **Estudo da influência do tamanho de bolha na flotação em coluna para diferentes granulometrias de apatita.** Tese (Doutorado em Engenharia Química), Universidade Federal de Uberlândia, Uberlândia, 2019.

REIS, A. S.; DEMUNER, L. R.; BARROZO, M. A. S. Effect of bubble size on the performance flotation of fine particles of a low-grade Brazilian apatite ore. **Powder Technology**, v. 356, p. 884-891, 2019. DOI: https://doi.org/10.1016/j.powtec.2019.09.029.

REIS, A. S.; MENDES, T. F.; PETRI JÚNIOR, I.; BARROZO, M. A. S. Influence of bubble size on performance of apatite flotation of different particle sizes. **Particulate Science and Technology,** v. 41, n. 7, p. 1044–1052, 2023. DOI: https://doi.org/10.1080/02726351.2023.2170840.

REIS, A. S.; REIS FILHO, A. M.; DEMUNER, L. R.; BARROZO, M. A. S. Effect of bubble size on the performance flotation of fine particles of a low-grade Brazilian apatite ore. **Powder Technology**, v. 356, p. 884-891, 2019. DOI: https://doi.org/10.1016/j.powtec.2019.09.029.

RUAN, Y.; HE, D.; CHI, R. Review on Beneficiation Techniques and Reagents Used for Phosphate Ores. **Minerals,** v. 9, n. 4, 253, 2019. DOI: https://doi.org/10.3390/min9040253.

RUBIO, J.; CAPPONI, F.; MATIOLO, E.; NUNES, G. N. Advances in flotation of mineral fines. *In:* PROCEEDING OF THE XXII INTERNATIONAL MINERAL PROCESSING CONGRESS, Cape Town, South Africa, 2003.

RUBIO, J.; CAPPONI, F.; RODRIGUES, R. T.; MATIOLO, E. Enhanced flotation of sulfide fines using the emulsified oil extender technique. **International Journal of Mineral Processing**, v. 84, n. 1-4, p. 41–50, 2007.

RUBIO, J. O Processo de Condicionamento em Alta Intensidade (CAI) na Flotação de Minérios. In: CHAVES, A. P. **Coleção Teoria e Prática do Tratamento de Minério: A Flotação no Brasil.** São Paulo, Oficina de Textos, 3 ed., 2013. p. 428-449.

ROSA, J. J. **O condicionamento a alta intensidade e a recuperação de finos de minérios por flotação**. Dissertação (Mestrado em Engenharia de Minas), Universidade Federal do Rio Grande do Sul, Porto Alegre, 1997.

SANTANA, R. C. **Efeito da altura da coluna na flotação de minério fosfático em diferentes granulometrias**. Tese (Doutorado em Engenharia Química), Universidade Federal de Uberlândia, Uberlândia, 2011.

SANTANA, R. C.; DUARTE, C. R.; ATAÍDE, C. H.; BARROZO, M. A. S. Flotation selectivity of phosphate ore: effects of particle size and reagent concentration. **Separation Science and Technology**, v. 46, p. 1511-1518, 2011. DOI: https://doi.org/10.1080/01496395.2011.561268.

SANTANA, R. C.; RIBEIRO, M. A.; SANTOS, A. S.; ATAÍDE, C. H.; BARROZO, M. A. S. Flotation of fine apatitic ore using microbubbles. **Separation and Purification Technology**, v. 98, p. 402–409, 2012.

SANTOS, A. R. **Estudo do comportamento dinâmico de colunas de flotação utilizando técnicas nucleares.** Dissertação (Mestrado) – CDTN/CNEN, Belo Horizonte, 2005.

SANTOS, M. A. **Estudo da influência de íons contaminantes na flotação de apatita em coluna**. Dissertação (Mestrado em Engenharia Química), Universidade Federal de Uberlândia, Uberlândia, 2010.

SAJJAD, M.; OTSUKI, A. Correlation between flotation and rheology of fine particle suspensions. **Metals**, v. 12, n. 2, 270, 2022. DOI: https://doi.org/10.3390/met12020270.

SEKAR, D. M. R.; PRABHULINGAIAH, G.; KUMAR, P. V.; KHADRI, S. A.; DASSIN, Y. Phosphate recovery from slime sized ore. *In*: PROCEEDINGS OF THE XIII INTERNATIONAL SEMINAR ON MINERAL PROCESSING TECHNOLOGY, Bhuvaneshwar, India, 2013.

SEVEROV, V. V.; FILIPPOVA, I. V.; FILIPPOV, L. O. Use of fatty acids with an ethoxylated alcohol for apatite flotation from old fine-grained tailings. **Minerals Engineering**, v. 188, 107832, 2022. DOI: https://doi.org/10.1016/j.mineng.2022.107832.

SHERMAN, H. Hydrodynamic forces on floating particles. Thesis (Doctoral in Chemical Enginnering), The University of Queensland, 2018. DOI: https://doi.org/10.14264/uql.2018.151

SILVA, A. A. M. **Estudo sobre a flotação de silicatos em coluna para processo de concentração da apatita.** Dissertação de Mestrado, PPG-EQ/UFU, Uberlândia, 2005.

SILVA, A. C.; SILVA, E. M. S.; SILVA, T. F. V.; FERREIRA, K. C. Influência do método de saponificação na microflotação de apatita utilizando óleo da castanha da macaúba. **Tecnologia em Metalurgia, Materiais e Mineração**, v. 14, n. 1, p. 30-38, 2017. DOI: http://dx.doi.org/10.4322/2176-1523.1187.

SILVA, E. M. S.; PERES, A. E. C.; SILVA, A. C.; FLORÊNCIO, D. L.; CAIXETA, V. H. Sorghum starch as depressant in mineral flotation: part 2 – flotation tests. **Journal of Materials Research and Technology**, v. 8, n. 1, p. 403-410, 2019. DOI: https://doi.org/10.1016/j.jmrt.2018.04.002.

SILVA, F. B. R. **Análise das principais variáveis na flotação industrial do complexo de mineração de Tapira – MG**. Dissertação (Mestrado em Engenharia Química), Universidade Federal de Uberlândia, Uberlândia, 2016.

SILVA, J. P. P.; BALTAR, C. A. M.; GONZAGA, R. S. G. Identification of sodium silicate species used as flotation depressants. **Mining, Metallurgy & Exploration**, v. 29, p. 207–210, 2012. DOI: https://doi.org/10.1007/BF03402458.

SIS, H.; CHANDER, S. Reagents used in the flotation of phosphate ores: a critical review. **Minerals Engineering**, v. 16, n. 7, p. 577-585, 2003. DOI: https://doi.org/10.1016/S0892-6875(03)00131-6

SNOW, R.; ZHANG, J. P.; MILLER, J. D. Froth modification for reduced fuel oil usage in phosphate flotation. **International Journal of Mineral Processing**, v. 74, n. 1-4, p. 91-99, 2004. DOI: https://doi.org/10.1016/j.minpro.2003.09.004.

SUBRAHMANYAM, T. V.; FORSSBERG, K. S. E. Fine particles processing: shear-flocculation and carrier flotation — a review. **International Journal of Mineral Processing**, v. 30, n. 3-4, p. 265-286, 1990. DOI: https://doi.org/10.1016/0301-7516(90)90019-U.

SUN, W.; HU, Y.; DAI, J.; LIU, R. Observation of fine particle aggregating behavior induced by high intensity conditioning using high speed CCD. **Transactions of Nonferrous Metals Society of China,** v. 16, n. 1, p. 198-202, 2006. DOI: https://doi.org/10.1016/S1003-6326(06)60035-6.

TABOSA, E. O. **Flotação com reciclo de concentrados (FRC) para recuperação de finos de minério: fundamentos e aplicações**. Dissertação (Mestrado em Engenharia de Minas), Universidade Federal de Porto Alegre, Porto Alegre, 2007.

TAKATA, L. A.; VALLE, T. Flotação em Coluna. In: CHAVES, A. P. **Coleção Teoria e Prática do Tratamento de Minério: A Flotação no Brasil**. São Paulo, Oficina de Textos, 3 ed., 2013. p. 65-104.

TAO, D. Role of Bubble Size in Flotation of Coarse and Fine Particles—A Review. **Separation Science and Technology**, v. 39, n. 4, p. 741–760, 2005. DOI: https://doi.org/10.1081/SS-120028444.

TEAGUE, A. J.; LOLLBACK, M. C. The beneficiation of ultrafine phosphate. **Minerals Engineering,** v. 27-28, p. 52-29, 2012. DOI: https://doi.org/10.1016/j.mineng.2011.12.007.

TESTA, F. G. **Avanços na flotação de finos de minério com condicionamento de alta intensidade.** Dissertação (Mestrado em Engenharia de Minas), Universidade Federal do Rio Grande do Sul, Porto Alegre, 2008.

TOHRY, A.; DEHGHAN, R.; HATEFI, P.; CHELGANI, S. C. A comparative study between the adsorption mechanisms of sodium co-silicate and conventional depressants for the reverse anionic hematite flotation. **Separation Science and Technology**, v. 57, n. 1, p. 141–158, 2021. DOI: https://doi.org/10.1080/01496395.2021.1887893.

TRAHAR, W. J. A rational interpretation of the role of particle size in flotation. **International Journal of Mineral Processing**, v. 8, n. 4, p. 289-327, 1981. DOI: https://doi.org/10.1016/0301-7516(81)90019-3.

TRAHAR, W. J.; WARREN, L. J. The flotability of very fine particles — A review. **International Journal of Mineral Processing**, v. 3, n. 2, p. 103-131, 1976. DOI: https://doi.org/10.1016/0301-7516(76)90029-6.

VALDERRAMA, L.; GÓMEZ, O.; PAVEZ, O.; SANTANDER, M. Recovery of Apatite from Magnetic Concentration Tailings by Flotation. **Minerals**, v. 14, n. 5, 2024.

VERAS, M. M. **Influência do tipo de espumante nas características de espuma produzida na flotação.** Dissertação (Mestrado em Engenharia Mineral), Universidade Federal de Pernambuco, Recife, 2010.

VIACAVA, G. E.; ROURA, S. I.; AGÜERO, M. V. Optimization of critical parameters during antioxidants extraction from butterhead lettuce to simultaneously enhance polyphenols and antioxidant activity. **Chemometrics and Intelligent Laboratory Systems**, v. 146, p.47–54, 2015. DOI: https://doi.org/10.1016/j.chemolab.2015.05.002.

WANG, D.; LIU, Q. Hydrodynamics of froth flotation and its effects on fine and ultrafine mineral particle flotation: A literature review. **Minerals Engineering**, v. 173, 2021. DOI: https://doi.org/10.1016/j.mineng.2021.107220.

WANG, G.; NGUYEN, A. V.; MITRA, S.; JOSHI, J. B.; JAMESON, G. J.; EVANS, G. M. A review of the mechanisms and models of bubble-particle detachment in froth flotation. **Separation and Purification Technology**, v. 170, p. 155-172, 2016. DOI: https://doi.org/10.1016/j.seppur.2016.06.041.

YU, L.; YU, P.; BAI, S. A Critical Review on the Flotation Reagents for Phosphate Ore Beneficiation. **Minerals**, v. 14, n. 8, 828, 2024. DOI: https://doi.org/10.3390/min14080828.

ZHANG, F.; CAI, H.; FAN, G.; GUI, X.; XING, Y.; CAO, Y. The role of interfacial nanobubbles in the flotation performance of microfine particles. **Colloids and Surfaces A: Physicochemical and Engineering Aspects**, v. 699, 134633, 2024. DOI: https://doi.org/10.1016/j.colsurfa.2024.134633.

ZHANG, J.; TANG, Z.; XIE, Y.; AI, M.; ZHANG, G.; GUI, W. Data-driven adaptive modeling method for industrial processes and its application in flotation reagent control. **ISA Transactions,** v. 108, p. 305-316, 2021. DOI: https://doi.org/10.1016/j.isatra.2020.08.024.

ZHAO, L.; ZHANG, Q. Study of oleic acid-induced hydrophobic agglomeration of apatite fines through rheology. **Minerals Engineering**, v. 218, 108911, 2024. DOI: https://doi.org/10.1016/j.mineng.2024.108911.

ZHOU, J. Z.; LI, H.; CHOW, R. S.; LIU, Q.; XU, Z.; MASLIYAH, J. Role of mineral flotation technology in improving bitumen extraction from mined Athabasca oil sands—II.

Flotation hydrodynamics of water-based oil sand extraction. **Canadian Journal of Chemical Engineering**, v. 98, p. 330–352, 2020. DOI: https://doi.org/10.1002/cjce.23598.

APPENDIX I

Figure I.1 - Fine XRD

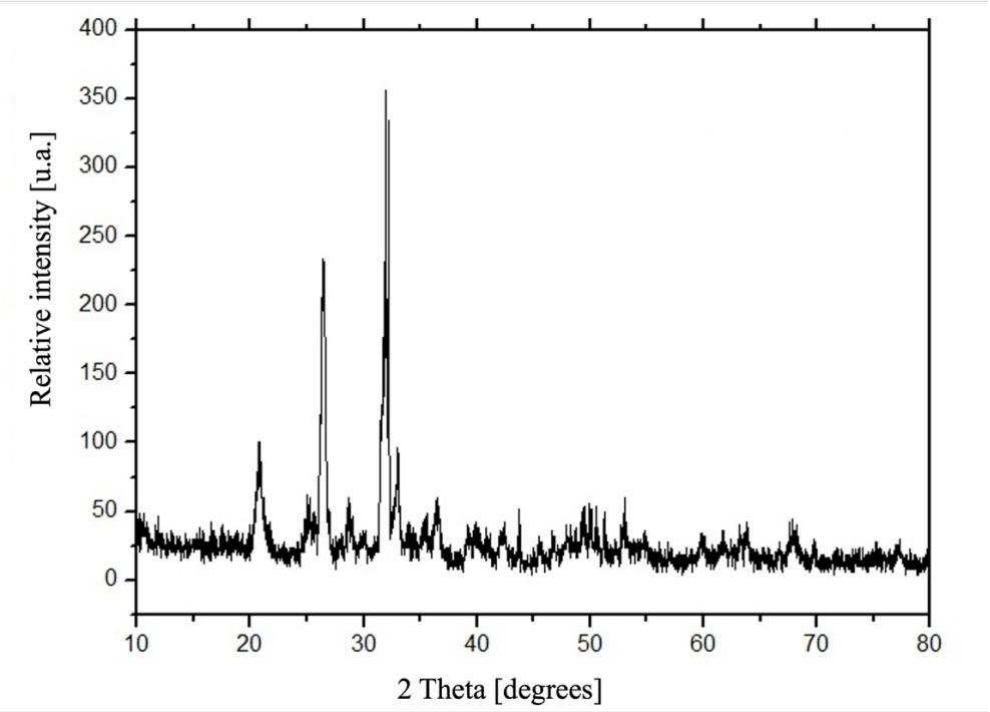

Source: Author (2025).

Figure I.2 Ultrafine XRD

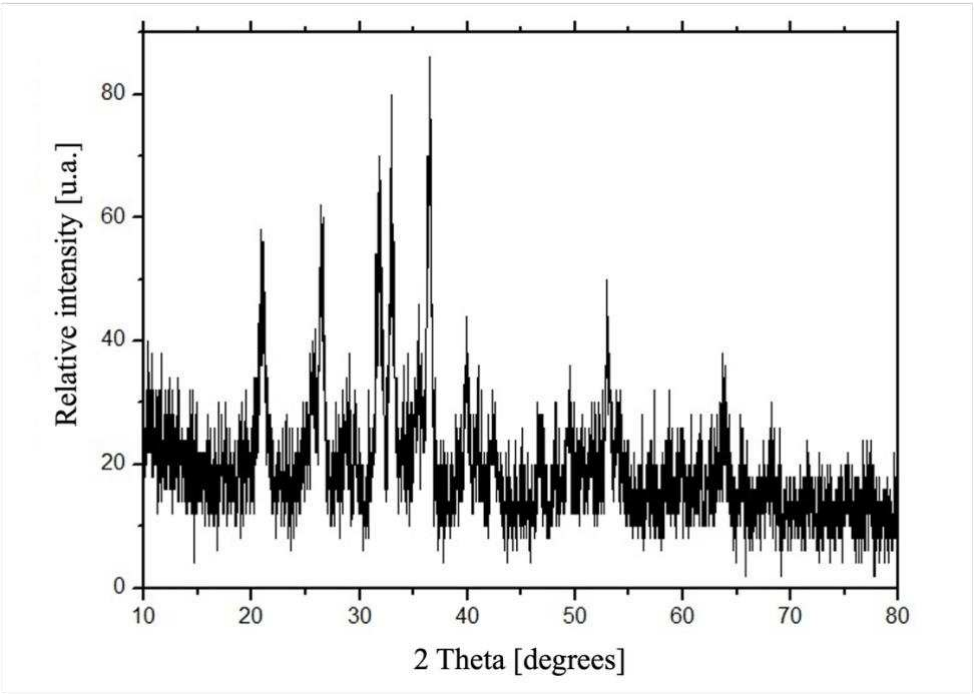

Source: Author (2025).

APPENDIX II

6. FINE ORE:

- Type of collector for fine ore:

Table 6.1 - Two-level factorial experimental design results

Test	Type of collector (x_1)	Collector dosage [ppm] (x_2)	Depressant dosage [ppm] (x_3)	P_2O_5 grade [%] (y_g)	Apatite recovery [%] (y_r)	SR Fe_2O_3 [%]	SR SiO_2 [%]
1	Rice oil	70	700	36.76	35.69	11.07	11.40
2	Agem A3	70	700	35.45	41.4	8.82	9.31
3	Rice oil	110	700	35.80	52.62	9.47	11.58
4	Agem A3	110	700	34.75	54.74	7.32	7.14
5	Rice oil	70	900	35.42	43.66	9.33	11.46
6	Agem A3	70	900	36.50	41.41	9.43	8.07
7 z	Rice oil	110	900	35.32	57.49	7.98	9.52
8	Agem A3	110	900	35.94	54.68	8.15	6.45

Source: Author (2025).

- Additional tests for fine ore:

Table 6.2 - Additional tests for fine ore

Test	pH	Collector dosage [ppm]	Depressant dosage [ppm]	Conditioning solid concentration [%]	Dispersant dosage [ppm]	P_2O_5 grade [%]	Apatite recovery [%]	SR Fe_2O_3 [%]	SR SiO_2 [%]	RI
3	12	110	700	40	0	35.80	52.62	9.47	11.58	0
1	12	70	700	40	0	36.76	35.69	11.07	11.4	0
9	12	30	700	40	0	37.24	20.79	12.47	14.78	0
7	12	110	900	40	0	35.32	57.49	7.98	9.52	0
5	12	70	900	40	0	35.42	43.66	9.33	11.46	0
10	12	30	900	40	0	36.62	25.11	11.46	13.56	0
11	12	110	900	40	250	36.35	49.30	10.60	12.04	0
12	12	110	900	40	2000	36.49	48.74	9.05	12.94	0
13	12	110	900	51	250	34.77	57.25	7.23	7.05	0
14	12	110	900	60	0	36.82	59.10	9.72	9.20	0
15	10	110	900	40	0	38.68	24.76	32.23	29.98	0
16	12	110	1100	40	0	37.48	39.33	18.19	18.19	0
17	12	150	900	40	0	34.80	64.39	7.45	7.07	3.31
18	10	150	900	40	0	34.66	72.46	8.73	7.34	3.57
19	10	400	400	40	0	34.36	81.29	8.36	5.34	3.86

Source: Author (2025).

- CCD tests for fine ore:

Table 6.3 - CCD conditions and results of fine ore

Test	Conditioning solid concentration [%] (x_1)	Collector dosage [ppm] (x_2)	Depressant dosage [ppm] (x_3)	pH (x_4)	P_2O_5 grade [%] (y_g)	Apatite recovery [%] (y_r)	SR Fe_2O_3 [%]	SR SiO_2 [%]	RI
20	40	350	300	10.00	33.43	81.42	8.3	4.26	3.83
21	40	350	300	11.50	35.7	82.14	8.90	9.39	3.93
22	40	350	500	10.00	35.02	81.92	9.62	6.14	3.9
23	40	350	500	11.50	36.11	77.3	9.92	9.68	3.78
24	40	450	300	10.00	33.85	87.19	7.56	4.99	4.03
25	40	450	300	11.50	35.27	85.91	8.56	7.38	4.04
26	40	450	500	10.00	34.72	84.14	9.07	5.06	3.96
27	40	450	500	11.50	34.40	79.26	7.56	5.85	3.79
28	60	350	300	10.00	29.90	84.14	4.06	2.86	0
29	60	350	300	11.50	34.46	82.92	6.29	6.42	3.91
30	60	350	500	10.00	35.17	85.21	9.11	6.86	4.01
31	60	350	500	11.50	36.14	85.9	8.71	8.58	4.07
32	60	450	300	10.00	33.55	88.25	6.85	4.65	4.06
33	60	450	300	11.50	35.03	87.96	7.77	8.42	4.1
34	60	450	500	10.00	34.24	89.44	8.39	6.06	4.12
35	60	450	500	11.50	35.03	84.79	8.13	8.63	3.99
36	35.17	400	400	10.80	34.16	80.34	8.41	4.99	3.82
37	64.83	400	400	10.80	33.2	84.2	5.57	4.76	3.91
38	50	325.87	400	10.80	34.66	87.95	7.97	6.84	4.09
39	50	474.13	400	10.80	34.62	91.58	8.03	6.36	4.21
40	50	400	251.74	10.80	34.02	85.1	7.68	5.85	3.97
41	50	400	548.26	10.80	35.67	85.19	8.40	7.29	4.03
42	50	400	400	9.69	35.37	86.39	9.59	6.34	4.06
43	50	400	400	11.91	35.34	84.5	8.30	6.98	3.99
44	50	400	400	10.80	34.59	85.82	8.52	5.12	4.01
45	50	400	400	10.80	34.74	86.14	8.94	5.45	4.03

Source: Author (2025).

7. ULTRAFINE ORE:

- Cell flotation tests for ultrafine ore:

Table 7.1 - Results and conditions of ultrafine flotation in cell

Test	Collector type	Collector dosage [ppm]	Depressant dosage [ppm]	pH	Conditioning solid concentration [%]	Flotation solids concentration [%]	P_2O_5 grade [%]	Apatite recovery [%]	SR Fe_2O_3	SR SiO_2
1	Agem A3	550	1200	12	52.78	38.78	12.92	92.47	0.38	0.75
2	Agem A3	110	1200	12	26.09	16.67	13.57	75.38	0.41	0.84
3	Agem A3	80	1400	12	21.05	11.43	13.84	75.46	0.42	0.91
4	Agem A3	80	1400	12	28.24	13.41	13.72	84.33	0.41	0.86
5	Agem A3	80	1400	12	31.78	17.35	13.99	86.45	0.42	0.87
6	Agem A3	80	2700	12	28.24	13.41	13.74	83.77	0.42	0.85
7	Agem A3	80	2700	9.5	28.24	13.41	15.55	25.18	0.49	1.17
8	Agem A3	80	3200	9.5	28.24	13.41	17.46	40.56	0.58	1.45
9	Agem A3	110	2700	9.5	28.24	13.41	17.09	42.81	0.57	1.43
10	Agem A3	110	3200	9.5	28.24	13.41	16.89	47.12	0.54	1.33
11	Agem A3	220	2700	9.5	28.24	13.41	16.47	71.95	0.53	1.25
12	Rice oil	220	2700	9.5	28.24	13.41	16.85	37.07	0.54	1.38
13	Flotigam	220	2700	9.5	28.24	13.41	17.08	69.00	0.57	1.38
14	Agem A3	220	3200	9.5	28.24	13.41	16.08	76.91	0.51	1.16
15	Agem A3	80	2700	9	28.24	13.41	16.12	27.67	0.51	1.32
16	Agem A3	80	3200	9	28.24	13.41	16.53	36.48	0.54	1.29
17	Agem A3	80	3500	9	28.24	13.41	16.92	43.44	0.56	1.35
18	Agem A3	80	3700	9	28.24	13.41	16.68	19.59	0.55	1.30
19	Agem A3	80	3900	9	28.24	13.41	-	-	-	-
20	Agem A3	220	2700	9	28.24	13.41	16.80	75.38	0.54	1.26
21	Agem A3	220	3200	9	28.24	13.41	16.31	75.92	0.52	1.20
22	Agem A3	80	3500	9	30.68	14.84	16.68	20.24	0.55	1.30
23	Agem A3	80	3500	9	32.97	16.22	14.20	15.79	0.42	0.99
24	Agem A3	100	3500	9	32.97	16.22	13.92	15.88	0.40	1.04
25	Agem A3	100	3500	9	35.11	17.55	14.03	17.95	0.40	1.01
26	Agem A3	100	3500	9	37.11	18.85	13.62	15.11	0.39	0.94
27	Agem A3	100	3500	9	39.00	20.10	13.26	14.83	0.37	0.91
28	Agem A3	100	3500	9	40.78	21.32	13.12	14.24	0.37	0.83

Source: Author (2025).

- Type of collector analysis of ultrafine ore:

Table 7.2 - Flotation conditions and results of two-level factorial experimental design of ultrafine ore

Test	Type of collector (x_1)	Collector dosage [ppm] (x_2)	Depressant dosage [ppm] (x_3)	P_2O_5 grade [%]	Apatite recovery [%]	SR Fe_2O_3 [%]	SR SiO_2 [%]
29	Rice oil	50	700	24.5	41.68	1.29	3.54
30	Agem A3	50	700	19.94	60.98	0.77	1.83
31	Rice oil	110	700	20.22	55.29	0.79	2.02
32	Agem A3	110	700	17.6	65.6	0.60	1.46
33	Rice oil	50	900	23.61	42.11	1.19	2.98
34	Agem A3	50	900	19.45	63.00	0.74	1.74
35	Rice oil	110	900	18.51	63.17	0.67	1.57
36	Agem A3	110	900	16.98	70.59	0.55	1.32

Source: Author (2025).

- Conditioning time and stirring speed analysis for ultrafine ore:

Table 7.3 - Conditioning time and stirring speed analysis of ultrafine ore

Test	Conditioning time for each reagent [min]	Stirring speed [rpm]	P_2O_5 grade [%]	Apatite recovery [%]	SR Fe_2O_3 [%]	SR SiO_2 [%]
41	5	1200	21.26	48.59	0.91	2.18
60	10	1200	21.4	48.07	0.92	2.16
61	5	1500	21.67	48.96	0.96	2.23

Source: Author (2025).

- Additional tests for ultrafine ore:

Table 7.4 - Additional tests in column of ultrafine ore

Test	Dispersant dosage [ppm]	Conditioning solid concentration [%]	pH	Collector dosage [ppm]	Depressant dosage [ppm]	P_2O_5 grade [%]	Apatite recovery [%]	SR Fe_{2O3} [%]	SR SiO_2 [%]
31	0	40	12	110	700	20.22	55.29	0.79	2.02
37	250	40	12	110	700	19.31	59.56	0.73	1.71
38	2000	40	12	110	700	17.3	44.89	0.58	1.31
39	0	40	12	70	700	19.75	49.44	0.84	1.96
40	125	40	12	70	700	20.61	50.96	0.86	2.04
41	250	40	12	70	700	20.67	51.46	0.91	2.18
42	400	40	12	70	700	19.73	40.93	0.78	1.83
43	0	50	12	70	700	-	-	-	-
44	0	50	10	70	700	16.82	6.07	0.48	1.94
45	0	20	12	70	700	-	-	-	-
46	0	40	10	70	700	17.82	7.52	0.55	2.02
47	250	40	10	70	700	17.49	5.60	0.52	2.00
29	0	40	12	50	700	24.5	41.68	1.29	3.54
35	0	40	12	110	900	18.51	63.17	0.67	1.57
48	0	40	12	70	900	20.16	50.10		
33	0	40	12	50	900	23.61	42.11	1.19	2.98
49	0	40	12	70	1100	20.47	50.79	0.83	2.02
50	0	40	12	70	1300	20.66	53.38	0.86	2.03
51	0	40	12	70	1500	20.02	51.38	0.79	1.82
52	0	40	12	70	1900	19.66	52.94	0.78	1.72
53	0	40	10	400	400	15.07	68.14	0.46	1.04
54	0	40	12	400	400	15	92.63	0.46	1.08
55	0	35	10	80	2618	15.34	22.14	0.45	1.25
56	0	35	12	80	2618	19.5	54.23	0.75	1.58
57	0	35	12	80	3000	18.77	51.00	0.70	1.54
58	250	35	12	80	2618	19.09	50.81	0.73	1.55
59	400	35	12	80	2618	19.09	50.46	0.73	1.53

Source: Author (2025).

- Dispersant tests for ultrafine ore:

Table 7.5 - Two factorial experimental design of dispersant analysis.

Test	Dispersant dosage [ppm] (x_1)	Collector dosage [ppm] (x_2)	Depressant dosage [ppm] (x_3)	P_2O_5 grade [%]	Apatite recovery [%]	SR Fe_2O_3 [%]	SR SiO_2 [%]
29	0	50	700	24.50	41.68	1.29	3.54
62	250	50	700	25.48	43.52	1.41	4.08
39	0	70	700	19.75	49.44	0.80	1.80
41	250	70	700	20.67	51.46	0.85	2.00
33	0	50	900	23.61	42.11	1.18	2.98
63	250	50	900	23.89	45.87	1.19	3.10
48	0	70	900	20.16	50.10	0.81	1.81
64	250	70	900	20.73	53.97	0.86	1.98

Source: Author (2025).

- CCD tests for ultrafine ore:

Table 7.6 - Experimental conditions and results of the CCD applied to ultrafine ore flotation

Test	Collector dosage [ppm] (x_2)	Depressant dosage [ppm] (x_3)	P_2O_5 grade [%] (y_g)	Apatite recovery [%] (y_r)	SR Fe_2O_3 [%]	SR SiO_2 [%]	RI
65	30	500	28.42	29.43	2.06	6.07	0
66	30	900	28.47	30.03	2.03	6.52	0
67	70	500	21.98	48.65	0.99	2.44	0
64	70	900	20.73	53.97	0.79	1.75	0
68	22	700	29.86	22.23	2.39	9.63	0
69	78	700	20.38	53.59	0.83	1.92	0
70	50	417	24.34	42.21	1.28	3.38	3.12
71	50	983	24.35	41.66	1.28	3.40	3.10
72	50	700	25.35	43.08	1.38	3.78	3.14
73	50	700	25.61	43.96	1.39	4.38	3.27

Source: Author (2025).